

FERMILAB Proposal No. 319

Spokesman: K. W. Chen

FTS 517-353-5459

FURTHER TEST OF SCALING AT HIGH MOMENTUM TRANSFERS

IN DEEP INELASTIC MUON SCATTERING

C. Chang, K. W. Chen, A. Kotlewski, L. Litt,

R. Renninger, and P. Schewe

Michigan State University

June 10, 1974

TABLE OF CONTENTS

	Page
I. SUMMARY	2
II. PHYSICS JUSTIFICATION	3
A. Introduction	3
B. Test of Scaling	4
C. $\mu^+/\mu^-$ Asymmetry Measurement	9
D. Pertinent Information From Experiment 26, Phase A	11
III. APPARATUS NEEDED	13
A. The Muon Beam--Conditions and Running Time	13
B. The Spectrometer and Associated Detectors	16
C. Resolution in $Q^2$ and $\nu$	17
D. Event Rate	18
IV. SCOPE OF THE EXPERIMENT	22
V. ACKNOWLEDGEMENTS	24
APPENDIX A. REVIEW OF THE SCALING TRANSFORMATION	25
APPENDIX B. SYSTEMATIC DIFFERENCES INHERENT IN RUNNING AT SEPARATE MACHINE ENERGIES	27
APPENDIX C. MOMENTUM RESOLUTION IN THE MAGNETIZED IRON SPECTROMETER	31
REFERENCES	33

## I. SUMMARY

In this proposal we outline a plan to follow-up progress made in Experiment 26. A status report for our 150 GeV and 56 GeV runs is available elsewhere.<sup>1</sup>

During the past three years, the E26 group originated, developed, and operated a magnetized iron spectrometer in the Muon Laboratory. A total of  $1.7 \times 10^{10}$  muons were made to strike an iron target during the period of our running (Phase A). The objectives of the Phase A run have been achieved. We now request a total of  $5 \times 10^{11}$  muons for the next phase. This amount of running should permit us to examine the structure of the nucleon in further detail up to a momentum transfer-squared of  $160 \text{ (GeV/c)}^2$ .

The original method of E26 will be used again.<sup>2</sup> As will be discussed later, this unique method offers an optimized way to test scaling with a minimum systematic bias.

Three muon beam energies are contemplated for the test of scaling: 90 GeV, 150 GeV, and 240 GeV. Data with negative muons will be taken at each energy to verify the absence of two-photon exchange processes, and to check on radiative corrections.

We fully expect to be ready in a relatively short time for a rigorous study of nucleon structure at high momentum transfers.

## II. PHYSICS JUSTIFICATION

### A. Introduction

The observed Bjorken scaling of the deep inelastic structure functions is a major issue in understanding the structure of the nucleon. At SLAC, electron scattering data at small  $\omega$  have been collected<sup>3</sup> up to  $Q^2 = 33 \text{ GeV}^2$ . The first presentation of these data will most likely come at the London Conference in July. For SLAC energies one must also carefully determine the parameter  $R = \frac{\sigma_s}{\sigma_t}$ . Theoretically, the existence of such scaling is also the basis for a suggestion that it must break down farther out in the  $Q^2$ - $\nu$  plane. (See, for example, Drell and Chanowitz, SLAC-PUB-1315, Oct. 1973, "Speculations on the Breakdown of Scaling at  $10^{-15} \text{ cm}$ ".) Experimentally, deep inelastic ep and  $\mu$ p scattering are basically measurements of the total  $\gamma^*p$  cross section. (Here  $\gamma^*$  denotes a space-like virtual photon of energy  $\nu$ , mass  $-Q^2$ .) Total pp,  $\pi$ p, and Kp cross sections have been seen to rise at FNAL energies. If  $\gamma^*p$  interactions continue to qualitatively follow the hadron-hadron interactions, then on experimental grounds alone one might expect scaling to start breaking down as  $Q^2$  stays fixed and  $\nu$  gets large. There is little disagreement these days on the importance of a sensitive test of Bjorken scaling. An experimental result on this question must be able to bear up under extensive scrutiny by the entire high energy physics community. In order to confidently understand such measurements, one must acquire ample amounts of data, have the opportunity to make careful checks of several experimental questions, and then follow up with a detailed and exhaustive analysis.

## B. Test of Scaling

Our main concern at this time is to continue a careful study of scaling out to higher values of  $Q^2$  and  $\nu$ , using different configurations--as in Experiment 26--of our magnetized iron spectrometer with nuclear targets. The significant advances to Experiment 26, Phase A, that we propose here are:

- 1) We now ask to run in a way that gives us a substantially larger  $Q^2$ - $\nu$  range. This means that the data/data ratio method (see Appendix A) can be used to test scaling to  $Q^2=160 \text{ GeV}^2$ , three times farther out than in E26, as shown in Figure 1. The increase in the  $Q^2$ - $\nu$  range comes about as a result of two simple changes from Experiment 26. (Compare Figure 2, which shows the original configuration, with Figure 3, which shows the proposed configuration.) The arrangement of equipment upstream of the first toroidal magnet has been changed to permit a "scaling configuration" in which the targets and magnets are substantially closer together. This improvement significantly increases the acceptance for  $Q^2 > 40 \text{ GeV}^2$ . The second factor enabling us to get to a larger kinematic range comes from running at higher muon beam energies. We would like to see the present muon beam line, N1, operate with pulsed magnets at 240 GeV/c. We realize that it might require some effort on the part of FNAL to get to 240 GeV in N1. But FNAL is planning to spend considerable time next year running with the accelerator energy at 400 GeV; and the muon laboratory has successfully pulsed the N1 magnets at this time. We therefore feel that this request is well matched to the muon laboratory's plans.

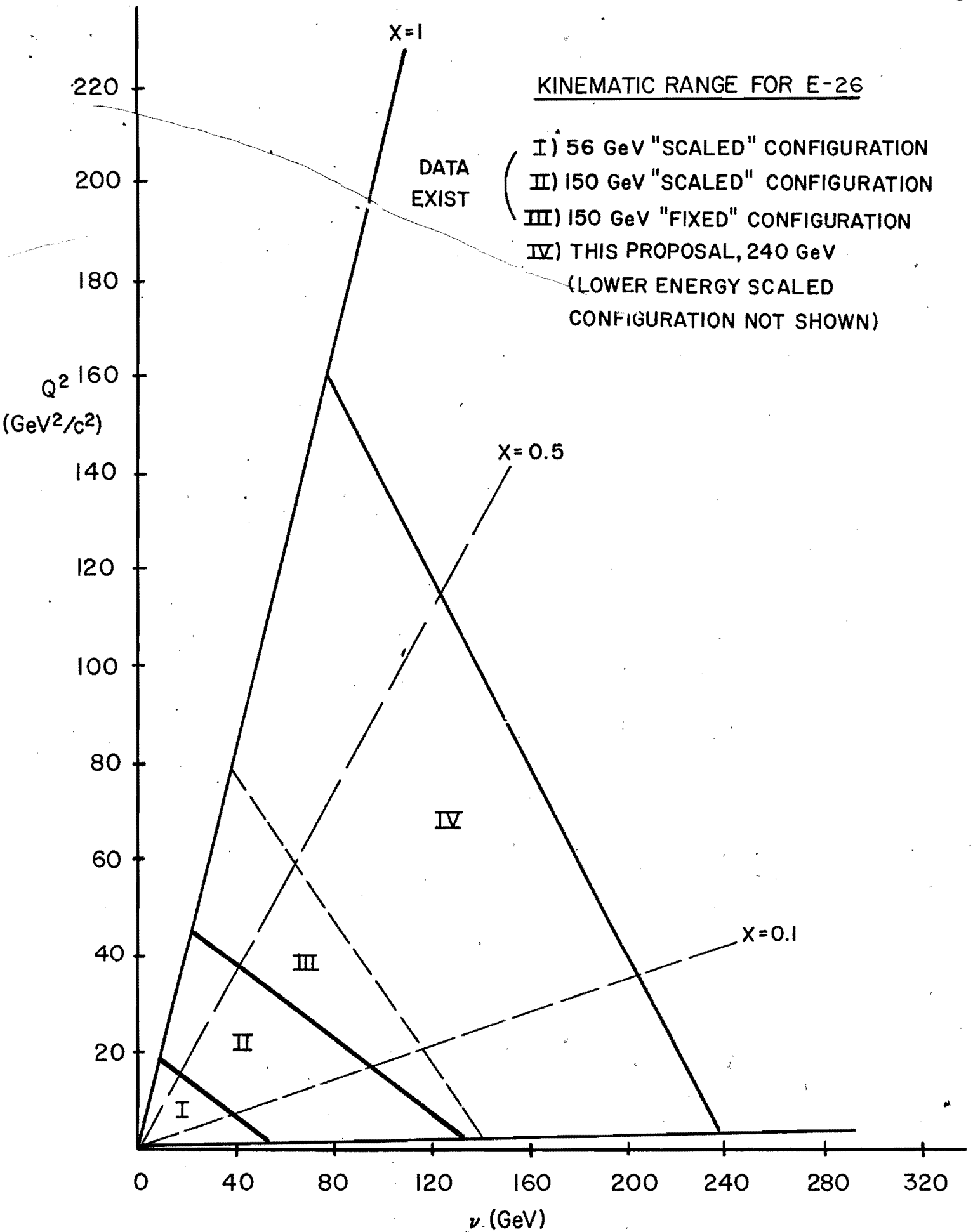
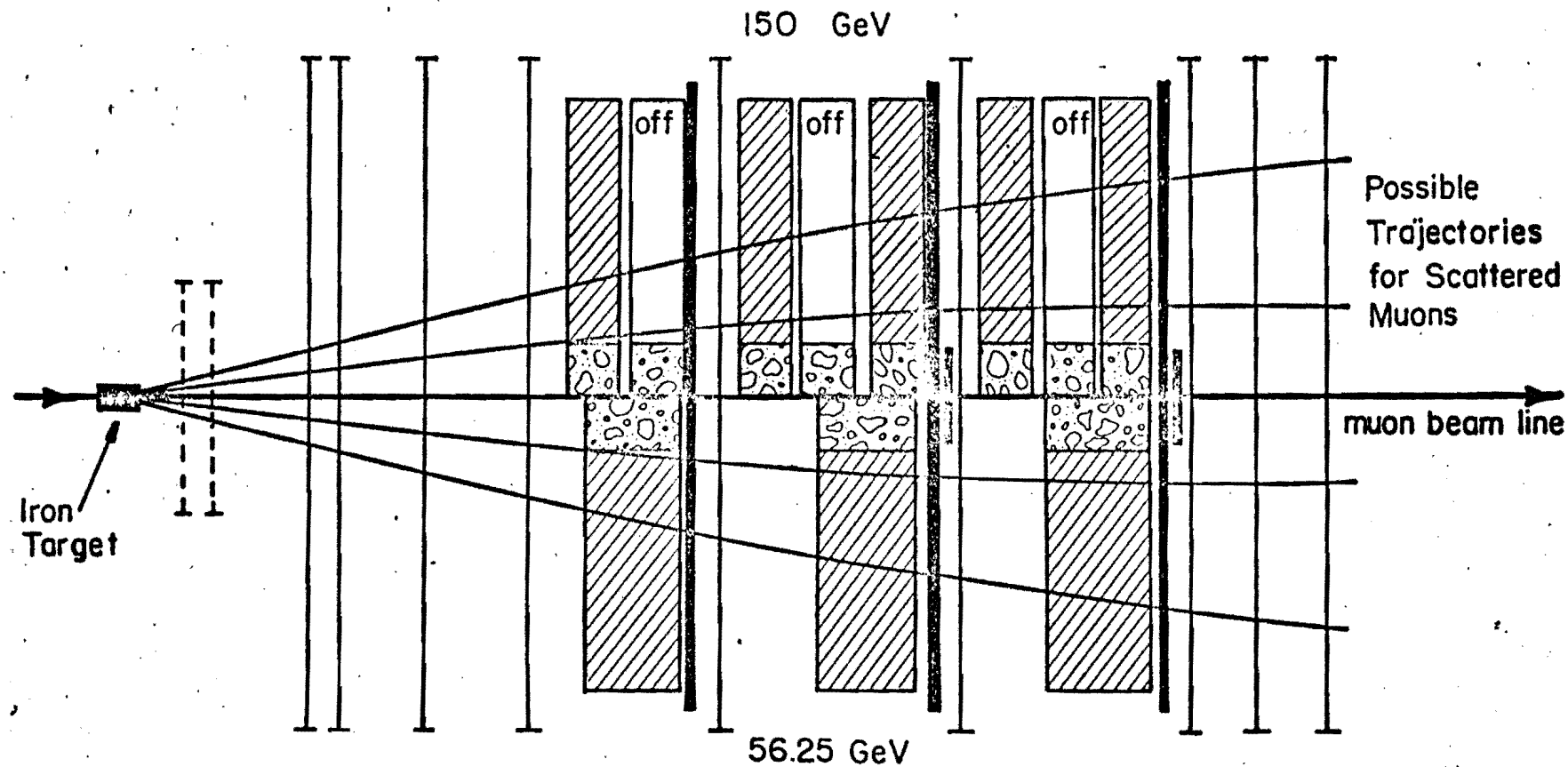


Figure 2. Schematic Diagram of the Apparatus in Experiment 26,  
**SCALE TRANSFORMATION OF MUON SCATTERING APPARATUS**

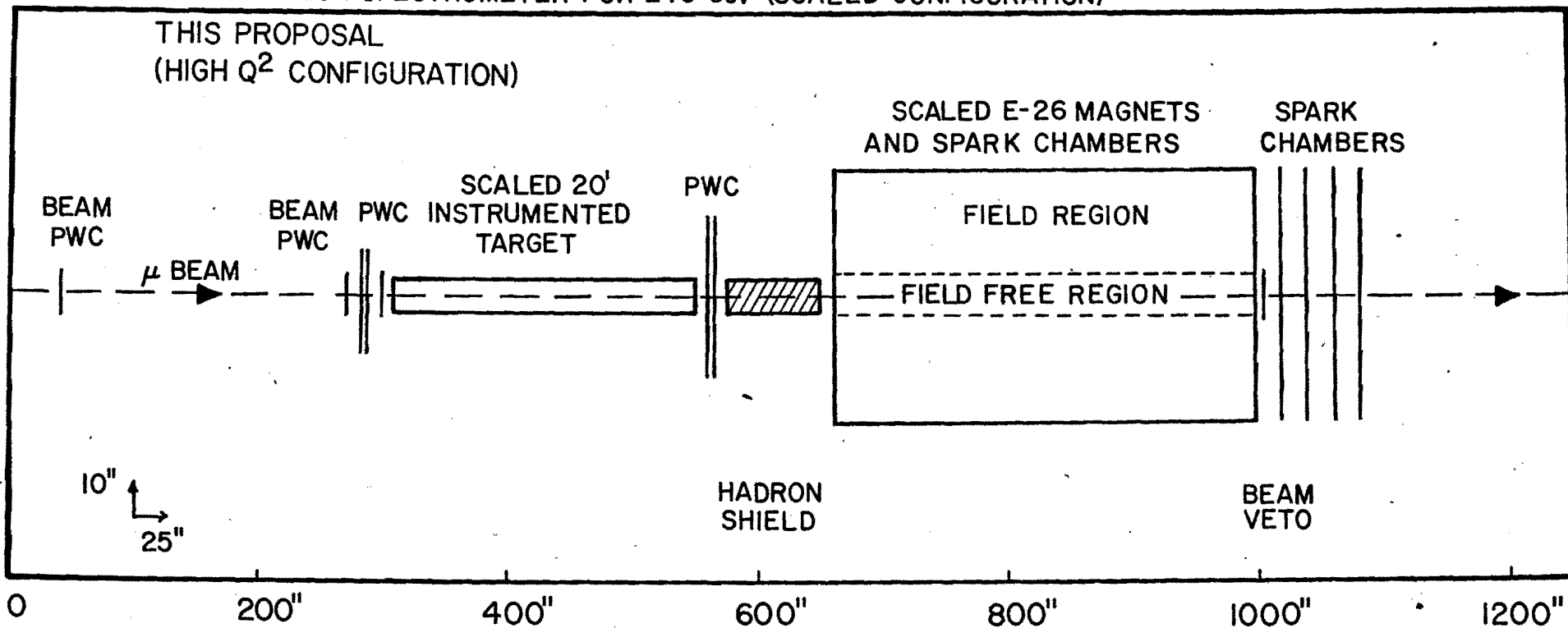


- Key
- |   |                             |   |                            |
|---|-----------------------------|---|----------------------------|
| I | Spark Chamber Module        |  | Magnetized Iron 17.3 KG    |
| I | Proportional Chamber Module |  | Demagnetized Iron          |
| ■ | Count Hodoscope             |  | High Density Concrete Plug |

0291173

Figure 3

SYMMETRICAL E-26 MUON SPECTROMETER FOR 240 GeV (SCALED CONFIGURATION)



FOOTNOTES:

- 1) INSTRUMENTED TARGET: 4" IRON +  $\frac{1}{4}$ " SCINTILLATOR, OPTIMIZED FOR LARGEST  $Q^2$ .  $Z_{center} = 425"$
- 2) MAGNETS: 8 TOTAL MAGNETS (5 ON, 3 OFF)
- 3) BEAM VETO: 3 TOTAL IN BEAM.
- 4) HADRON SHIELD: 75" LEAD OR EQUIVALENT

- 2) Besides the rearrangements discussed above, we intend to make simple improvements and additions to the present apparatus, resulting in: a) the ability to take data at higher rates and at higher beam energies; b) our having better halo rejection at large and small radial distances from the muon beam; c) our having finer granularity in the sampling of hadronic cascades in the target; and, d) our having more protection against punch-through that occurs for events with a large hadronic cascade. All of these improvements are designed to give a good signal-to-noise ratio at high  $Q^2$ .

We believe that in this new phase we can complete a study that has the systematic uncertainties down to the intrinsic limitations of the apparatus. (See Appendix B.)

It is our belief that the E-26 apparatus is the best nuclear target/ magnetized-iron spectrometer system for FNAL to support. Its resolution and acceptance are hard to improve upon; it is the least expensive for FNAL to use, and its output of physics per dollar will be high; and, finally, it has an optimized and reliable time scale for the investigation of  $\nu W_2$ .

### C. $\mu^+ / \mu^-$ Asymmetry Measurement

The present quantitative understanding of deep inelastic muon scattering is based entirely on the assumption that all observed processes are due to one-photon exchange. The expectation here is that two-photon exchange amplitudes are suppressed by  $\alpha = \frac{e^2}{\hbar c}$ . Before Experiment 26, there were no asymmetry measurements beyond  $Q^2 = 2.1 \text{ GeV}^2$ .

The asymmetry parameter,  $\epsilon$ , is defined as follows:

$$\epsilon = \frac{\sigma(\mu^+) - \sigma(\mu^-)}{\sigma(\mu^+) + \sigma(\mu^-)} = \frac{2R_1 R_2}{R_1^2 + R_2^2 + I_2^2} \approx \frac{2R_2}{R_1}$$

where  $R_1$  is the one-photon exchange amplitude, and  $R_2$  and  $I_2$  are the real and imaginary parts of the two-photon exchange amplitude. In the literature<sup>4</sup> one finds  $\epsilon$  placed at  $0.002 \pm 0.017$  for the range  $0.5 < Q^2 < 2.1 \text{ GeV}^2$ . An alternate way of expressing this is:

$$\epsilon = 0.0 + b Q^2 \quad ; \quad \text{with } b = 0.003 \pm 0.014 \quad .$$

During the 150 GeV run of Experiment 26 we took sufficient  $\mu^+$  and  $\mu^-$  data to place a 1% upper limit on  $\epsilon$  out to higher  $Q^2$ , (i.e.,  $Q^2 < 60 \text{ GeV}^2$ .) The incident flux here was  $3.4 \times 10^9 \mu^+$  and  $2.9 \times 10^9 \mu^-$ . These runs occurred under identical conditions, except for the reversal of magnetic fields.

No corrections have been applied, and we expect no evidence of a large asymmetry to appear after all corrections have been included.

The two dominant effects that one must watch here are muon beam shape and radiative corrections. We note that the toroidal magnets are particularly well suited for this measurement thanks to :1) their rotational symmetry about the incident beam direction; and, 2) the fact that the beam does not traverse a magnetic field. Corrections to changes in radial beam distributions, or to offset of the beam, are more easily made because of the first point; the incident muon is not subject to hysteresis effects or other possible sources of unsymmetric field reversal thanks to the second point.

We now propose to expand the range of the  $\mu^+/\mu^-$  measurement to the range  $10 \text{ GeV}^2 < Q^2 < 160 \text{ GeV}^2$ .

D. Pertinent Information from Experiment 26, Phase A

The preliminary results on muon scattering from Experiment 26 indicate a possible complication of perfect scaling predictions at  $Q^2$  in the vicinity of  $\approx 50 \text{ GeV}^2$ . (5) (See Table I for a list of conclusions presented at the Chicago APS Meeting in February, 1974.) Possible deviations from the predictions of perfect scaling need not be simple. The best way to represent the data might be in terms of both  $Q^2$  and  $x = (Q^2/2Mv)$ . Because of the possible admixture of  $x$  and  $Q^2$  dependence in  $vW_2$ , a sensitive measure of scaling must determine a functional form for  $vW_2$  and then indicate the errors on whatever coefficients are involved. Large statistics are required to do this. Regardless of the outcome of the final analysis of the existing E26 data at 150 GeV and 56 GeV, it is important to continue tests at higher energy and higher  $Q^2$ .

Data taken so far as part of Experiment 26 does not yet match the inherent precision of the apparatus. The statistical sensitivity in the present data correspond to a mass of approximately  $25 (\text{GeV}/c)^2$ . The limiting systematic errors are discussed in detail in Appendix B. The systematic sensitivity of this experiment can now be increased to  $\approx 50 (\text{GeV}/c)^2$ . The proposed run will have statistical errors at this level.

No corrections have been applied, and we expect no evidence of a large asymmetry to appear after all corrections have been included.

The two dominant effects that one must watch here are muon beam shape and radiative corrections. We note that the toroidal magnets are particularly well suited for this measurement thanks to : 1) their rotational symmetry about the incident beam direction; and, 2) the fact that the beam does not traverse a magnetic field. Corrections to changes in radial beam distributions, or to offset of the beam, are more easily made because of the first point; the incident muon is not subject to hysteresis effects or other possible sources of unsymmetric field reversal thanks to the second point.

We now propose to expand the range of the  $\mu^+/\mu^-$  measurement to the range  $10 \text{ GeV}^2 < Q^2 < 160 \text{ GeV}^2$ .

TABLE I. PRELIMINARY CONCLUSIONS ON THE 150 GeV DATA  
 TAKEN IN EXPERIMENT-26 -- PRESENTED AT THE  
 CHICAGO APS MEETING, FEBRUARY, 1974

1. No catastrophic change occurs in  $\nu W_2$  for  $Q^2$  less than  $50(\text{GeV}/c)^2$ .  
 There is no evidence for "color thaw" up to  $W$  of 150 GeV.
2. The combined effects of a scaling violation, a photon propagator modification or a muon form factor<sup>†</sup> can be limited to masses greater than 12 GeV, i.e., distances less than .02 fermi.
3. A systematic decrease relative to the Bodek fit to the SLAC data appears in both of the full data analyses made so far. This could be explained by either a mass in a form factor of about 12 GeV ( $1/\Lambda^2 \approx 70 \times 10^{-4}$ ) or by the assumption that the SLAC data had not reached a true asymptotic limit, i.e., that the  $x$  dependence of  $\nu W_2$  is different at NAL energies.
4. A self contained test of scaling at NAL energies will be available when the 56 GeV data is taken. This will be independent of Monte Carlo comparisons with SLAC and in principle free of systematic errors.
5. The  $\omega$  variation of  $\nu W_2$  at large  $\omega$  appears to be either flat or slightly rising. Present statistics do not permit binning the data in  $\omega$  before studying the  $Q^2$  behavior.

† Possibilities Include: 1) Breakdown of Scaling in the structure function; 2) a finite size muon; 3) a heavy photon (Lee-Wick  $B^0$ )

### III. APPARATUS NEEDED

#### A. The Muon Beam - Conditions and Running Time

During the course of Experiment 26, steady improvements were made in the FNAL muon beam. Our group participated and contributed heavily along with staff members of the neutrino laboratory in these developments. The full potential of the FNAL muon beam was not realized until very recently, when a flux of  $1.2 \times 10^6$  muons/pulse were observed in the muon area. With such a flux, our request for  $5 \times 10^{11}$  muons can now be met with reasonable running time.

In estimating muon beam intensities we have assumed that the present muon line is unchanged. A fair estimate of the muon yield per proton from a 12" Al target can be made using the formula:

$$\frac{\mu^+}{p} = 7 \times 10^{-8} \times \frac{dN}{dp_{\pi} d\Omega_{\pi}} \times (1 - \gamma c \tau)$$

where the cross section shown is that produced by the thermodynamical model via the CERN program SPUKJ, and where the last factor represents the number of pions that decay in 700 meters. The numerical constant in front comes from "guesstimating" a variety of numbers. This constant was made to agree with the  $1.2 \times 10^{-7} \mu^+/p$  value observed in past 150 GeV muon runs at an accelerator energy of 300 GeV. Thus we are extrapolating from measured yields to unmeasured higher energy ones. For a 400 GeV proton energy, we have the following numbers. They agree with a more detailed computer calculation of S. Loken.<sup>6</sup>

ESTIMATED MUON YIELDS WHEN THE ACCELERATOR  
RUNS AT 400 GEV

---

$p_{\mu}$	$\mu^+ / p$
90 GeV	$4.0 \times 10^{-7}$
150 GeV	$2.2 \times 10^{-7}$
240 GeV	$4.0 \times 10^{-8}$

(Particle yields were obtained from runs of SPUKJ on the Argonne IBM 370. The calculation was done for an Al target; sample curves for other types of targets may be found in FNAL Report FN-216/1111.20 by M. Awschalom and A. Van Ginneken, "Secondary Particle Yields Produced by 400 and 500 GeV/c Protons Interacting on H, Be, and Pb", October, 1970.)

Furthermore, we assume a ten second repetition rate of acceleration cycles, with  $10^{13}$  protons/cycle coming to the Al target for 240 GeV muon runs. We also have assumed that the present muon beam will not be operated at more than  $10^6$  muons per cycle, due to radiation safety levels. This results in the following request for machine time, with the accelerator operating at 400 GeV for the 240 GeV muon runs. (See Table II.)

TABLE II. RUNNING TIME REQUEST

<u>Hours of Machine Time</u>	<u><math>\mu</math> Energy</u>	<u>Total #<math>\mu</math>'s</u>	<u>Use of the Time</u>
300	240 GeV	$10^{11} \mu^+$	High $Q^2$ - $\nu$ Data for Scaling Test, check $\nu W_2(x, Q^2)$ .
300	240 GeV	$(.3-.5) \times 10^{11} \mu^-$	Check one-photon exchange. Further useful scaling data.
100	150 GeV	$10^{11} \mu^+$	Fe target, high $Q^2$ data, Check E26 150 GeV run.
100	150 GeV	$(.3-.5) \times 10^{11} \mu^-$	Fe target, high $Q^2$ , check one-photon exchange, further useful scaling data
100	150 GeV	$10^{11} \mu^+$	Be and Pb targets. High $Q^2$ look at A-dependence. A tungsten target (Hevimet) would be interesting. This will be further explored.
100	90 GeV	$10^{11} \mu^+$	Fe target--scaling test
100	90 GeV	$(.3-.5) \times 10^{11} \mu^-$	Fe target--check of one-photon-exchange, scaling test.
<hr/>			
1100 Hours Total	---	$\sim 5 \times 10^{11} \mu$ 's	

## B. The Spectrometer and Associated Detectors

The proposed configuration of elements in our spectrometer is indicated in Figure 3. The target, counter, and chamber positions, as well as the number of magnets and the magnet positions, are scaled exactly as in Experiment 26. (See Figure 2 and Appendix A for a review of the scaling transformation.)

During Experiment 26 the acceptance of the system was studied as a function of target position. Data exist for each of six different target positions, covering a range more than 400" upstream of the first magnet. We looked into the event rate vs.  $Q^2$  for the different targets, and have concluded that we would like a 20' target that ends about 120" upstream of the first magnet. The target is segmented and scintillation counters that go to ADC's are placed every four inches for aid in vertex identification. Large proportional chambers<sup>†</sup> are upstream and downstream of the target to facilitate identification of incoming halo tracks. Three large xy hodoscopes at various places downstream of the second magnet are used for defining a scattered muon in the trigger, and for accurate timing that will reject "stale" spark chamber tracks. A smaller xy hodoscope upstream of the target will eliminate the consideration of "out-of-time" beam tracks in the proportional chambers. The trigger will be as in Experiment #26. An additional beam veto counter will be added, as will some shielding in the region upstream of the plug in the first magnet. We wish to continue using all of the NAL equipment presently allocated to Experiment 26.

<sup>†</sup> Now under construction at Michigan State University.

### C. Resolution in $Q^2$ and $\nu$

The muon spectrometer used in Experiment 26 was carefully checked out during the course of Phase A running. Its acceptance and resolution have been measured and tested. There are two types of measurements in this experiment: relative and absolute. The data/data method requires a thorough understanding of non-scaling effects arising from systematic differences in the different configurations. The data/monte-carlo method, on the other hand, requires an absolute energy calibration. In some sense these two methods are complimentary.

In the new phase, we are required to examine the details of  $\nu W_2(x, Q^2)$ . This involves searching for a  $Q^2$  variation at fixed  $x$ . For certain types of scaling violations, this approach can yield better understanding than the present approach, where one looks for  $Q^2$  variations alone. It is important, then, to have good resolution in both  $x$  and  $Q^2$ . The following facts relate to this issue:

1.  $E'$  and  $Q^2$  Resolution-- The spectrometer resolution in  $(1/E')$  been measured to be 14%. For  $Q^2$  the resolution is worse, ~18%. These values are close to the best one can do with a magnetized iron spectrometer, since the dominant effect is the multiple coulomb scattering. (See Appendix C.)
2.  $\omega$  or  $x$  Resolution--Resolution in  $\omega$  for the case where one knows only  $E'$  is highly  $\nu$  dependent. For  $\nu < .4 E_0$ ,  $\Delta\nu/\nu$  exceeds the smallest value it can have: ~12% due to Fermi motion. An independent measurement of  $\nu$  significantly improves the  $\omega$  resolution. A sampling of hadronic cascades in the target provides such a measurement. This calorimetry is not new to FNAL

We plan to have such instrumentation in future running. The 20' instrumented target contains a sufficient number of elements for fine granularity of the sampling. We look forward to accuracy of 15% in  $\Delta v/v$  for the range  $0.1E_0 < v < E_0$ . In this range  $\Delta\omega/\omega$  is  $\sim 20\%$ , a significant improvement over E26, Phase A.

D. The Event Rate

Monte Carlo calculations of the event rate for the proposed configuration may be summarized by the following Table and graphs. Table III lists the expected number of events above various values of  $Q^2$  for the high energy run. Figure 4 shows how such events can be expected to populate the  $Q^2$ - $v$  plane. Finally, Figure 5 shows the detection efficiency as a function of  $Q^2$  and  $v$ .

# No. OF EVENTS ACCEPTED BY APPARATUS

$10'' \mu's \quad (\nu > 40 \text{ GeV})$

$E_\mu = 240 \text{ GeV}$

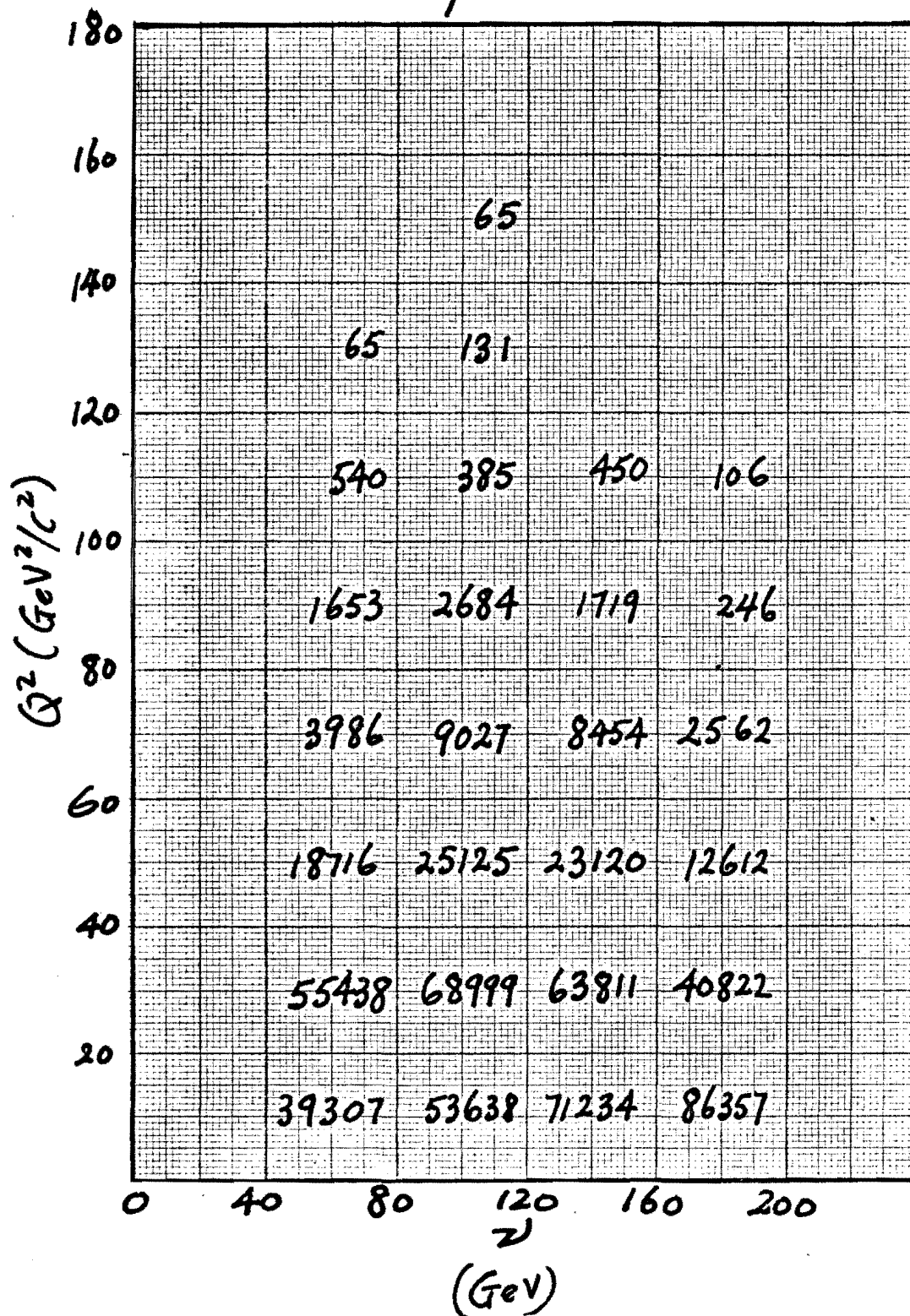


FIGURE 4

DETECTION EFFICIENCY vs  $Q^2$

(SCALED CONFIGURATION)

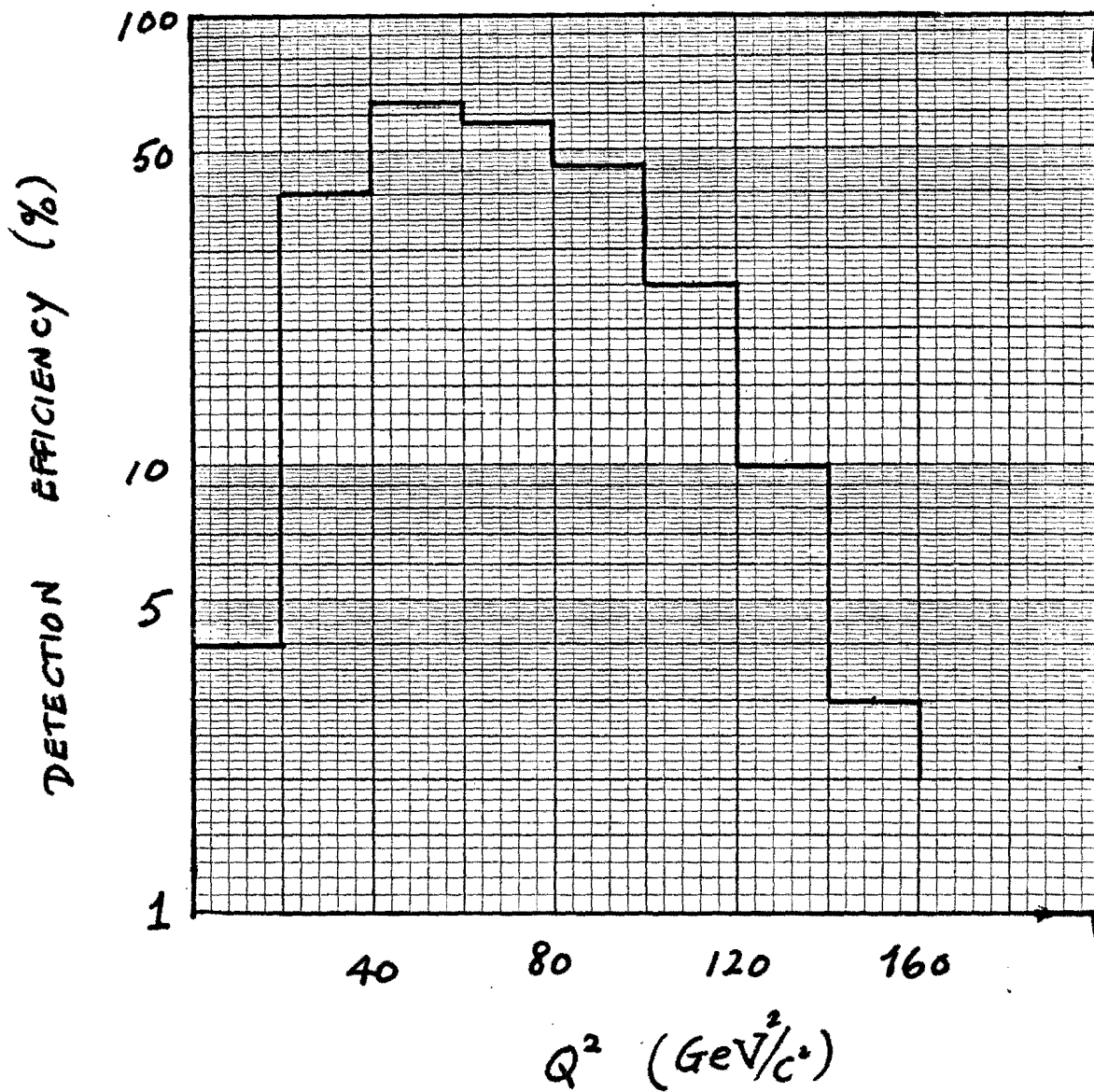


FIGURE 5a

DETECTION EFFICIENCY vs  $\nu$   
(SCALED CONFIGURATION)

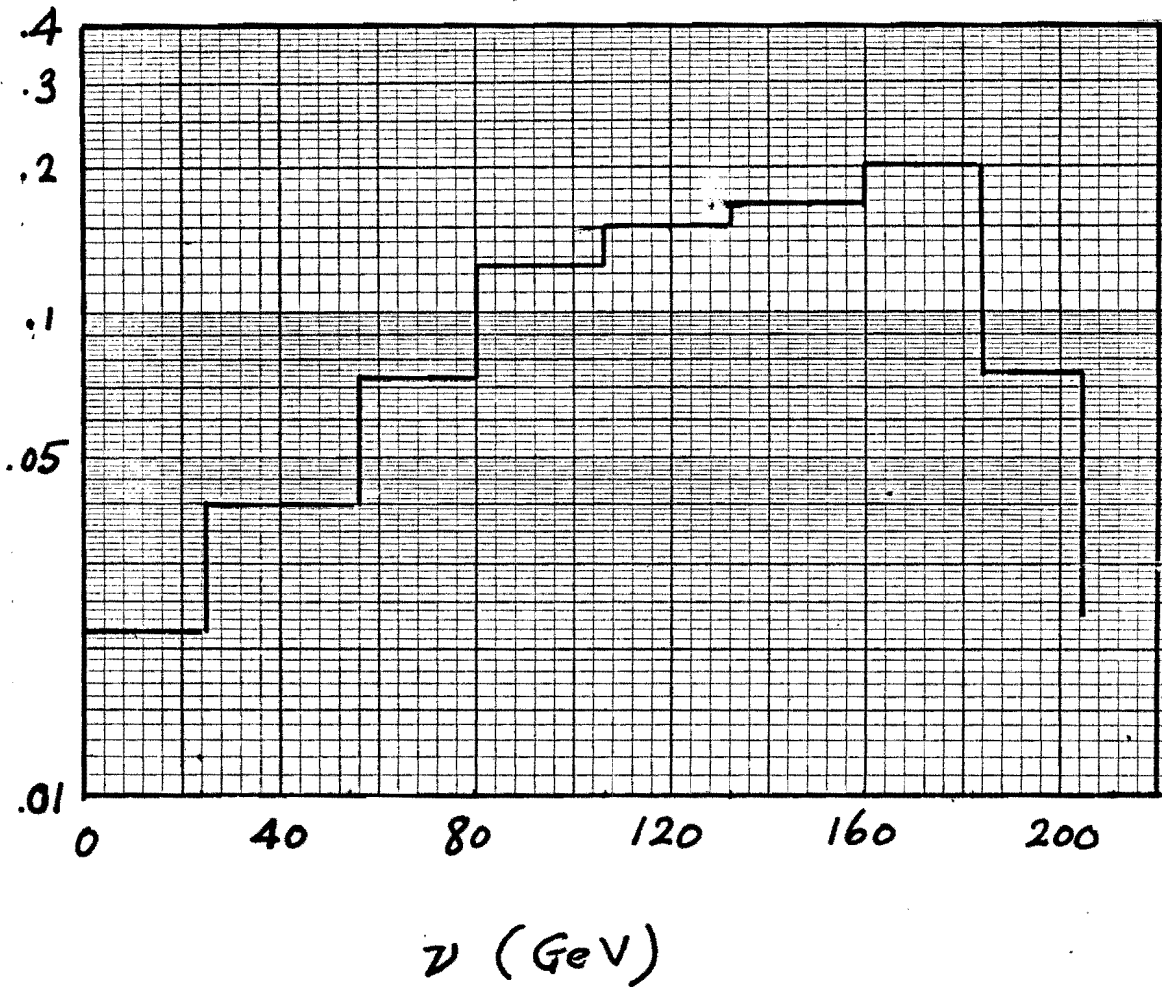


FIGURE 5b

TABLE III. MONTE-CARLO ESTIMATE OF EVENT RATES FOR  $10^{11}$  MUONS  
 AT 240 GEV. THE CONFIGURATION SCALES--SEE FIGURE 3

Assuming Perfect Scaling		Assuming $\Lambda = 12$ GeV	
$Q^2$	Events Beyond $Q^2$	$Q^2$	Events Beyond $Q^2$
20	$3.77 \cdot 10^5$	20	$2.47 \cdot 10^5$
40	$1.21 \cdot 10^5$	40	$6.67 \cdot 10^4$
60	$3.50 \cdot 10^4$	60	$1.67 \cdot 10^4$
80	$9.23 \cdot 10^3$	80	$3.93 \cdot 10^3$
100	2079	100	810
120	456	120	178
140	60	140	20

#### IV. SCOPE OF THE EXPERIMENT

The physics program outlined by this proposal is a natural continuation of Experiment 26. Much of the equipment is already in place. Detector and read-out electronics for the spark chambers and proportional chambers have been thoroughly checked out during the past two years. There will be no fundamental changes to the spectrometer. The modifications that must be completed before running can begin are the following:

- 1) Target Instrumentation--Modifications must be made to the target cart; the remaining portion of the target must be fabricated in the machine shop (72" of target already exists from E26); the ADC set-up must be assembled and tested.
- 2) Hodoscope Construction--Three large xy hodoscopes and two small xy hodoscopes must be assembled and tested.
- 3) Proportional Chamber Construction and Installation--Some large proportional chambers must be ready for installation upstream of the first toroidal magnet. One chamber has already been assembled at Michigan State University. There will be a complete check-out of that chamber, the electronics, and the gas system this summer at FNAL.
- 4) On-Line Computer Modifications--We currently have a FNAL PDP 11/20 with 12k storage. The on-line program will have to be modified so as to monitor and record information from the newly installed equipment.
- 5) Miscellaneous--An additional counter or two will be added. Some minor modifications might be made to the electronic

logic. For example, fast-timing using TDC's might be installed to get off-line timing to 1 rf bunch. Also, some extra "triggers" or "latches" might be added. No major revision is foreseen here.

We feel that a realistic time-scale for the completion of these changes is six months. That is, we plan to be ready to run by the end of January 1975. Our group will consist of five post-doctoral physicists and three graduate students. Three of the physicists have been intimately involved with the running and analysis of Experiment 26. One of us (L. Litt) plans to work closely with the neutrino laboratory to insure that a 240 GeV beam is ready by July 1975 for reliable, experimental operation.

We expect to request a total of ~50 hours this year for test runs and for calibration. We wish to begin our data taking at 150 GeV because the initial data to come in would then overlap with E26 data at the same kinematical values.

Some other groups have expressed an interest in the possibility of joining us in collaboration. We intend to fully explore these possibilities. Things will most likely become more certain by the time we negotiate our "Agreement" with FNAL.

#### V. ACKNOWLEDGEMENTS

Many of the ideas and plans presented here were developed jointly with our Cornell and UC-San Diego collaborators from Experiment 26: L. Hand, S. Herb, S. Loken, W. Vernon, and Y. Watanabe. We especially thank S. Loken for generously sharing his thoughts, calculations and opinions. We also acknowledge the help and encouragement of the staff of the Neutrino Laboratory, in particular F. R. Huson and P. Limon, for information concerning the feasibility of 240 GeV running. A. Skuja and L. Verhey are to be thanked for sharing their insight into the muon beam. Conversations with R. Wilson of Experiment 98 have also been stimulating.

## APPENDIX A. REVIEW OF THE SCALING TRANSFORMATION

1. Incident Energy:  $E \rightarrow \lambda E$
2. Scattered Muon Energy:  $E' \rightarrow \lambda E'$
3. Scattered Muon Angle:  $\sin(\theta/2) \rightarrow \frac{1}{\sqrt{\lambda}} \sin(\theta/2)$

Done as follows: spatial separation of elements along the muon beam change as  $z \rightarrow \sqrt{\lambda} z$ ; positions transverse to the beam line are unchanged:  $x, y \rightarrow x, y$ .

4.  $\Delta$ (p-transverse) for trajectories:  $\int B dl \rightarrow \sqrt{\lambda} \int B dl$ ; but  $B \rightarrow B$ .
5. Multiple Scattering Material: For both the target and the magnets,

$$(\text{gm/cm}^2) \rightarrow \lambda (\text{gm/cm}^2); \quad (\text{spatial extent along } \mu \text{ beam}) \rightarrow \sqrt{\lambda} (\text{spatial extent along } \mu \text{ beam})$$

so that (d-transverse)<sub>mult. scat.</sub>  $\rightarrow$  (d-transverse)<sub>mult. scat.</sub>

6. The Kinematical Variables:  $Q^2 \rightarrow \lambda Q^2$ ;  $v \rightarrow \lambda v$ ; so that

$$\frac{2Mv}{Q^2} = \omega \rightarrow \omega$$

7. The Deep-Inelastic Cross Section:

$$\left( \frac{d\sigma}{dE' d\Omega} \right) = \left( \frac{d\sigma}{d\Omega} \right)_{\text{Mott}} v W_2 \left\{ 1 + 2 \frac{(1 + v\omega/2M) \tan^2(\theta/2)}{(1 + R)} \right\}$$

$$\text{where } \left( \frac{d\sigma}{d\Omega} \right)_{\text{Mott}} = \frac{e^2 \cos^2(\theta/2)}{4E^2 \sin^4(\theta/2)}$$

Clearly,

$$\left( \frac{d\sigma}{d\Omega} \right)_{\text{Mott}} \rightarrow \left( \frac{d\sigma}{d\Omega} \right)_{\text{Mott}}$$

$$dE' d\Omega \rightarrow dE' d\Omega$$

and  $vW_2 \rightarrow vW_2$  (Scaling Hypothesis!)

Thus  $(d\sigma)_{\text{inelastic}} \rightarrow (1/\lambda) \times (d\sigma)_{\text{inelastic}}$  ; although  
 (counts per incident muon)  $\rightarrow$  (counts per incident muon)

because the target mass along the beam was increased by  $\lambda$ . (See 5.)

#### 8. The Data/Data and Data/Monte-Carlo Comparisons:

Suppose that scaling is broken by a multiplicative factor of the form  $(1+Q^2/\Lambda^2)^{-2}$ . Then one will not get the same counting rate at  $\lambda Q^2$  in the second configuration that one has at  $Q^2$  in the first configuration. In fact, one will have

$$\frac{\text{Data in second config. at } \lambda Q^2}{\text{Monte Carlo assuming Scaling at } \lambda Q^2} = \{ 1 + (\lambda Q^2/\Lambda^2) \}^{-2} \quad (1)$$

and

$$\frac{\text{Data in second config. at } \lambda Q^2}{\text{Data in first config. at } Q^2} = \frac{\{ 1 + \lambda Q^2/\Lambda^2 \}^{-2}}{\{ 1 + Q^2/\Lambda^2 \}^{-2}} \quad (2)$$

So, the effect of a scaling violation is different in data/data comparisons and in data/monte-carlo comparisons; the deviation from scaling is always smaller in data/data comparisons. For low  $Q^2$  the right side of Eq.(2) becomes  $\{ 1 - 2(\lambda - 1)Q^2/\Lambda^2 \}$ . For energies of 240 GeV and 90 GeV,  $\lambda = 8/3$ .

## APPENDIX B

## SYSTEMATIC DIFFERENCES INHERENT IN RUNNING AT SEPARATE MACHINE ENERGIES

We have looked into the nature and magnitude of those systematic differences that arise in comparing data from two configurations. The fact that some systematic uncertainties tend to cancel raises obvious questions: how big are these uncertainties? How exact is the cancellation? What is the resulting error in the ratio, after all proper analysis procedures have been followed? Briefly, there are the following issues:

1. Differences in the incident  $\mu$  beam. The intensity, geometrical shape and position, and the momentum-space shape and position, can all vary from one setting to another. The geometrical shape and position, as well as the  $\Delta p/p$  shape, however, can be corrected for in the analysis. The trigger uses an ordinary pulse generator to randomly sample the beam tracks. The data tapes therefore contain unbiased distributions of all the independent beam variables. One can take data/data ratios (i.e., for different  $\lambda$ 's) in a bin-by-bin fashion, and then combine the ratios, with the result of each bin weighted according to its error. For data/ monte carlo comparisons one uses the actual unbiased sample of beam tracks as input to the monte carlo program. Furthermore, cuts can be made on  $\Delta p/p$ , eliminating the possibility of contamination by low or high energy tails in the incident muon beam. In conclusion, the apparatus monitors and records all relevant properties of the muon beam, and our analysis properly removes the variation of

beam shape when doing data/data comparisons.

The absolute incident energy has, in the past, been calibrated by steering the beam into the spectrometer, where we now know the absolute magnetic field to  $\pm 1\%$ . In the future this limit might be reduced to  $\pm .5\%$ .<sup>7</sup> We also expect that in future runs there will be additional measurements of the muon beam energy with beam-line magnets. The goal of a  $\pm .5\%$  absolute energy calibration seems feasible.

## 2. Triggering Biases and Inefficiencies

There are two sets of anti-counters in the experiment. The first is used to define the incident beam, while the second is used to define the scattered beam. (That is, an event is vetoed if the incident beam track is too far away from the target, or if the scattered muon is too close to the incident beam.)

Special runs were taken to look for any bias originating from the first set of counters; no bias was found. Special bits set by the second set of counters permitted off-line searches for a bias there; no bias was found.

## 3. Reconstruction Inefficiencies

A more interesting set of questions relates to the reconstruction inefficiencies. What per cent of all triggers will have zero reconstructions? What about halo contamination and halo-induced misidentification of scattered muon tracks? Do extra sparks significantly mess up the assignment of momentum and angle?

Such questions have been carefully investigated as part of the current E26 analysis. A counter-telescope, installed during the 56 GeV April run, maps out a road through the magnets, making

a direct efficiency measurement possible. The hodoscopes we propose to use in our next set-up have finer bins, and will provide a more extensive, direct check.

#### 4. Pion Contamination in the Incident Muon Beam

This effect is negligible. Experiment 98 has measured an upper limit of  $5 \times 10^{-5}$   $\pi$ 's/ $\mu$  in the muon beam. Experiment 26 has looked for wrong-sign muons on the data tapes, and so far a limit of 0 per  $10^4$  triggers has been set.

The table on the following page summarizes our discussion of systematic differences. In conclusion, we feel that the intrinsic limit of sensitivity of the apparatus is  $\Lambda = 50$  GeV.

## SUMMARY TABLE OF ESTIMATED SYSTEMATIC UNCERTAINTIES

<u>Effect</u>	Resulting Limit on the $Q^2$ -Dependence Due to the Indicated Effect--in units of $(10^4/\Lambda^2)$	
	<u>DATA</u> <u>DATA</u>	<u>DATA</u> <u>MONTE-CARLO</u>
1. Incident Energy-- Normalization and $\Delta p/p$ shape	---	$\pm 2.5$
2. Magnetic Field-- Normalization and Shape	---	$\pm 3.0$
3. De-Gaussed Field in the 150 GeV Configuration	$\pm 2.5$	$\pm 2.5$
4. Spatial Distribution of the incident beam	---	---
5. Error in assumed $dE/dx$ formulae	$\pm 2.5$	$\pm 2.5$
6. Trigger Biases and Reconstruction Inefficiencies	$\pm 1.0$	$\pm 2.0$
7. Halo Contamination	$\pm 1.0$	$\pm 2.0$
8. Pion Contamination	---	---
<hr/> TOTAL (Added in Quadrature)	<hr/> $\pm 4$	<hr/> $\pm 6$

## APPENDIX C. MOMENTUM RESOLUTION IN THE MAGNETIZED-IRON SPECTROMETER

Here we consider multiple coulomb scattering, which is the dominant component. If  $\theta_B$  is the bend-angle, and  $p$  is the momentum of a ray through the spectrometer, then

$$p \text{ (GeV/c)} = .03 \times \left\{ \left( \int B \, dl \right) / \theta_B \right\} \quad \text{( KG-m/radians)}$$

or,

$$p = \eta / \theta_B \quad .$$

$$\text{But,} \quad \delta p = (-1/\eta) p^2 \delta \theta_B \quad ; \quad \text{or,} \quad \frac{\delta(1/p)}{(1/p)} = \frac{p \delta \theta_B}{\eta} \quad .$$

Thus, to first order,

1. The variable  $(1/p)$  has a gaussian distribution when momenta are assigned to monochromatic muons incident upon the system.
2. The per cent width of the gaussian is linearly dependent on the square root of the number of radiation lengths of iron; and inversely proportional to  $\int B \, dl$ .

Under the scaling transformation described in Appendix A,  $\{ \delta(1/p) \} / (1/p)$  is unchanged.

Besides multiple scattering, there is energy loss. The average energy loss is compensated for when one assigns production variables to fitted trajectories. There are also fluctuations in energy loss, which are asymmetric. The existence of straggling means that the curve of  $\{ \delta(1/p) \} / (1/p)$ , when generated by a monte-carlo program, is not pure gaussian, but rather gaussian

with an additional tail on the high side. The effect of this tail upon our analysis is negligible, as shown by the analysis of monte-carlo generated events where stragglings has been turned on and off. (The stragglings was computed using the knock-on formulae in Rossi, and the  $\mu$ -bremsstrahlung and pair production formulae of Tsai, SLAC-PUB-1365 (1974), "Pair Production and Bremsstrahlung of Charged Leptons".)

REFERENCES

1. "Status Report to the PAC on the Status of Experiment 26", June 1974.
2. Proposal 26, by K. W. Chen and L. N. Hand.
3. R. Taylor (private communication)
4. The Brookhaven Collaboration (see A. Entenberg et al. Phys. Rev. Letters 32, p. 486 (1974) ) will soon publish their results. (A. Melissinos, private communication.)
5. Invited talk at the Chicago APS Meeting in February, 1974 by K. W. Chen.
6. Private Communication. We are indebted to Loken for these results. Loken's program agrees to within a factor of two with all measured muon fluxes.
7. Meticulous studies of this limit have been made by S. Herb of Cornell. See the appropriate memo, or his write up in reference 1.

Addendum to Proposal 319

by

E-26 Collaboration

Presented by K. W. Chen at the January 17, 1975

Muon Physics Workshop

PROPOSAL # ~~319~~  
MASTER  
DO FILE  
ELG  
JRS

## I. Review of the Physics Reasons for Testing Scaling

The observed Bjorken scaling of the deep inelastic structure functions is a major issue in understanding the structure of the nucleon. Two prominent notions that are questioned by tests of scaling are the parton model<sup>1</sup> and asymptotic freedom. Theoretically it appears that Bjorken scaling requires asymptotic freedom, and that this throws one into the arena of non-Abelian gauge theories.<sup>2</sup> In this talk, however, we are thrown into a different kind of arena.

About one year ago the parton model started running into some trouble. After having nearly exhausted their program for studying  $\nu W_2$  using space-like photons, SLAC, CEA, and DESY turned their attention to time-like investigations of  $\nu W_2$ . Surprisingly, all of the colliding beam measurements<sup>3</sup> pointed to a rising  $e^+e^-$  total cross section, which is in contradiction with a simple parton model. As far as hadron-hadron production of time-like photons was concerned, Drell-Yan<sup>4</sup> production of massive  $e^+e^-$  pairs was still in a hazy state.<sup>5</sup> Last April the first results appeared from the E26 Collaboration:<sup>6</sup> a (data/monte-carlo) ratio for deep-inelastic  $\mu$ -Fe scattering at an incident energy of 150 GeV. The ratio varies as a function of  $Q^2$ . All in all, the status of Bjorken scaling beyond the SLAC region was not clear.

It is comforting to note that although each of the above experimental results have not changed since April 1974, the question marks hanging over scaling have. Everybody certainly knows about the discoveries recently made in  $e^+e^-$  colliding beam experiments,

JASO 084  
 831110  
 51110

and in hadron production of massive  $e^+e^-$  pairs.<sup>7,8</sup> But nobody yet understands whether Bjorken scaling will be a valid notion after all the data are in and the full consequences of the discoveries are taken into account.<sup>9</sup> The new information provided by E-26 answers some questions, but now it is raising more.

## II. Review of Results from E-26

### A. General Features

The scaling tests are preformed in two ways to answer these questions.

1. Comparison with absolute predictions given by a Monte-Carlo program assuming SLAC's  $\nu W_2$ . (Are  $\mu p$  data at higher  $q^2$  and  $\omega$  described by the  $\nu W_2(\omega')$  which best fits  $ep$  data at SLAC?)
2. Comparison of data at one energy and configuration with data at another energy and configuration. (Does a model-independent test of  $\mu p$  data at high  $q^2$ ,  $\omega$  (far away from SLAC region) indicate Bjorken scaling?)

The absolute kinematical variable distributions of method 1 are predicted by a Monte-Carlo program that uses the best fit to the SLAC-MIT  $ep$  results.<sup>10</sup> The Monte-Carlo calculation includes all known physical effects when it allows the scattered muon to traverse the target and the spectrometer. The comparison of data to Monte-Carlo in E-26 is not a flat function of  $q^2$  and  $\omega$  throughout the kinematic region of E-26.<sup>6</sup> The apparent  $q^2$  variation, however, cannot be immediately interpreted as a deviation of Bjorken scaling because:

1. SLAC-MIT fit may be not the asymptotic form for the structure function, i.e., it may have anomalous  $\omega$  dependence at large  $\omega$ .

2. Even if the variations observed indicated  $q^2$  variations at fixed  $\omega$ , the asymptotic statement that  $\lim_{q^2 \rightarrow \text{large}} \nu W(x, q^2) = \nu W_2(\omega')$  still may be valid farther out in the  $q^2 \nu$  plane.

Let us dwell on the first point. The absolute studies in E-26 shows that the data have an  $\omega$  dependence. At fixed  $q^2$  the high  $\omega$  data ( $\omega > 10$ ) tend to be higher than the data at low  $\omega$  ( $\omega < 10$ ). The very low  $\omega$  ( $\omega < 4$ ) data in fact shows no evidences of a rise but gives a strong indication that it might have fallen below unity (by as much as 30% at  $q^2 \geq 60 \text{ GeV}^2/c^2$ ). At lower  $q^2$ , ( $q^2 < 5$ ) and  $\omega < 16$ , E-26 data shows good agreement with SLAC, indicating a good absolute normalization of our experiment. We shall discuss these points in detail.

#### B. Large $\omega$ Region (Intermediate $q^2$ Region)

For larger  $\omega$ , we have taken data at several target positions. We took the data at these various target positions primarily to test that the data sample is stable against severely different acceptances. At a fixed  $q^2$  and  $\omega$ , the acceptances vary by as much as a factor of 6 (100% to 15%). All data sample at the present state of analysis shows an internal consistency of the order of 10%. We can entertain two explanations of the data.

1. The  $\omega$  rise at fixed  $q^2$  is a pure variation of  $\nu W_2(\omega')$ .

For  $\omega \approx 20$  the apparent rise amounts to 20-30%, from 1.0 at  $q^2 = 1 \text{ GeV}^2/c^2$  to about 1.25 at  $10 \text{ GeV}^2/c^2$ . How is the transition taking place in  $q^2$ ? Possibly, then, there is non-scaling in the low  $q^2$  region between  $q^2 = 1$  and  $10$  at  $\omega \approx 20$ . This could be indicating uninteresting features of  $\nu W_2$  at high  $\omega$  that go away at higher  $q^2$ .

2. The second possibility of the  $\omega$  rise is that we are really seeing some particle production mechanism in deep inelastic scattering.

This is, however, a really exciting possibility that we are then seeing new physics that is originating from effects such as those of Ref. 7 and 8.<sup>11</sup> This is because in deep inelastic scattering the missing-mass-squared is given by:

$$W^2 = 2M\nu - q^2 + M^2$$

$$W^2 = q^2 \cdot (\omega' - 1)$$

Thus at fixed  $q^2$ , the variable  $W^2$  is directly related to  $\omega$ . An observed  $\omega$  rise at fixed  $q^2$  can in principle be plotted as a rise in the invariant-mass-squared distribution.

These two possibilities are still entangled with further analysis efforts and the possibility of more data that would come as an E-26 extension. Analysis of existing data, however, cannot resolve all the questions. More data are required. We can list some tests that must be made:

1. Does the  $W^2$  distribution scale? (Since  $q^2 \rightarrow \lambda q^2$ ,  $\omega \rightarrow \omega$ ,  $W^2 \rightarrow \lambda W^2$ ) The  $W^2$  distribution observed at 56 GeV and 250 GeV should exhibit the same characteristics if the rise is caused by a  $\nu W_2$  increase in the  $\omega$  alone. If it is particle production, then the two distributions will not "scale", thus giving support to the latter possibility.
2. Is there structure in the  $W^2$  distribution? If there is structure that is not caused by apparatus effects,

then it is an unambiguous vote for the latter possibility. To do this one subtracts the "background" (yield from scaling) from the data and looks for "bumps". We note that the  $v$  resolution for large  $v$  of the E-26 apparatus is very good. For example, if  $E'$  is 30 GeV,  $v = E_0 - E' = 120$  GeV. Our estimate is that  $\frac{\Delta v}{v} \approx \pm 7\%$ .

3. Examine events which are of the following kind:

$$\mu^+ + p \rightarrow \mu^- + \text{anything}$$

If such events trigger the apparatus, they could come from either decays of  $\rho$ 's, other produced particles, or from pion decay. We found this process to be small. In general,  $\mu^-$  is a small background.

4. Look at transverse momentum distribution. Maybe there are bumps there! In other words, E-26 type data is very rich. We do not have all the answers yet. But we are now working on this.

C. High  $q^2$  Region (Low  $\omega$  Region)

Let us return to the high  $q^2$  region ( $q^2 > 30$ ). Previous data at  $\omega > 15$  are nonexistent at intermediate values of  $q^2$  ( $q^2 \approx 20$ ). Thus it is not completely fair to look at super high  $q^2$  without recognizing that  $\omega$  is necessarily very low.

At low  $\omega$  ( $\omega < 4$ ) and high  $q^2$ , the test of Bjorken scaling will have to be precise. There are no dramatic effects, such as a rise in  $\omega$ . The fairest statement that can be made from E-26 at this time is scaling is good (or bad, depending on your point of view!) to 30% up to  $q^2 = 60 \text{ GeV}^2/c^2$ . An attempt to fit the E-26 data/Monte-Carlo

to a propagator type of violation yield a value of the form:

$$\frac{\text{data}}{\text{MC}} = N \left(1 + \frac{q^2}{\Lambda^2}\right)^{-2} \quad \text{gives}$$

$$\frac{1}{\Lambda^2} = (11 \pm 5) \times 10^{-4} \text{ GeV}^{-2}$$

This corresponds to a mass of 25 to 30 GeV!

One may reflect that the mass keeps going up. It was 12 GeV about a year ago.<sup>6</sup> But we have learned more from our data. We cut at  $\omega < 9$  previously for this comparison; now we cut at  $\omega < 4$ . The  $\omega$  rise contribution from events between  $4 < \omega < 9$  is now removed.

We would like to cut even closer, say  $\omega < 2$ , the present sample data cannot yield good information due to:

1. The  $\omega$  resolution is poor at low  $\omega$ . As is seen in Figure 8, the resolution is ~50%! P-319 will do much better by means of a calorimeter.
2. More data are needed since  $\nu W_2$  varies as  $(\omega' - 1)^3$ . At small values of  $\omega$ , yields are low, and become lower as  $\omega' \rightarrow 1$ . P-319 is <sup>excellent</sup> since it gives more events near  $\omega' \approx 2$  at  $q^2 \sim 100-140$  than any apparatus.

#### D. Data/Data Comparisons

This basic method has two well known advantages; it is independent of what you take for  $\nu W_2$ , and it has reduced systematic uncertainties.

The data/data method worked very well in E-26. We note that the rise observed in data/data is diminished, indicating that part of the  $\nu W_2$  rise, if not all, is removed by the data/data ratio.

The scaled ratio of LARGE ANGLE data shows within our statistics that Bjorken scaling works well. Note that the 150 LA data corresponds to  $\sim 10^9$  incident muons (equivalent to  $\sim 1$  hour of data taking at  $2 \times 10^6$   $\mu$ /pulse). It is therefore somewhat low in statistical accuracy. The 56 LA data has better statistics, but suffers from having a smaller range of  $q^2$ .

Analysis on SMALL ANGLE data is currently being completed by all collaborators.

The initial running of E-26 is such that we did not have sufficient running time at 150 GeV (October, 1973) in the scaled configuration. We look forward to more data very soon.

### III. Objectives of Future Running

Guided by the trends in the data of E-26, we next consider P-319. In P-319 the large spark chambers upstream of the target have been removed, and the target itself is longer and closer to the toroids. A schematic layout is shown in Figure 1' .

The basic objectives of P-319 are:

1. Continued Use of the Scaling Technique for Further Exploration of the  $q^2$ - $\nu$  Plane.

Figures 4a and 4b show the detection efficiency and rate per  $10^{11}$  muons for the 240 GeV scaling configuration. As we have mentioned earlier, the values of  $\omega$  must also be kept in mind. Figures 5a and 5b show that we will be looking at very high  $q^2$  where  $\omega$  is low, at intermediate  $q^2$  where  $\omega$  is low, at intermediate  $q^2$  where  $\omega$  is moderate, and at modest  $q^2$  where  $\omega$  is very high. Figure 6 shows the total  $q^2$  rate for  $10^{11}$  muons.

2. Better  $\omega$  and  $\nu$  Resolution Due to a Target-Calorimeter.

Table I shows the formulae that apply when  $\nu$  and  $\omega$  are obtained from knowledge of the incident beam and either the scattered muon alone or the target calorimeter alone. Use of both pieces of information, of course, permits background rejection due to redundancy. However, it is apparent that the calorimeter is crucial to measurements of  $\nu W_2$  at very low  $\omega$ . Some details on the assembly of the arrangement have been given elsewhere. <sup>12</sup>

3. Reduced Systematic Uncertainty in Energy and Acceptance as a Result of More Extensive Calibration Running

Once the apparatus is assembled in a particular configuration, it is possible to calibrate the energy and acceptance by running with a small toroid in place of the target. The incident beam energy can be varied over the entire momentum range of the spectrometer, and one can compare the deduced energy spectrum with that obtained from a knowledge of the muon beam line. This was, in E-26, a check on the alignment constants for the spark chambers. The symmetry of the apparatus was crucial to the many checks made. One can also check the energy loss by closing the shutter in E-98's muon identifier. Again, the techniques here were established in E-26; and one merely intends to fully exploit them.

4. Preliminary Trigger Studies Related to MultimMuon Production and Heavy Lepton Searches

We are very interested in pursuing the physics that can be done in second generation muon experiments at high beam intensities. The idea behind it all is well known:<sup>13</sup> if one is interested in reactions where one only studies the initial-state and final-state muons, then one can use long, heavy targets in a muon beam, gaining factors of  $\approx 10^3$  in the number of target nucleons. The physics of two such endeavors has been outlined in proposals 225 and 368. It is possible to do preliminary trigger studies for such endeavors by connecting up separate logic that can be used

in OR with the E-26 triggering. We plan to look at several rates, including those involving no beam veto counters in the spectrometer; multimMuon events; and large and small pulse heights in the calorimeter.

#### IV. Conclusions

Our basic conclusions are that P-319 will take us well beyond E-26. The systematic and statistical uncertainties will be reduced. The data will span a larger kinematical region. The resolution in  $\nu$  and  $\omega$  will be better. We will have better halo rejection and will be capable of running at high rates. In the region  $\omega < 5$ , we will be able to sense Bjorken scaling breakdowns of  $\Lambda = 33$  GeV.

A new objective dictated by the E-26 data is to resolve questions regarding the observed  $\omega$  rise in the moderate  $q^2$  range. This is a key question requiring clarification. There is a possibility we are looking at a particle production phenomenon.

Footnotes and References

1. R. P. Feynman, Photon-Hadron Interactions, W. A. Benjamin, Inc. (197
2. D. J. Gross and F. Wilczek, Phys. Rev. D 9, p. 980 (1974).
3. G. Tarnopolsky et al., Phys. Rev. Letters 32, p. 432 (1974); and references therein.
4. S. D. Drell and T. M. Yan, Annals of Physics 66, p. 578 (1971).
5. J. Christenson et al., Phys. Rev. D 8, p. 2016 (1973).  
F. W. Büsler et al., Physics Letters 48B, p. 377 (1974).
6. K. W. Chen, Invited Talk at the Chicago APS Meeting, February 1974. The curve presented at the talk corresponds to Figure 2g of D. J. Fox et al., "Early Tests of Scale Invariance in High-Energy Muon Scattering", Phys. Rev. Letters 33, p. 1504 (1974).
7. J. J. Aubert et al., Phys. Rev. Letters 33, p. 1404 (1974).
8. J. E. Augustin et al., Phys. Rev. Letters 33, p. 1406 (1974); and p. 1453 (1974).
9. For suggestions of trends in the SLAC ep data, see (for low  $\omega$ ) A. Bodek et al., "Observed Deviations From Scaling of the Electromagnetic Structure Functions", SLAC-PUB-1442 (June 1974). For the high  $\omega$  region see: E. M. Riordan et al., Phys. Rev. Letters 33, p. 561 (1974).
10. A. Bodek, thesis, MIT Report C00-3069-116
11. H. T. Nieh, T. T. Wu, and C. N. Yang, Phys. Rev. Letters 34, p. 49 (1975).
12. K. W. Chen and L. Litt, Group Memo (August 1974). We have estimated our calorimeter resolution using the 2"-plate curves from S. Mori, J. Pine, and J. Scheid, FNAL-TM-479/2050 (unpublished, March 1974). We have also consulted J. Engler et al., Nucl. Inst. & Methods 106 (1973), p. 189; and, B. C. Barish et al., Nucl. Inst. & Methods 116 (1974), p. 413.
13. See for example, L. M. Lederman and M. J. Tannenbaum, "High Energy Muon Scattering", Advances in Particle Physics (edited by R. L. Cool), 1972.

See also, C. Carimalo et al., Phys. Rev. D 10, p. 1561 (1974).

List of Tables

- I. Formulae Relevant to the Calorimeter's Role  
in  $\omega$  and  $\nu$  Resolution.
- II. Systematic Uncertainties in P319
- III. Summary of Desired Improvements Over E26

## TABLE I.

FORMULAE FOR CALORIMETER  
RESOLUTION $E_0 =$  incident energy

$$\nu = \frac{k \cdot p}{m} \quad \omega = \frac{2m\nu}{Q^2}$$

$$\frac{\Delta(\nu/E')}{(\nu/E')} = c$$

$$y = \frac{\nu}{E_0}$$

- 1)  $\frac{\Delta\nu}{\nu} = c \left[ \frac{1-y}{y} \right]$  No Fermi Motion.  
 $\nu$  obtained from  $E'$
- 2)  $\frac{\Delta\nu}{\nu} = \left\{ \left( c \left[ \frac{1-y}{y} \right] \right)^2 + (.12)^2 \right\}^{1/2}$  Fermi Motion  
 $\nu$  obtained from  $E'$
- 3)  $\frac{\Delta\omega}{\omega} = \frac{c}{y}$  No Fermi Motion,  $\omega$  obtained from  $E'$
- 4)  $\frac{\Delta\omega}{\omega} = \frac{\Delta\nu}{\nu} \frac{1}{1-y}$  No Fermi Motion,  $\omega$  obtained  
by estimating  $\nu$  from calorimeter
- 5)  $\frac{\Delta\omega}{\omega} = \left\{ \left( \frac{\Delta\nu}{\nu} \right)^2 + (.12)^2 \right\}^{1/2} \left( \frac{1}{1-y} \right)$  Fermi-Motion,  $\nu$   
obtained from calorimeter

Table II. Systematic Uncertainties in P319. Given in Units  
of  $\pm 10^4 / \Lambda^2$

	Data/Data	Data/Monte-Carlo	Assumed Accuracy
Incident Energy	5	7	0.5%
B-Field	4	8	1.0%
Field Shape	--	4	0.5%
Degaussed Magnet	4	4	100 gauss
Chamber Inefficiency	1	2	5% radial dep.
dE/dx	3	6	Measure it to 5%
Halo Contamination	.5	1	2% at low $Q^2$
Misalignment	1	1	
Different R	0-4	4	Variation from .18 less than $.52M^2/Q^2$
TOTAL	$\pm 9$	$\pm 14$	

$$\Lambda = 33 \text{ GeV} \quad \Lambda = 27 \text{ GeV}$$

TABLE III

DESIRABLE FEATURES OF A IMPROVED E-26 APPARATUS (THIS PROPOSAL)  
 (AS SUGGESTED BY THE TREND OF DATA IN E-26)

1. SMALLER AND UNDERSTANDABLE SYSTEMATIC ERRORS
2. IMPROVED CHAMBER EFFICIENCIES BY REDUNDANT USE OF CHAMBERS ESPECIALLY THOSE IN THE MAGNET.
3. REDUNDANT AND UNIFORM MEASUREMENT OF  $\nu$  : INCORPORATION OF CALORIMETRY.
4. REDUNDANT INFORMATION DOWNSTREAM OF THE TARGET: USE OF WIRE-PROPORTIONAL CHAMBERS.
5. INCREASED MATERIAL USED IN THE HADRON SHIELD DOWN STREAM OF THE TARGET.
6. IMPROVED HALO REJECTION BY FINER HODOSCOPE BINNING. AS A SUGGESTION TO MUON BEAM DESIGNERS, USE HERB ANDERSON'S HALO SPOILERS.
7. DESIRABLE TO USE E98 BEAM PWC AND HODOSCOPE ARRANGEMENT IF THEY ARE CONSIDERED AS A FACILITY. IF NOT, SOME IMPROVEMENT ON E26 BEAM TRIGGER DETECTION ASSEMBLY.

THE ABOVE MENTIONED SYSTEM WILL WORK PERFECTLY WELL AT 240 GeV AT MUON INTENSITY IN EXCESS OF  $10^6$  MUONS. TIME SCALE FOR THESE IMPROVEMENT IS SIX MONTHS OR LESS.

FURTHER IMPROVEMENTS FOR E-319  $+ e$  :

1. ADD DRIFT CHAMBERS a LA RUBBIA.
2. REPLACE PRESENT TOROIDS WITH LARGER TOROIDS

## List of Figures

## I. Figures Relevant to Proposal 319

1. Schematic Layout of the Apparatus.
2. Schematic of a Toroid
3. Kinematic Ranges in the  $Q^2-\nu$  Plane.
4. a) Detection Efficiency in the  $Q^2-\nu$  Plane.  
b) Accepted Events in the  $Q^2-\nu$  Plane.
5. a) Rates per  $10^{11}$  Muons in the  $Q^2-\omega$  Plane (Region I)  
b) Rates per  $10^{11}$  Muons in the  $Q^2-\omega$  Plane (Region II)
6. Rates Beyond a Given  $Q^2$  in P319
7.  $\Delta\nu/\nu$  Resolution
8.  $\frac{\Delta\omega}{\omega}$  Resolution

## II. Preliminary Analyses From E26

9. a) Data/Monte-Carlo vs  $\omega$  (all  $Q^2$ )  
b) Data/Monte-Carlo vs  $\omega$  ( $Q^2$  bins)
  10. Long Target Data
  11. (Data/Monte-Carlo) vs. Missing Mass. 150 GeV, Small Angle Data. 30 GeV Energy Cut in Analysis.
  12. (Data/Monte-Carlo) vs. Missing Mass. 150 GeV, Small Angle and Large Angle Data. 30 GeV Energy Cut in the Analysis
  13. (Yield minus Scaling Prediction) vs. Missing Mass. 150 GeV Data. 30 GeV Energy Cuts.
  14. Data/Monte-Carlo Results in the  $Q^2-\nu$  Plane.
-

# SCALED CONFIGURATION FOR P319

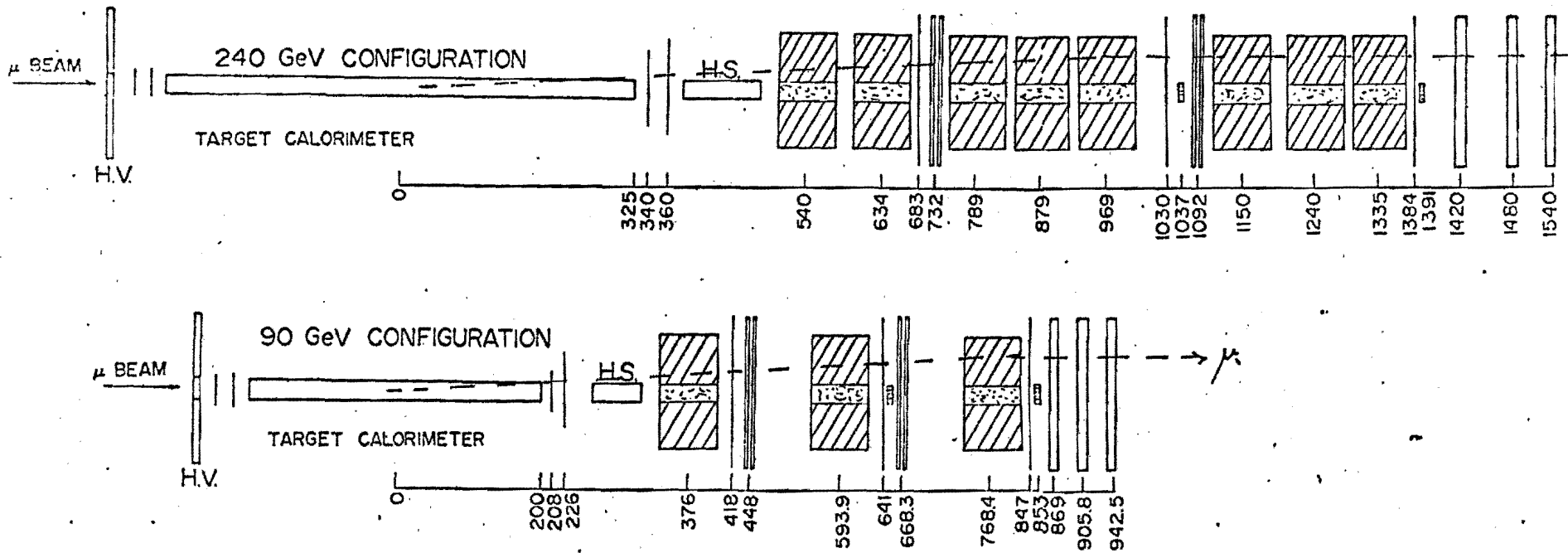
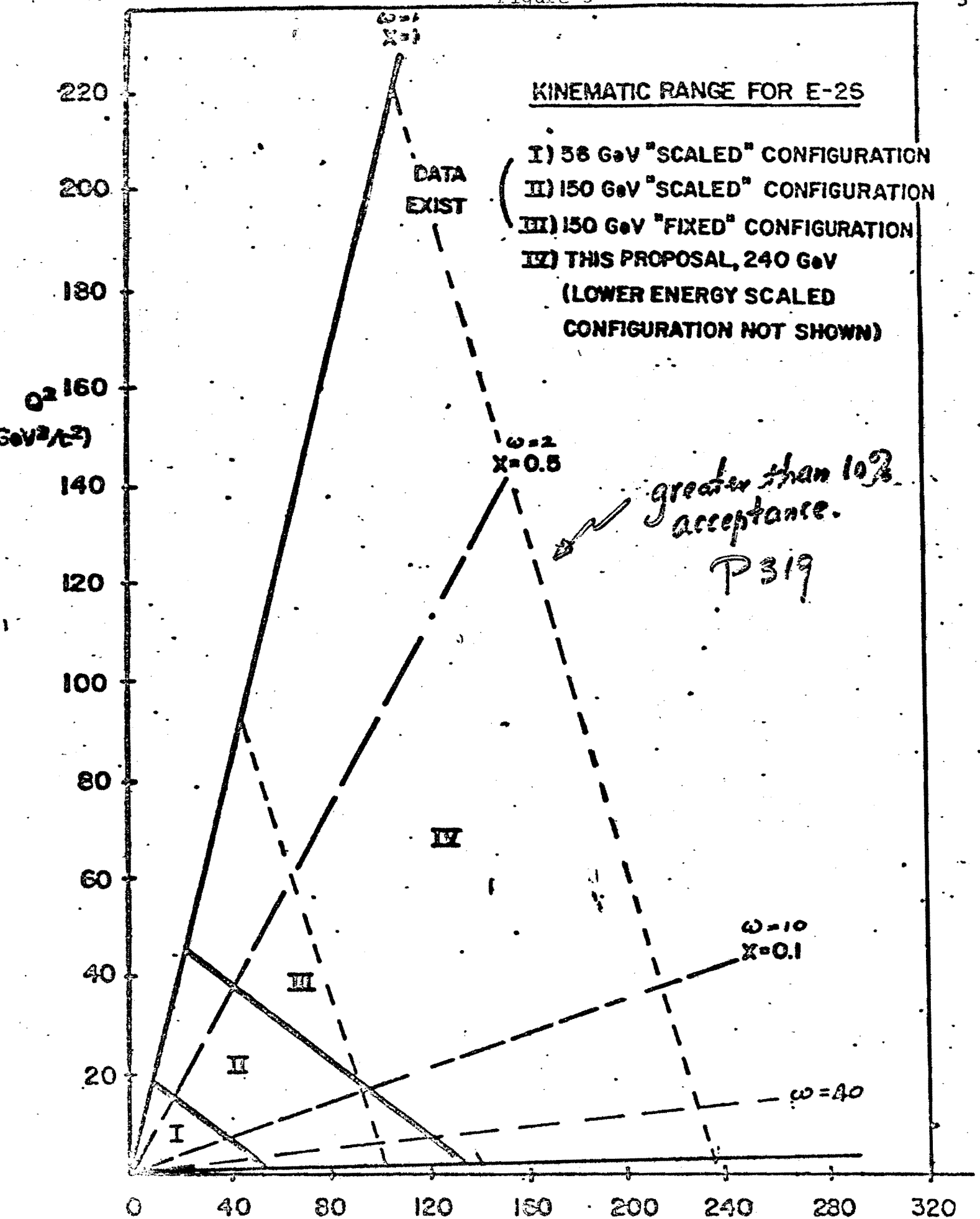


Figure 1

→ μ BEAM  
 4T





## DETECTION EFFICIENCY (%)

200								13	7	5						
190								18	11	14	3	1	1			
180								17	22	24	6	15	8	1	1	1
170								58	14	22	24	5	10	6	1	1
160								17	14	28	18	14	15	8	4	1
150								66	22	16	28	39	26	26	8	12
140								34	42	41	51	56	30	37	20	10
130								59	30	31	50	48	52	56	34	22
120								42	45	51	57	73	64	54	44	42
110								65	41	41	66	85	69	72	67	79
100								24	42	53	52	79	75	67	81	83
90								74	30	37	54	76	75	84	86	89
80								17	30	56	59	84	75	89	94	99
70								36	39	50	69	78	63	73	79	87
60								28	45	65	58	59	66	77	78	84
50								28	45	65	58	59	66	77	78	84
	40	60	80	100	120	140	160	180	200							

) (GeV)

Figure 4a

180		10	31	16		
160	10	42	78	104		
140	10	83	411	400	68	
120	83	796	1,227	1,430	312	
100	270	1,092	3,255	3,702	1,508	
80	1,596	4,176	8,887	9,852	5,470	
60	6,542	17,238	25,116	23,654	17,243	
40	22,594	68,120	77,600	62,514	51,194	
20	23,561	103,100	104,733	95,378	122,788	
0						
	0	40	80	120	160	200

$Q^2$   
(GeV/c)<sup>2</sup>

$\nu$  (GeV)

NO. OF EVENTS ACCEPTED BY APPARATUS  
10<sup>11</sup> INCIDENT MUONS

Figure 4b

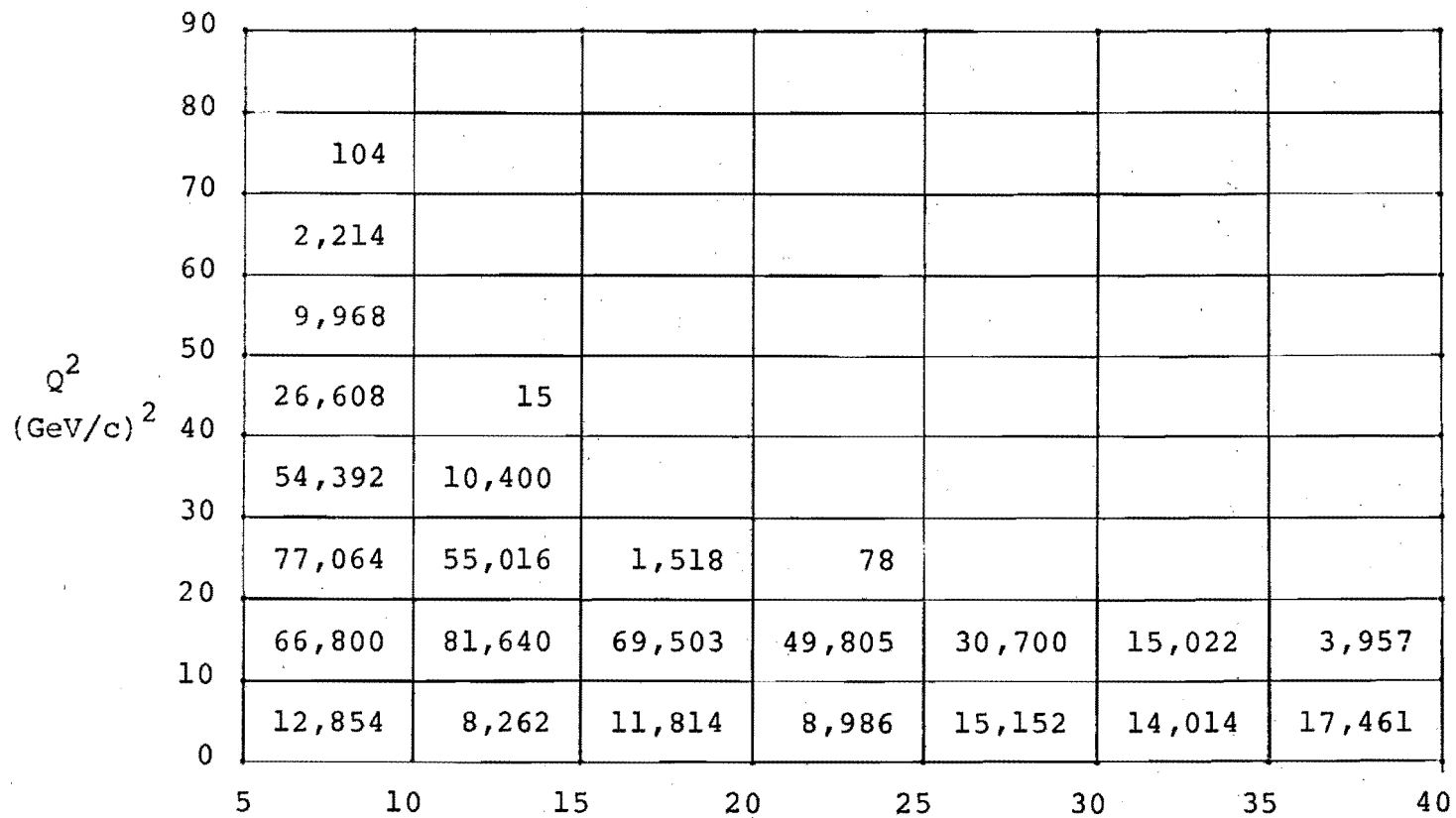
11  
NO. OF EVENTS / 10 MUONS

200		5									
180		26	36	21							
160											
140	10	36	99	114	10						
120	5	62	224	458	234	42					
100	47	177	484	941	1113	640	166				
80	114	312	588	1264	2096	2307	1877	1019	302	31	
60	484	712	1258	2408	3344	4051	4779	4347	3561	2751	
40	1082	1643	3484	4472	4852	6391	8122	7894	9058	7779	
20	1799	3271	3822	3936	7852	8450	10603	11534	15012	15038	
	0.0	0.5	1.0	1.5	2.0	2.5	3.0	3.5	4.0	4.5	5.0

ω

Figure 5a

NO. OF EVENTS /  $10^{11}$  MUONS



ω

Figure 5b.

Figure 6

# NUMBER OF EVENTS HIGHER THAN $Q^2$ FOR 10" INCIDENT MUONS

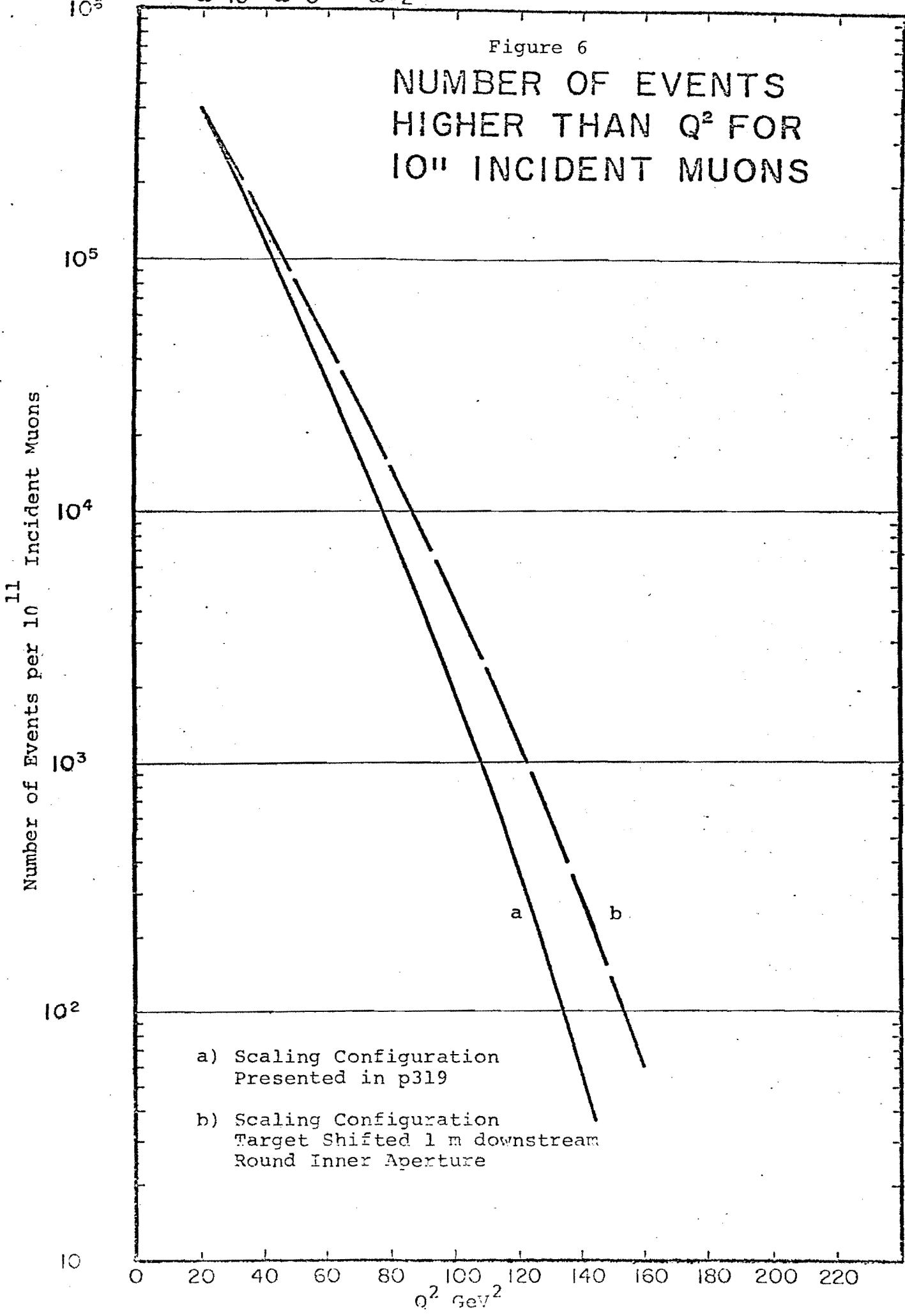
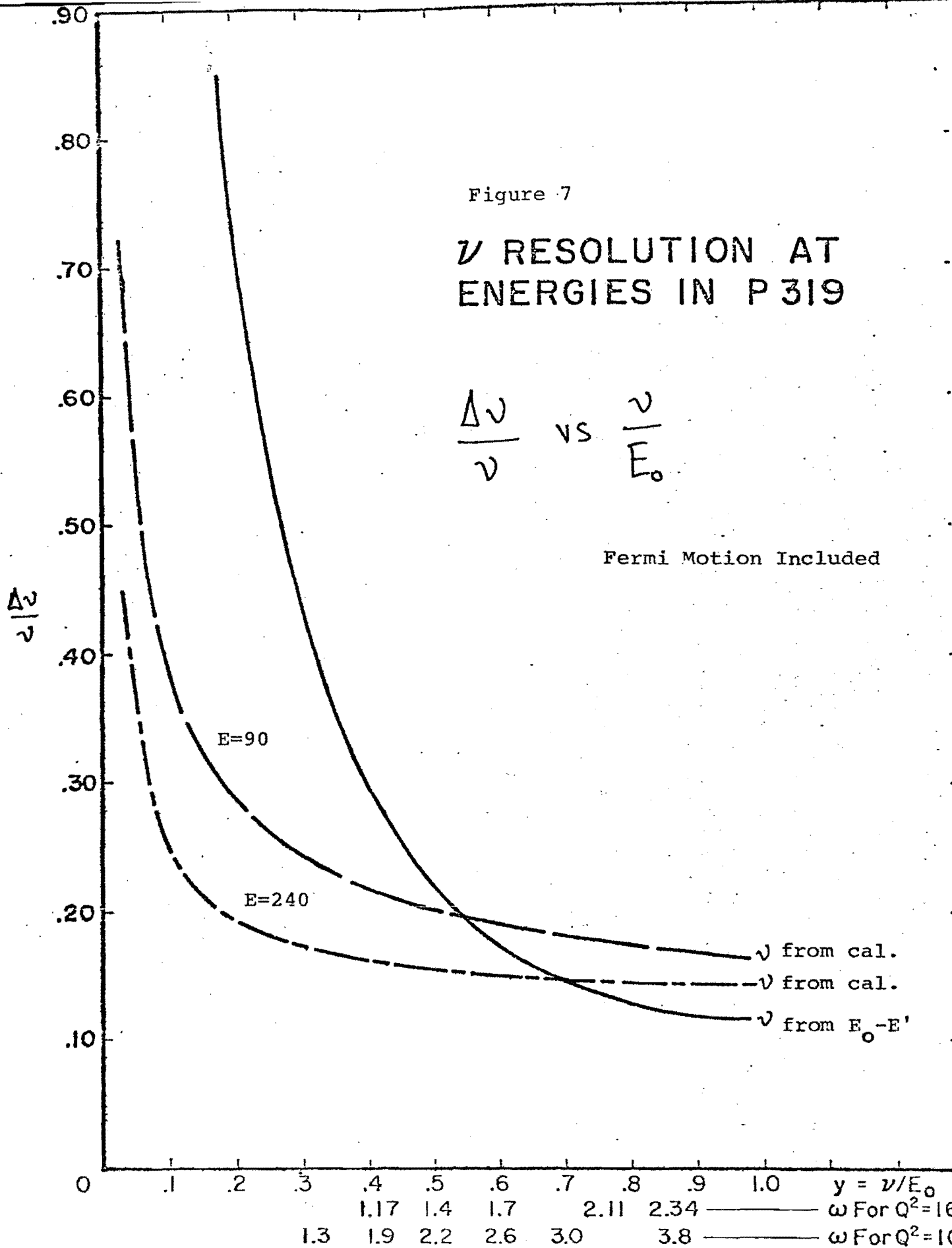


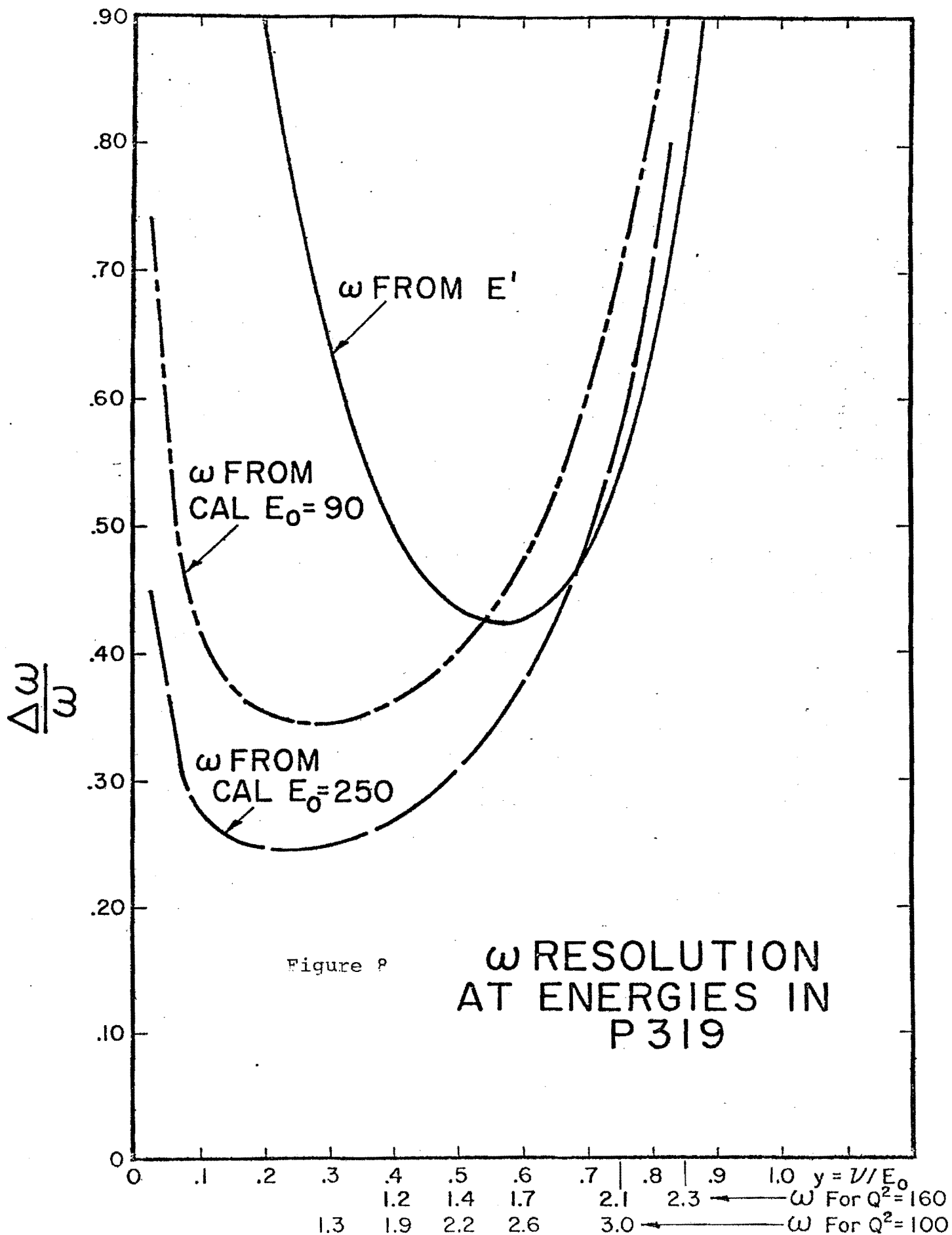
Figure 7

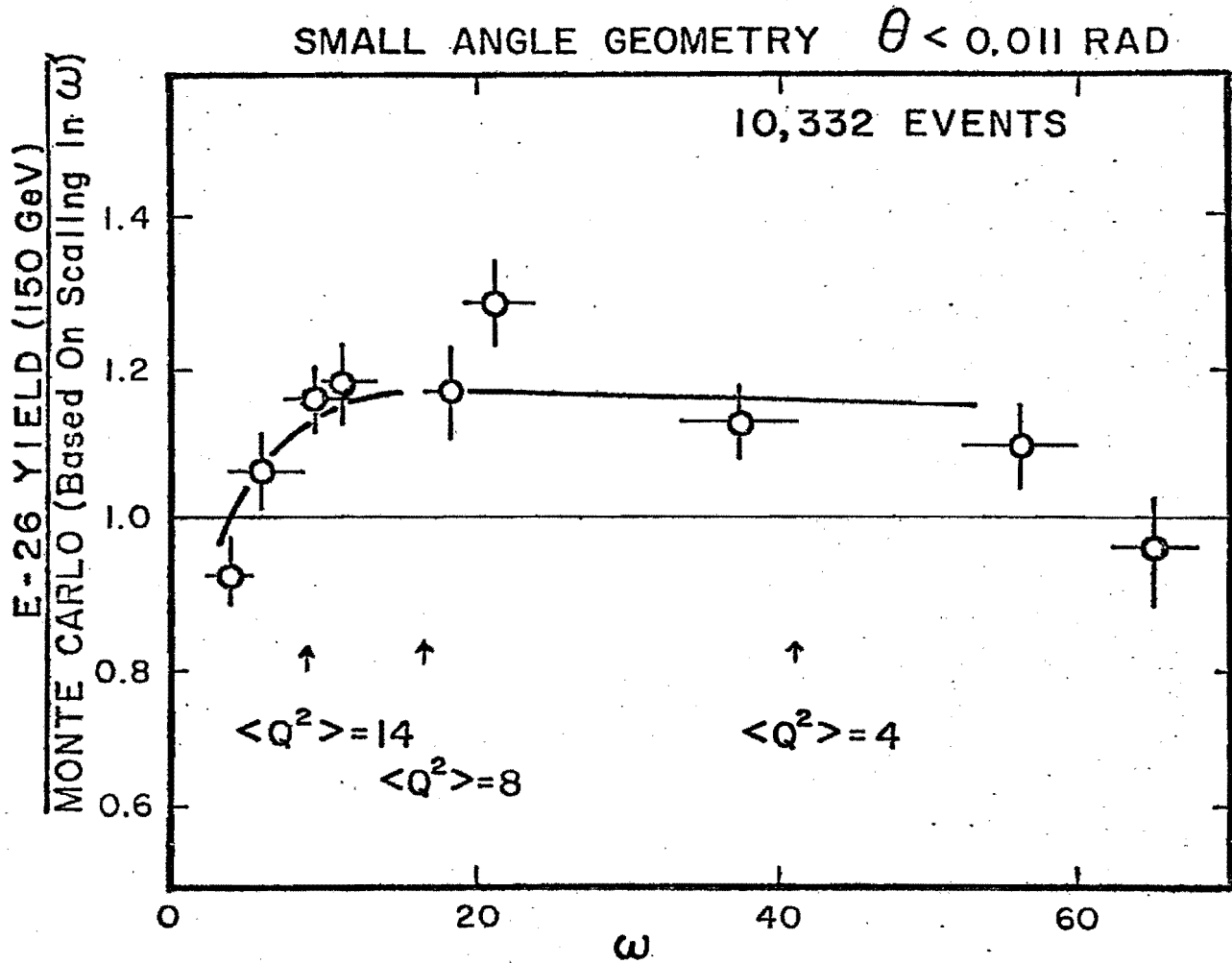
# $\nu$ RESOLUTION AT ENERGIES IN P 319

$$\frac{\Delta\nu}{\nu} \text{ vs } \frac{\nu}{E_0}$$

Fermi Motion Included







DATA / MONTE CARLO vs  $\omega$

Figure 9a

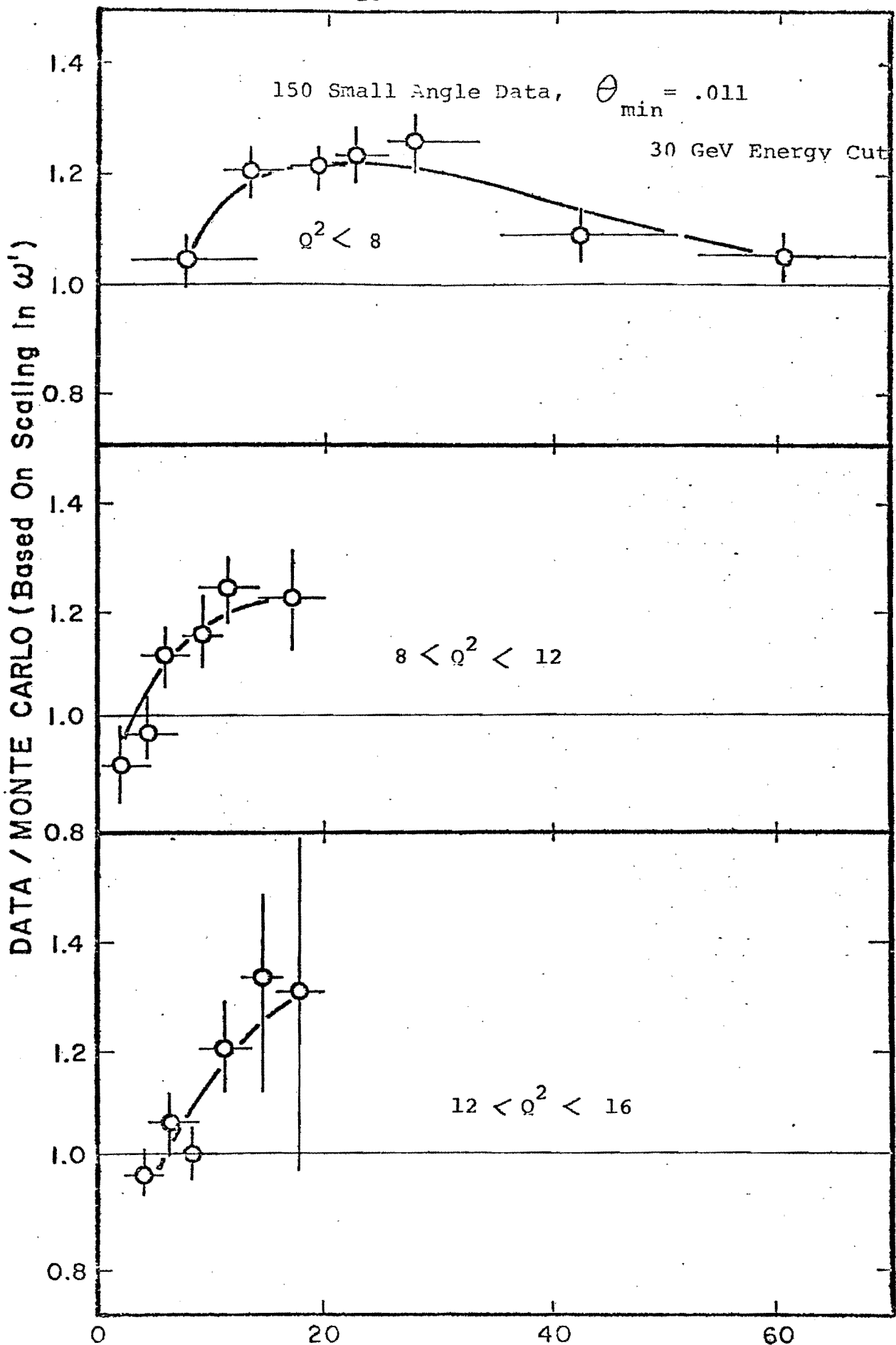
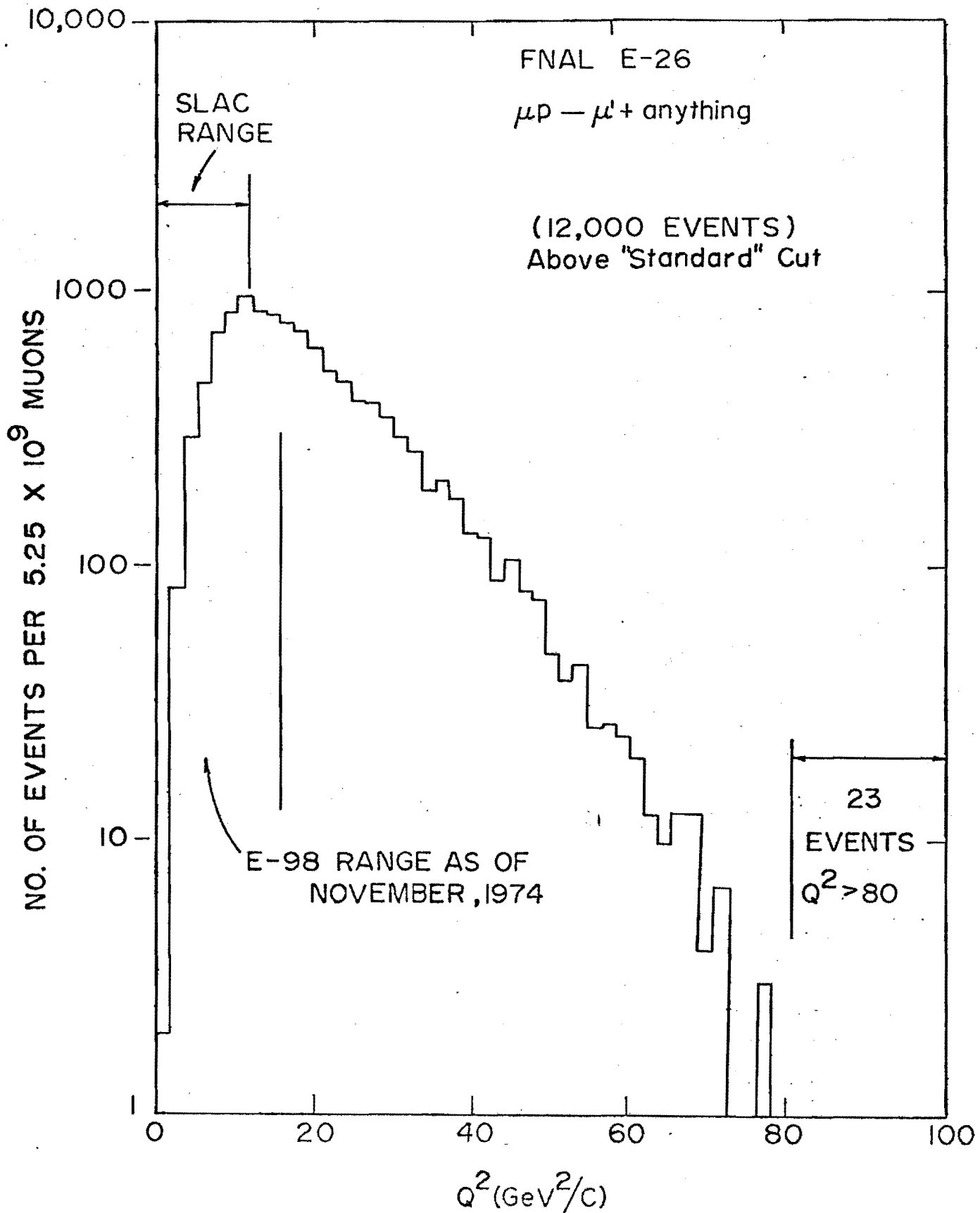


Figure 9b DATA / MONTE CARLO vs  $\omega$   
The curves shown are not fits. They are drawn to guide the eye.

Figure 10.

## "LT" DATA



RATIO OF YIELD (DATA/MONTE CARLO)

DATA  
MONTE CARLO (SA)

$\mu p \rightarrow \mu^+ \text{ ANYTHING}$

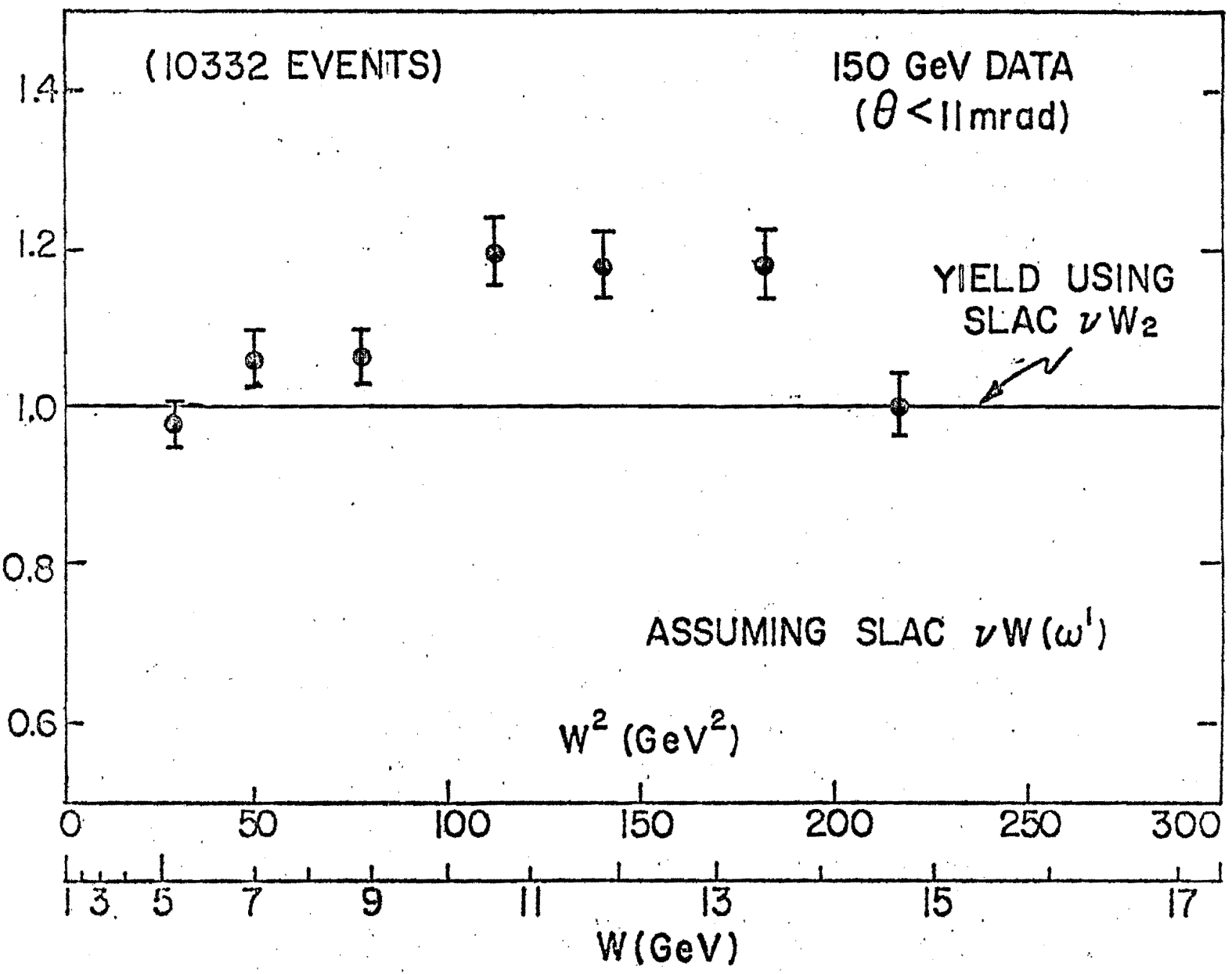


Figure 11.

MISSING MASS

DATA  
 MONTE CARLO BASED ON SCALING IN W

exp → μ ANYTHING

○ SA (10332)  
 ○ LA (3691)

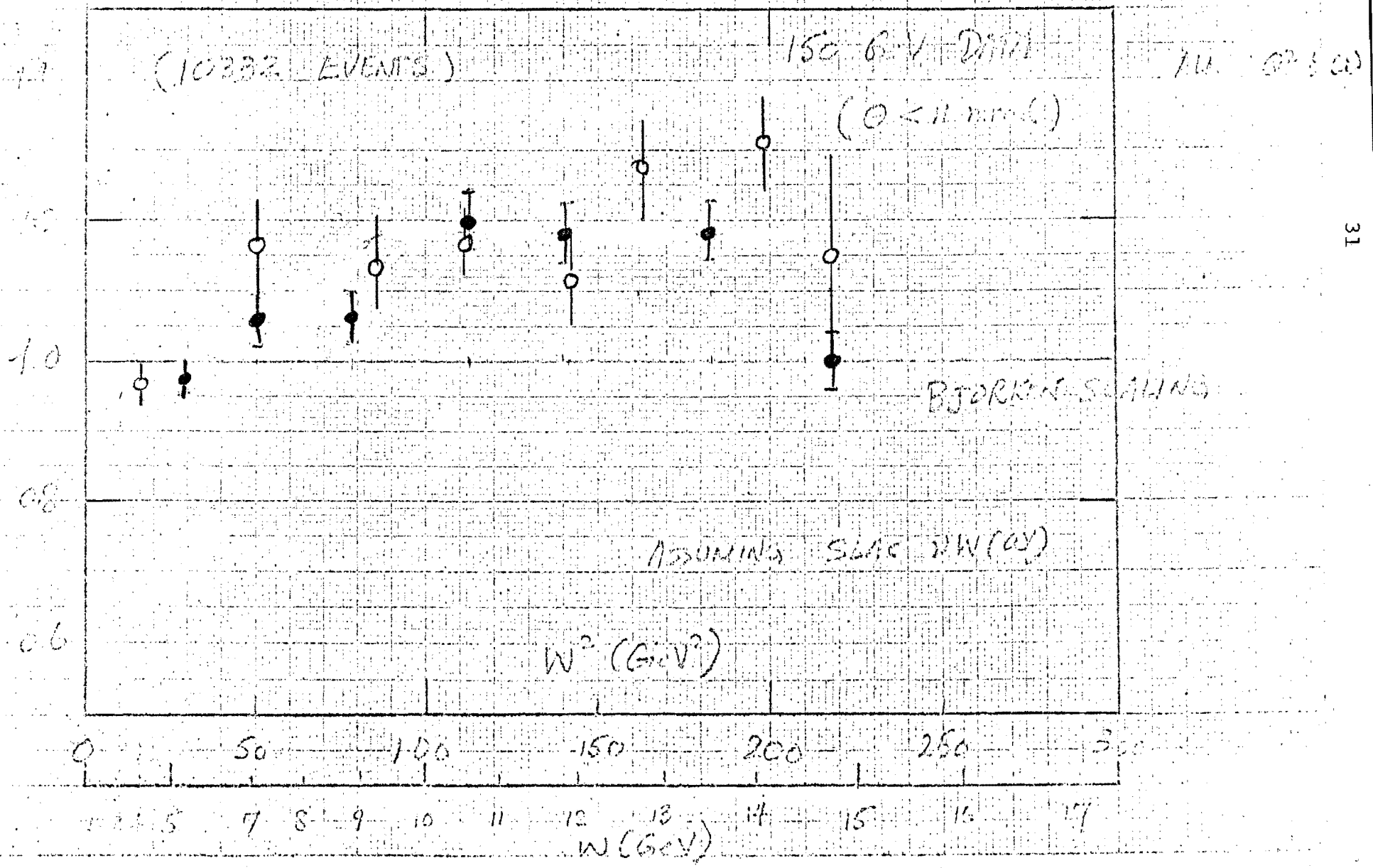


Figure 12

PRELIMINARY!

Figure 13.

YIELD OF EVENTS AFTER  
SUBTRACTING DEEP IN-  
ELASTIC CONTRIBUTION  
(BASED ON SLAC  $\nu W_2(\omega')$ )  
SMALL ANGLE DATA  
 $\theta_{MIN} < 0.011 \text{ RAD}$

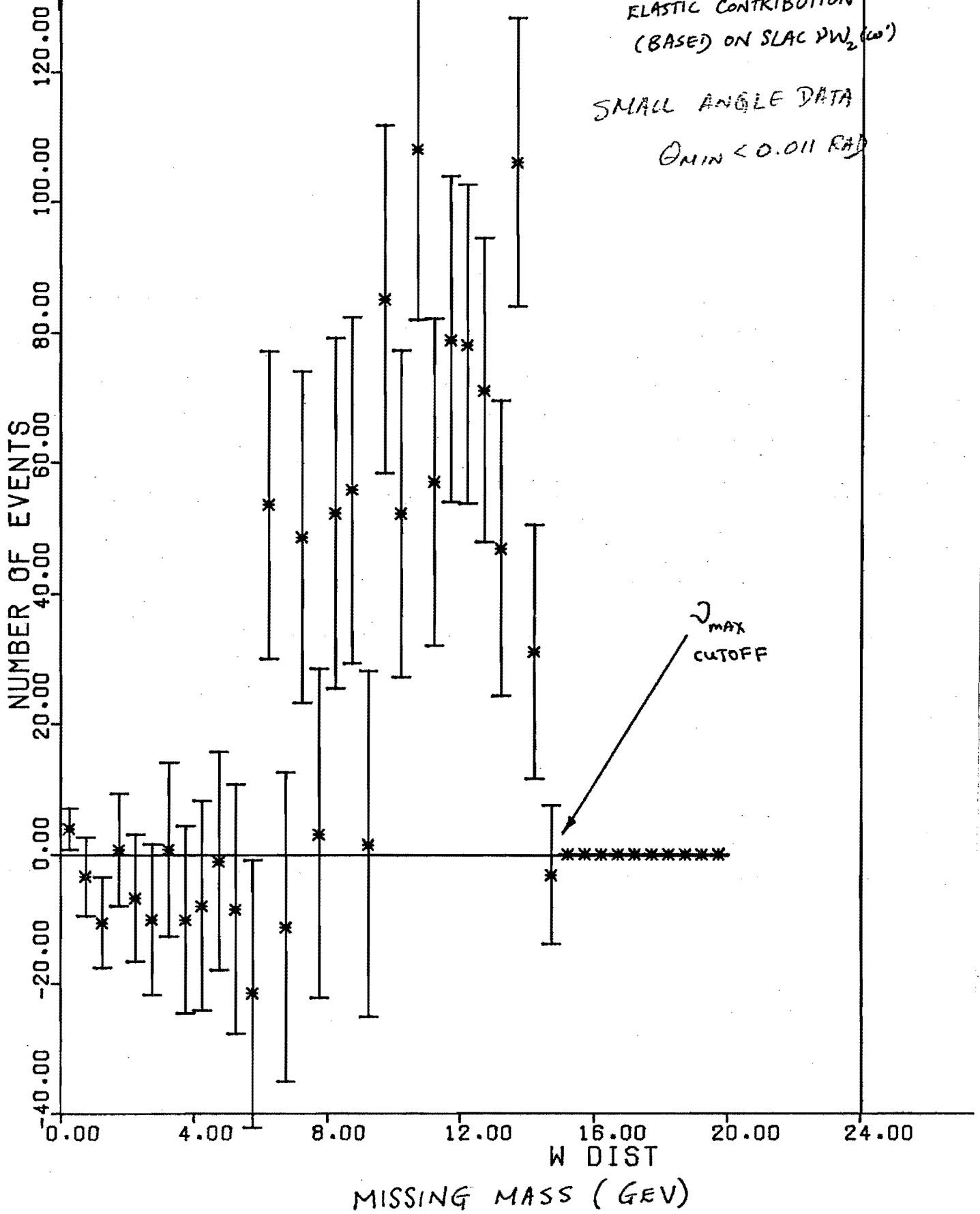


Figure 14.

RATIO OF DATA / MONTE CARLO (BASED ON SCALING IN  $\omega'$ )

SMALL ANGLE (SA) \*

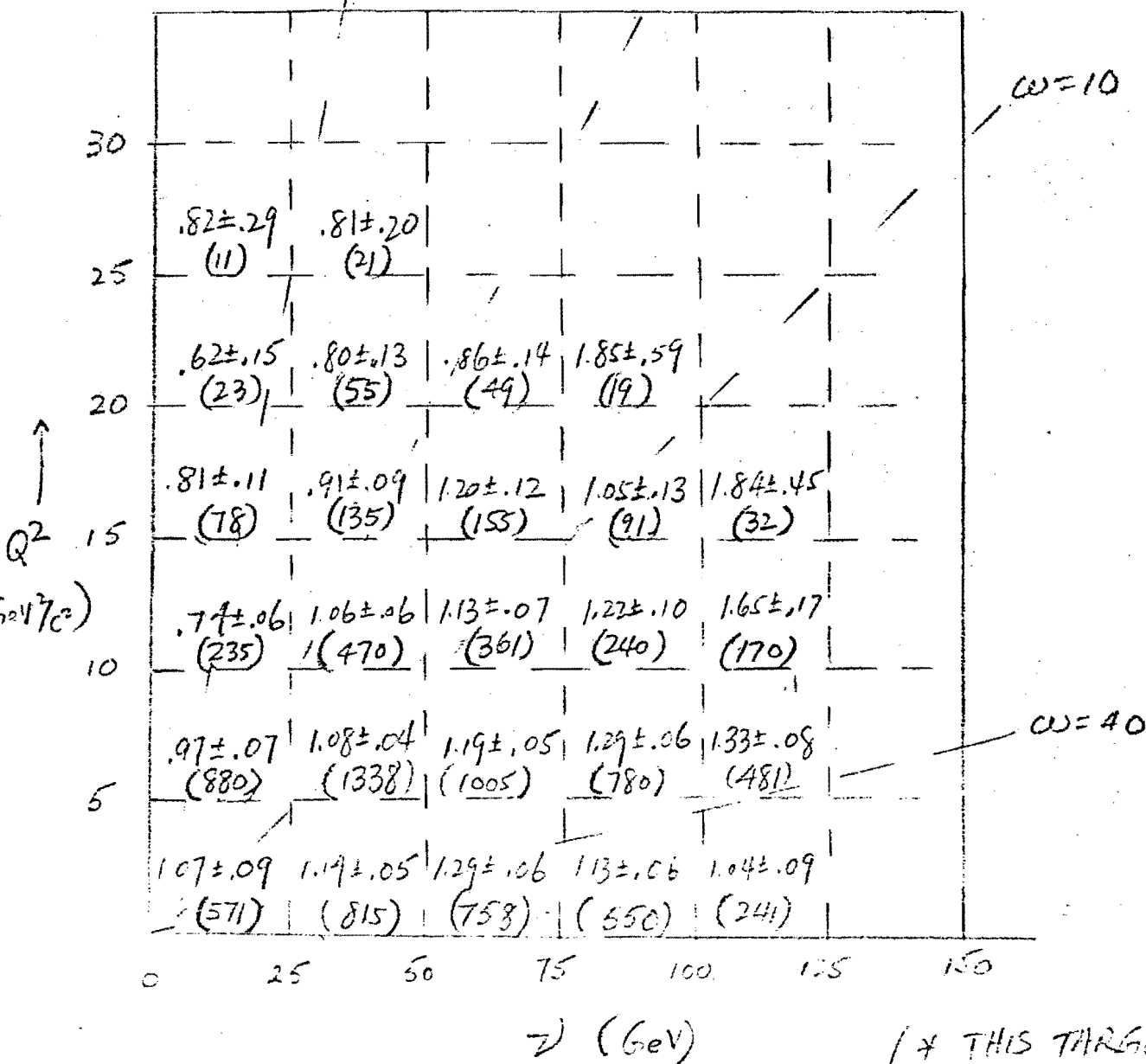
$\theta_{\text{Min}} < 0.011 \text{ RAD.}$

(THIS DATA STILL SUBJECT TO +5% TO +10% CORRECTION IN  
ABSOLUTE NORMALIZATION)

$\omega = 2$

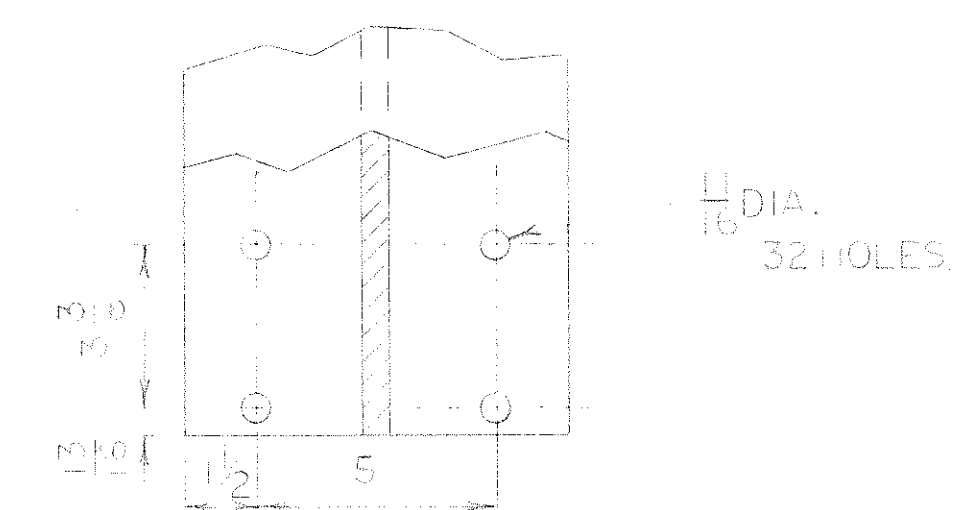
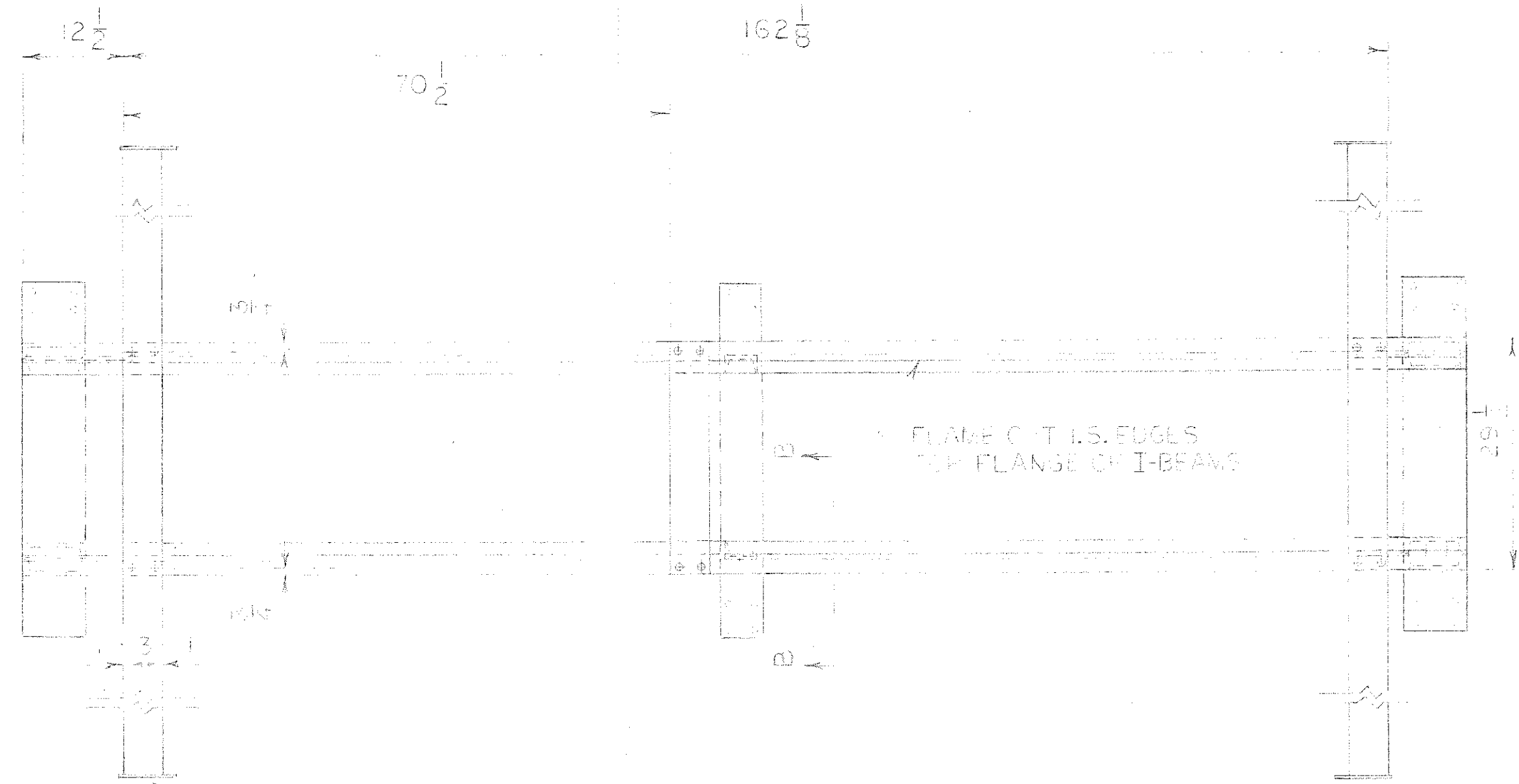
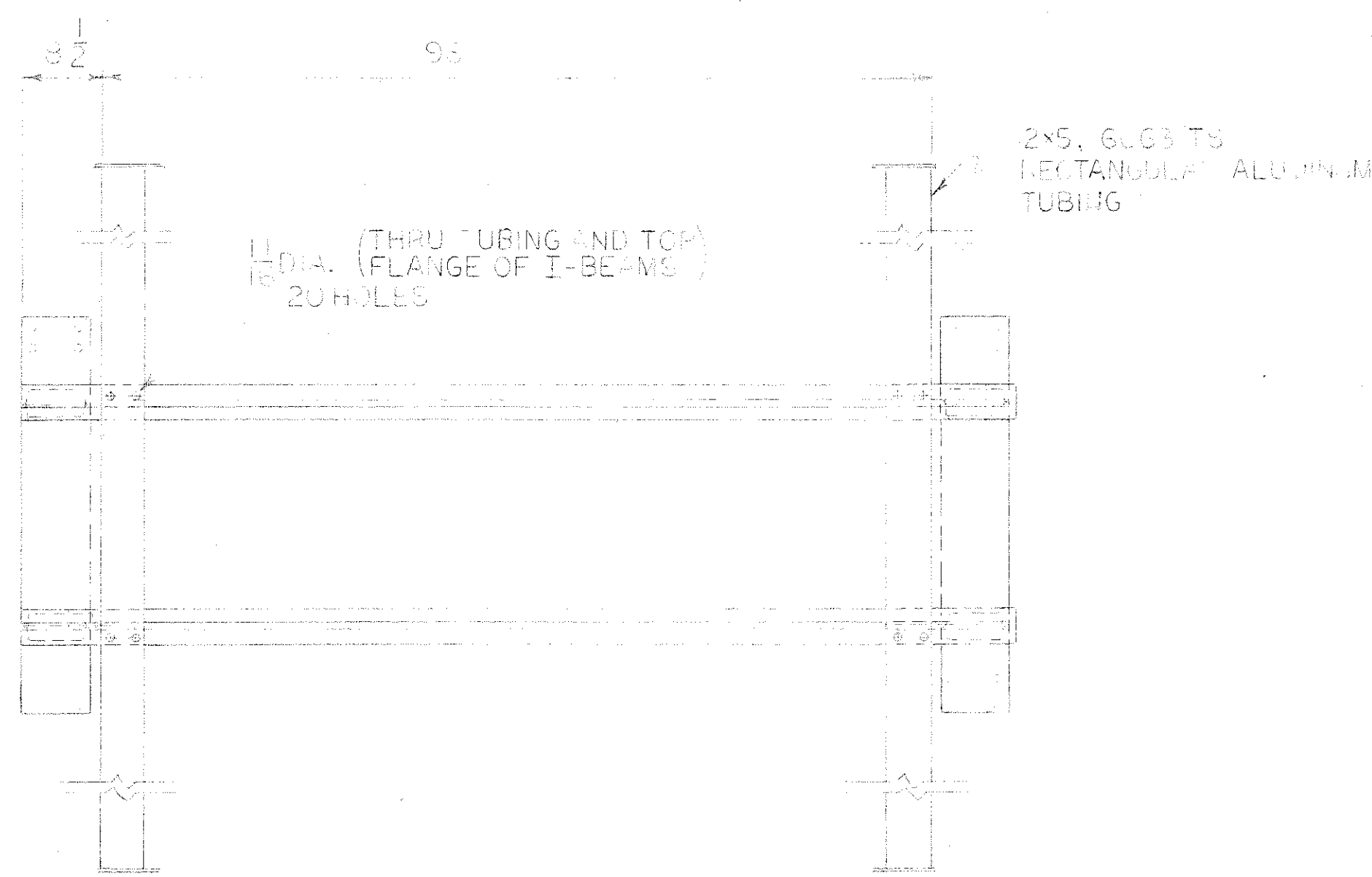
$\omega = 5$

$\omega = 10$

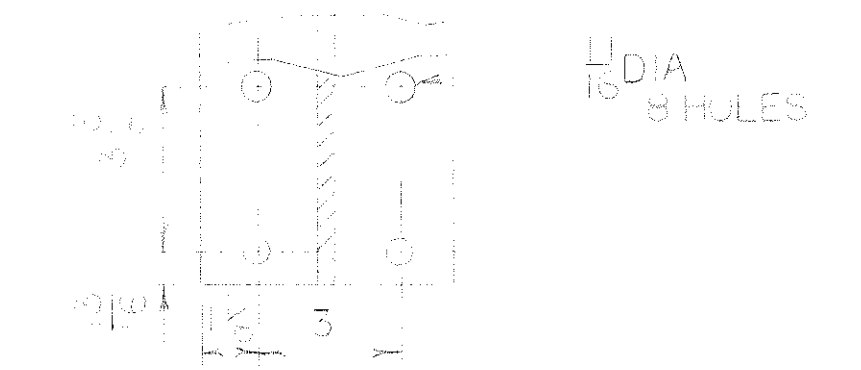


(No of events  
in data)

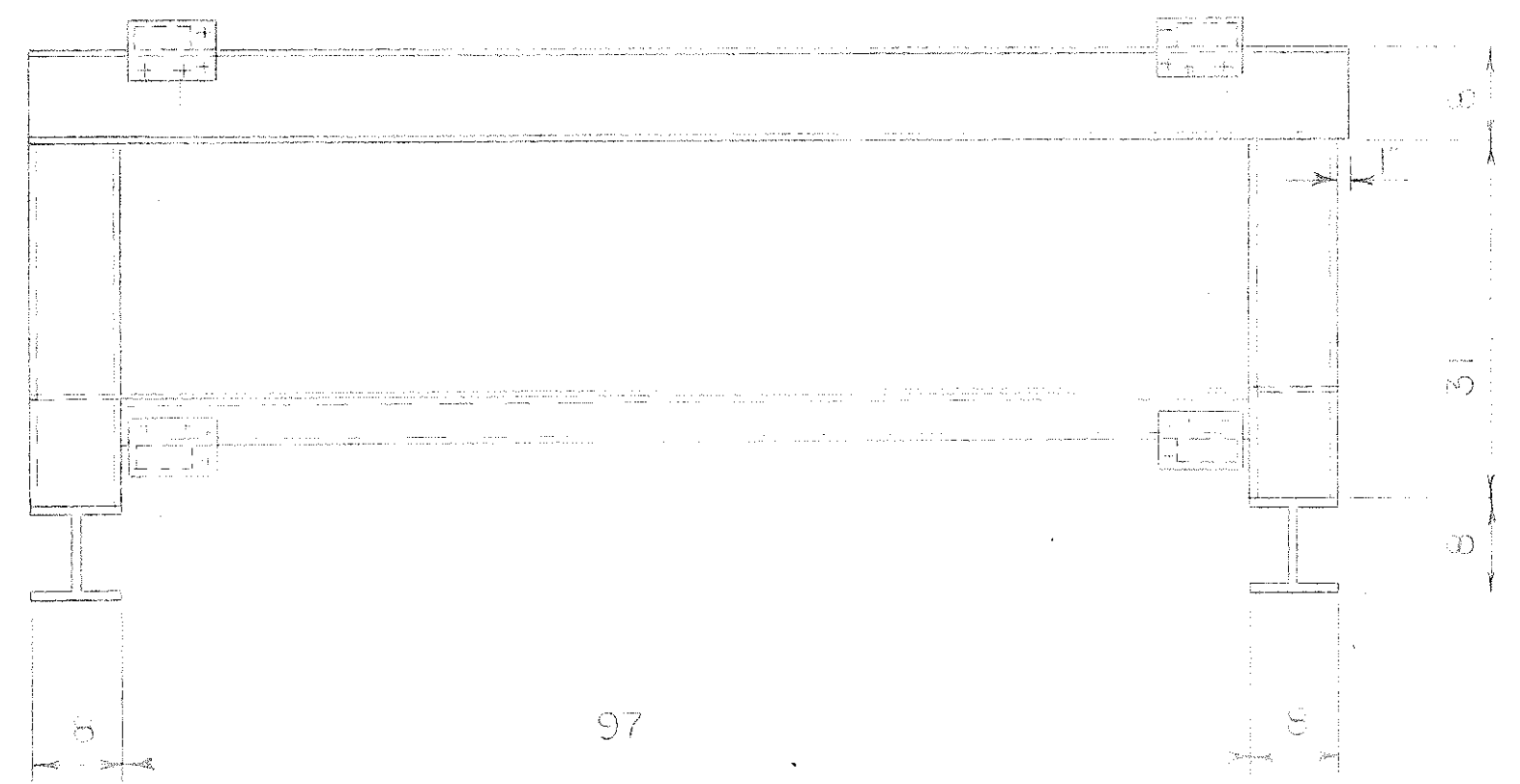
(\* THIS TARGET POSITION  
FAVORS LOW  $Q^2$  HIGH  
 $\omega$ .)



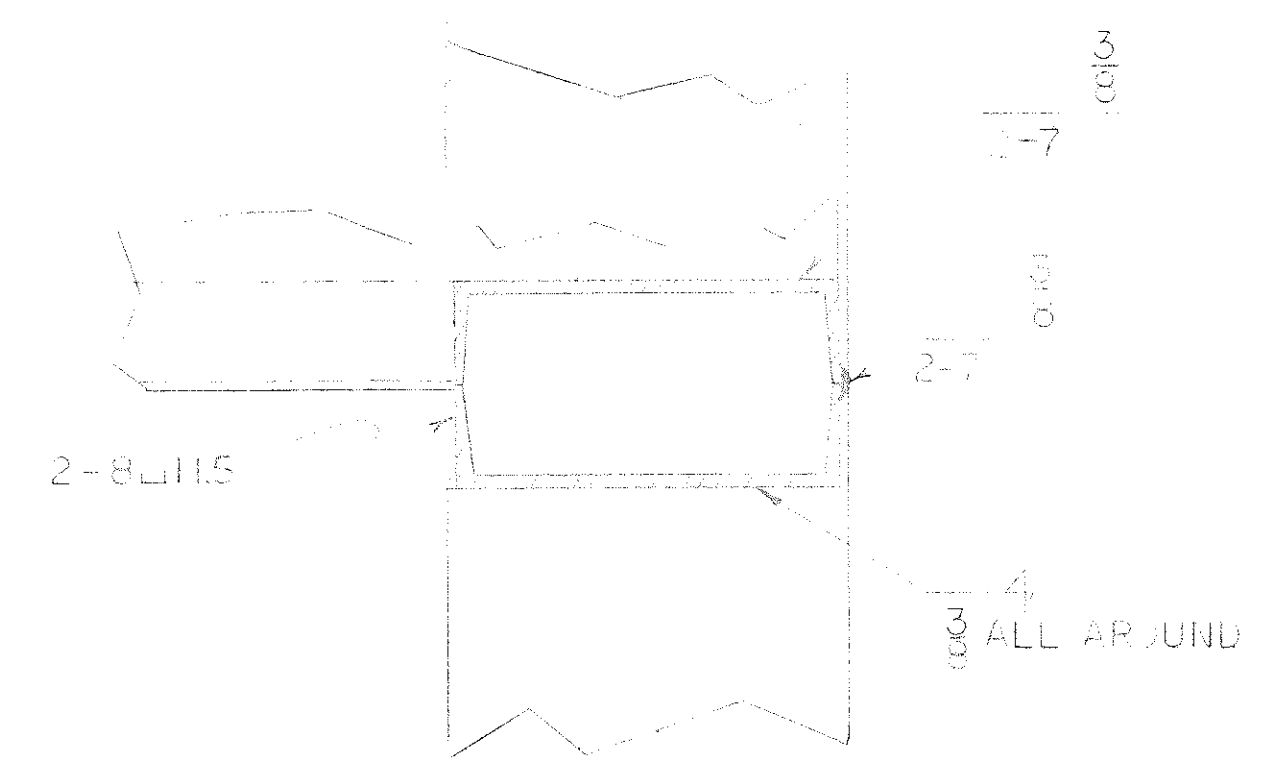
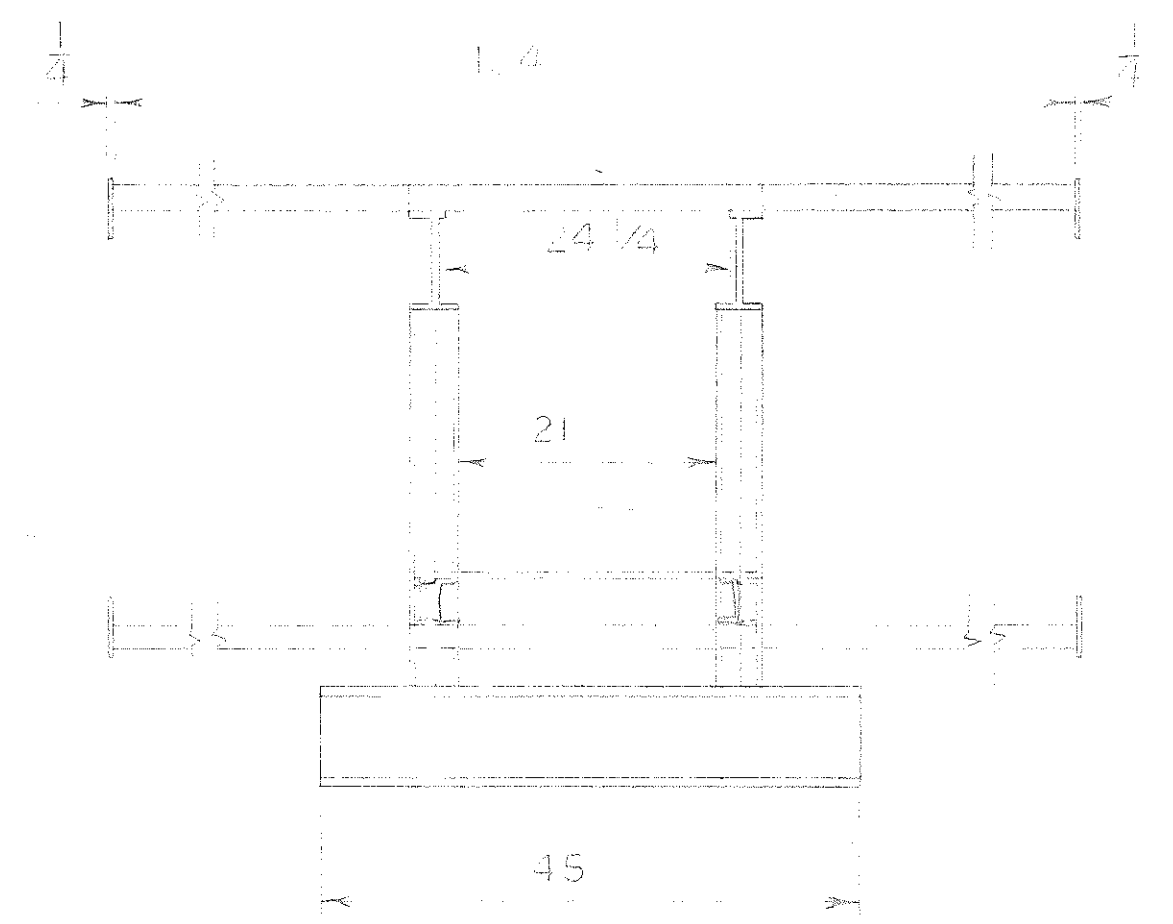
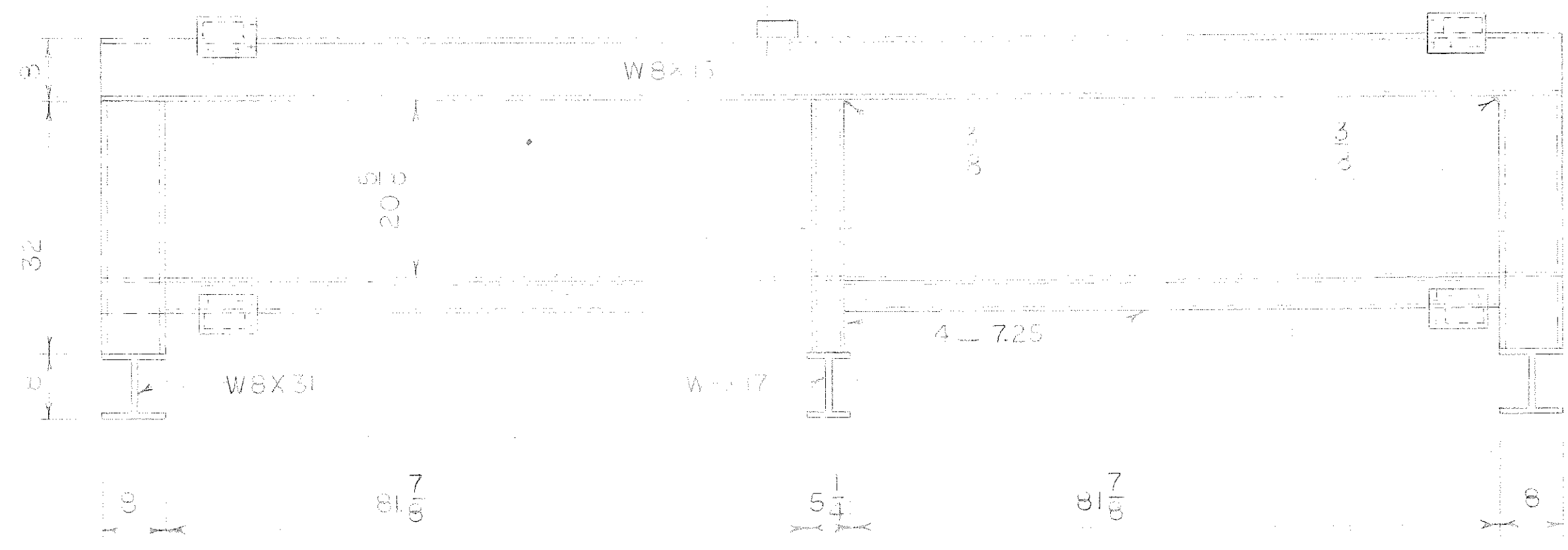
HOLE DETAIL FOR W8x31 BEAMS



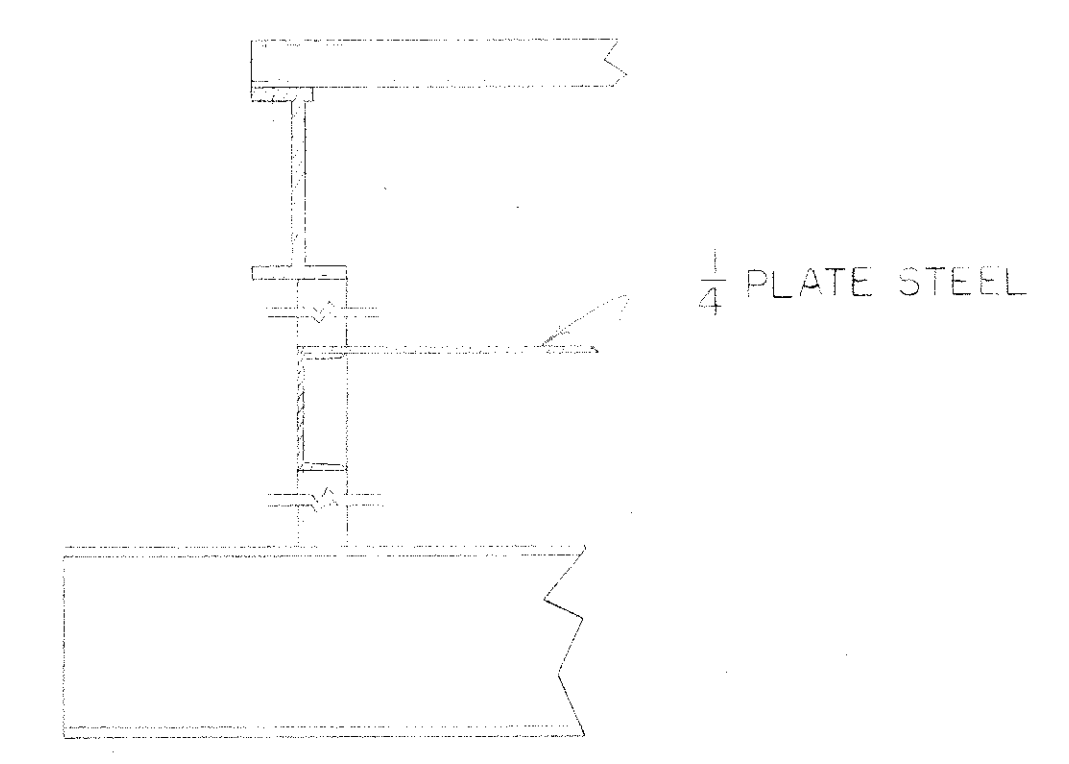
HOLE DETAIL FOR W8x17 BEAM



97



SECTION A-A  
SCALE 1/4" = 1"



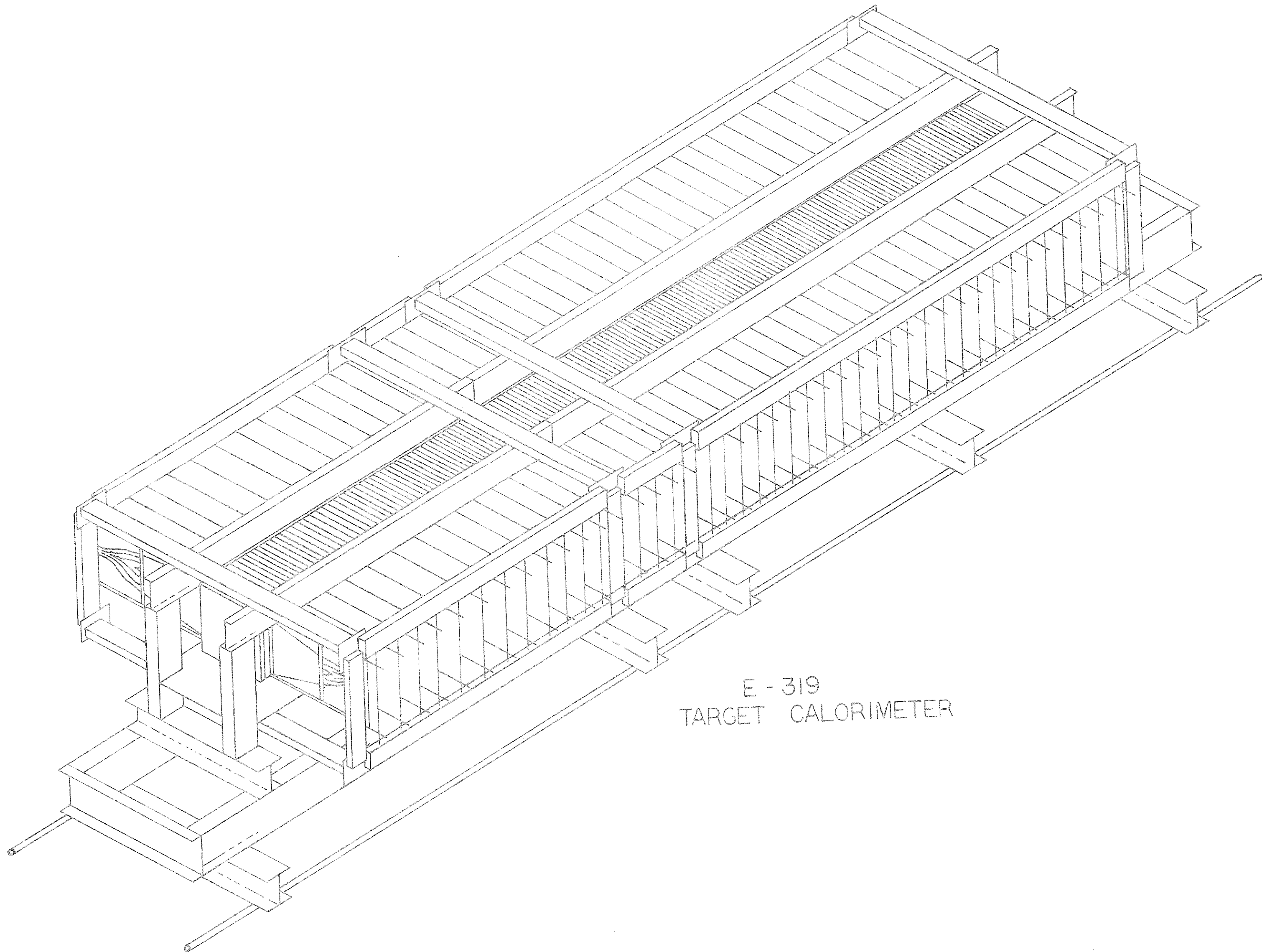
SECTION B-B  
SCALE 1/8" = 1"

MSU TARGET  
IRON SUPPORT

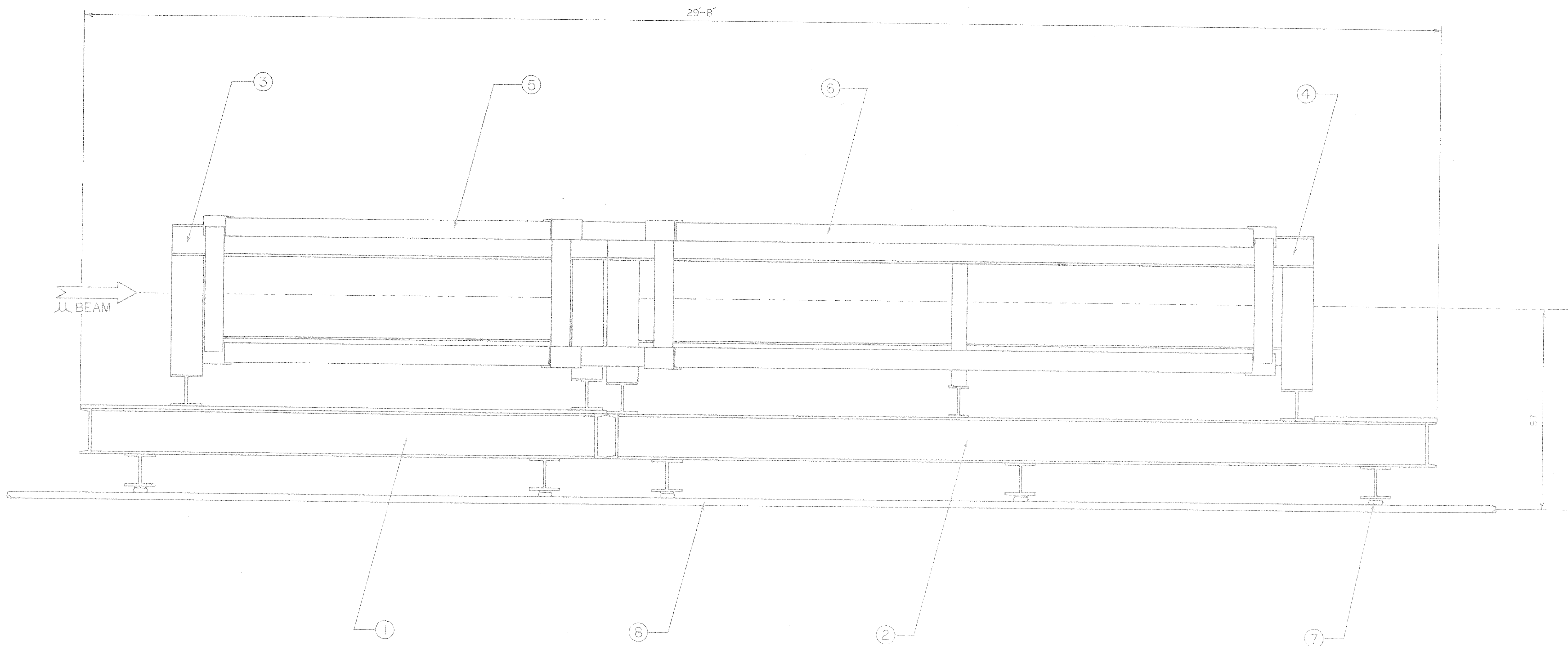
MICHIGAN STATE UNIVERSITY  
COUNTER SPARK CHAMBER LAB  
EXPERIMENT 319

TOLERANCE: ± 1/16	DRAWN BY: F. EARLEY	DATE:
SCALE: 3/4" = 1"	CHECKED BY:	DWG. NO. TC 200





E - 319  
TARGET CALORIMETER



NO.	DESCRIPTION
1	FRAME #1
2	FRAME #2
3	IRON SUPPORT #1
4	IRON SUPPORT #2
5	OUTER COUNTER SUPPORT #1
6	OUTER COUNTER SUPPORT #2
7	THOMPSON BEARING
8	THOMPSON RAIL SYSTEM

MSU TARGET  
CALORIMETER ASSEMBLY

MICHIGAN STATE UNIVERSITY  
COUNTER SPARK CHAMBER LAB.  
EXPERIMENT 319

SCALE 1" = 1'	DRAWN BY F. EARLEY	DWG. NO. TC 203
DATE 5-17-75	CHECKED BY	

MECHANICAL DESIGN OF INSTRUMENTED  
TARGET FOR PARTICLE CALORIMETRY  
FOR USE IN EXPERIMENT 319 AT  
THE FERMI NATIONAL ACCELERATOR LABORATORY

May, 1975  
Michigan State University  
Counter Spark-Chamber Lab

Robert Mills  
Frank Earley

CONTENTS

10.1	Contents
10.2	Description
10.3	Physical Criterion
20.1	Strength Calculations
20.2	Assembly Drawing
20.3	Drawings
30.1	Introduction to Assembly
30.2	Assembly Flowgraph
30.3	Written Assembly Instructions
30.4	Conclusion
40.1	Appendix
	Required bolts and nuts
	Project Time Table
	Moving Target on Rail

Designed By  
Robert Mills

Drawings By  
Frank Earley

Also  
Dr. K. W. Chen  
Dr. L. Litt  
Dr. A. Kotlewski  
Mr. L. Funkhouser  
Dr. J. Terze

Editor  
Jim Kiley

10.2

DESCRIPTION

The Michigan State University Instrumented Target for Particle Calorimetry has the following physical specifications:

Length	Total	356"
	Target	298"
	Frame #1	138"
	Frame #2	218"
Width	Max	104.5"
	Frame	40"
	Thomson	60.25"
Height	Max	68"
	Frame	12"
	Iron Hanger	60.12"
Rail	For 60.25" spaced Thomson rails as per E-319 Muon Lab Fermi National Accelerator, bearings are RW-32.	
Weight Bearing	Max	17.5 tons
	Min	none
Weight of Assembly	4.1 tons	
Iron Target	Length	240"
	Size	20" x 20"
Scintillation Counters	MSU Counters 20" Square Support Frame TC 210	

DESCRIPTION

The Michigan State University Instrumented Target For Particle Calorimetry.

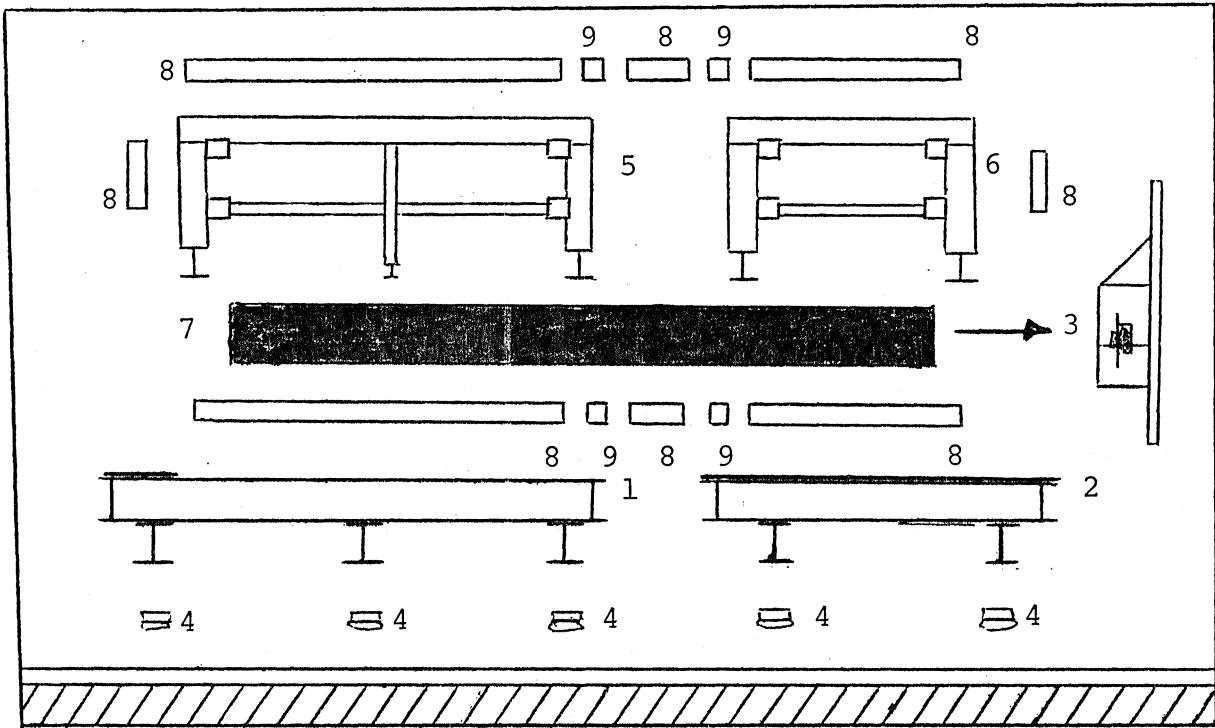


Figure 1

EXPLODED VIEW OF TARGET CALORIMETER

The target calorimeter is made of structural steel except for the outer counter frame which is aluminum to have low magnetic effects near photo tube bases. Construction is welded or bolted and requires on-site final assembly.

PARTS OF TARGET CALORIMETER

- |    |                                   |
|----|-----------------------------------|
| 1  | Target Frame #2                   |
| *2 | Target Frame #1 (Old Target Cart) |
| *3 | Halo Veto/MWPC Assembly           |
| 4  | Thomson Bearings                  |
| 5  | Iron Support Frame #2             |
| 6  | Iron Support Frame #1             |
| 7  | Target Iron                       |
| 8  | Outer Counter Support (Aluminum)  |
| 9  | Connect Plates (Aluminum)         |

\*From FNAL E-26

### 10.3

The Michigan State University Instrumented Target for Particle Calorimetry, called here the Calorimeter, is designed to satisfy the following criterion:

- 1) Conforms to physical size and shape of the Princeton-Penn truck frame drawing 1042-75-D-2 as modified for Fermi National Accelerator (FNAL) Experiment 26.
- 2) Total length of Iron Counter Sandwichs is 298 inches.
- 3) Scintillation counters are read from sides and allows for existence of double readout type counters.
- 4) Target Iron is 20" x 20" square and can be any thickness, the target may also use lead or other materials.
- 5) The two frame assemblies may be used independently or as one large assembly.
- 6) Existing E-26 Halo Veto counters are used as well as one small Cornell Multiwire Proportional Chamber.
- 7) This design must require minimum changes on existing target from FNAL E-26.
- 8) Single readout counter should be able to be used from either side or top of assembly.
- 9) Support should exist to hold photo tube ends of counters that extend away from truck frame.
- 10) Lowest cost should be maintained.
- 11) Frame should bear weight of worstcase lead target.
- 12) Holes for proportional chambers as per Drawing TC 202, Michigan State University specifications.
- 13) Gross physical specification supplied by Dr. K. W. Chen, Michigan State University, as per requirements for FNAL Experiment E-319.

STRENGTH CALCULATIONS

Iron Hanging Frames as shown in Drawing TC 202.

24000 lb. Total Load  
 12000 lb. on each beam for solid iron target  
 20" x 20" x 298"  
 Length ~ 298"  
 Load is fully distributed  
 $12000/25=480$  P.L.F.  
 For  $w=Load/Ft.$   
 $w=480$  P.L.F.

$$m = \beta \times w \times (L)^2$$

L is Max Unsupported span

$$m = 8 \times 480 \times (9)^2$$

$$m = 4.86 \text{ KFT.}$$

$$s = m/Ft.$$

$$s_{reqd.} = 4.86 \times \frac{12}{24}$$

$$= 2.43 \text{ in.}$$

For w8 x 15 Beam

$$S \text{ spec} = 11.8 \text{ in.}^3$$

Factor of 4 safety margin from  $2.43 \times 4 = 9.72$

$$9.72 < 11.8$$

This allows for the possibility of a lead target that would give a safety factor of 2, the classical value of safety.

Worst Case Deflection at full load, 20" x 20" x 298" solid iron.

$$\Delta = 5 \times w \times (L)^4 / 384 \text{ EI}$$

$$= 5 \times 480 \times (108)^4 / 384 \times 12 \times 30 \times 10^6 \times 48$$

$$= .148 \text{ inches}$$

The maximum bending of the main iron support will never exceed 1/8" under full iron load and nowhere will the shear exceed the weld strength of 1.66, the equivalent uniform iron load.

All welds are compression, no shear on weight bearing components.

20.15

### BEARINGS

Load on each bearing =  $L_B$

$$L_B = 1/6 (17.5 + 4.1) 2000$$

$$L_B = 7200 \text{ lb.}$$

Rated Load for Rolling

$$L_R = 12360 \text{ lb.}$$

This allows a 40% safety factor on each bearing.

### LIFE EXPECTANCY

Roundway hardness = 60 Rockwell C

Expectancy =  $10^6$  inches

Then  $E = \frac{\text{Capacity Required}}{K_L \times K_H}$

Where  $K_L =$  Load Correction Factor for Life.

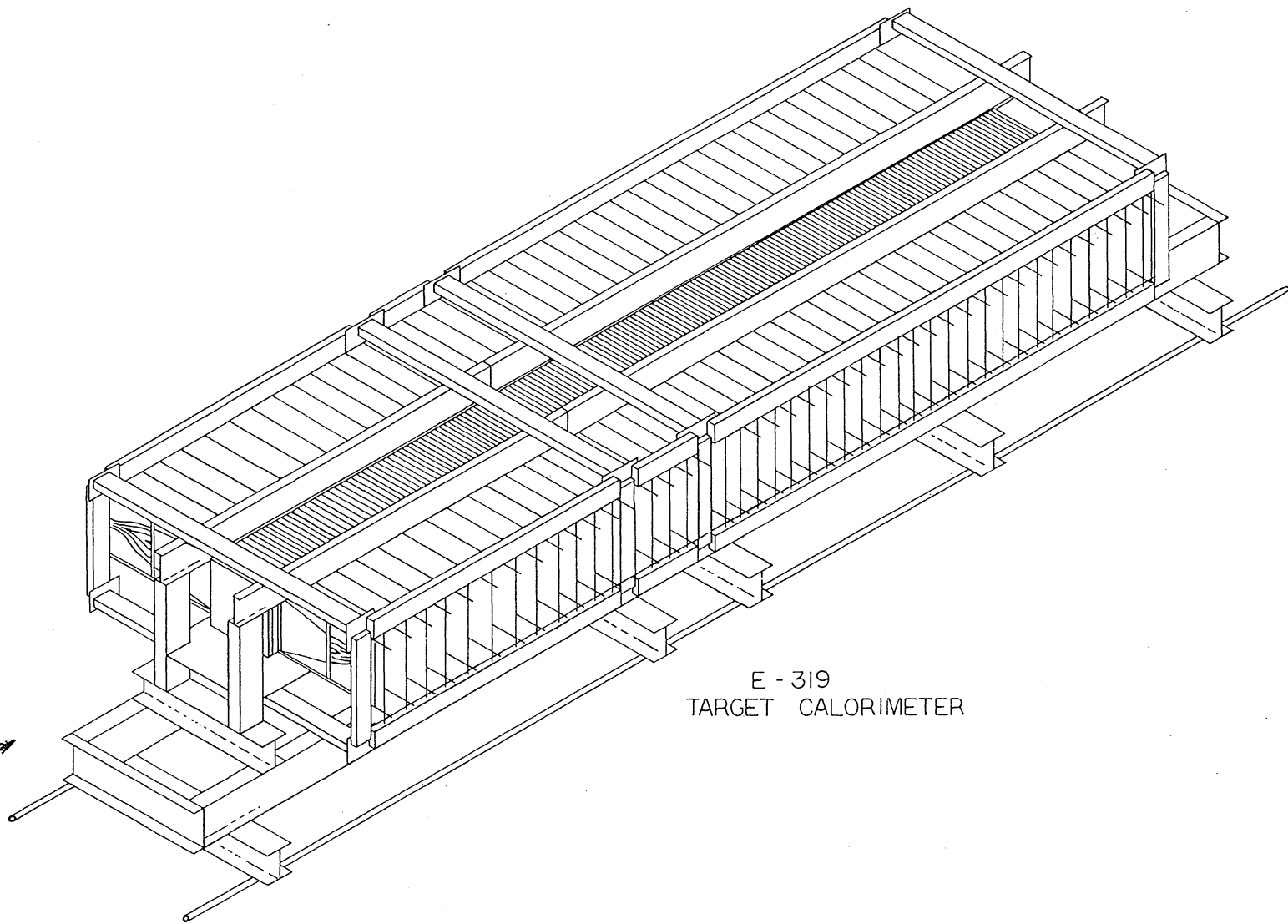
$K_H =$  Load Factor for Hardness

$$E = \frac{13,000}{1 \times 1}$$

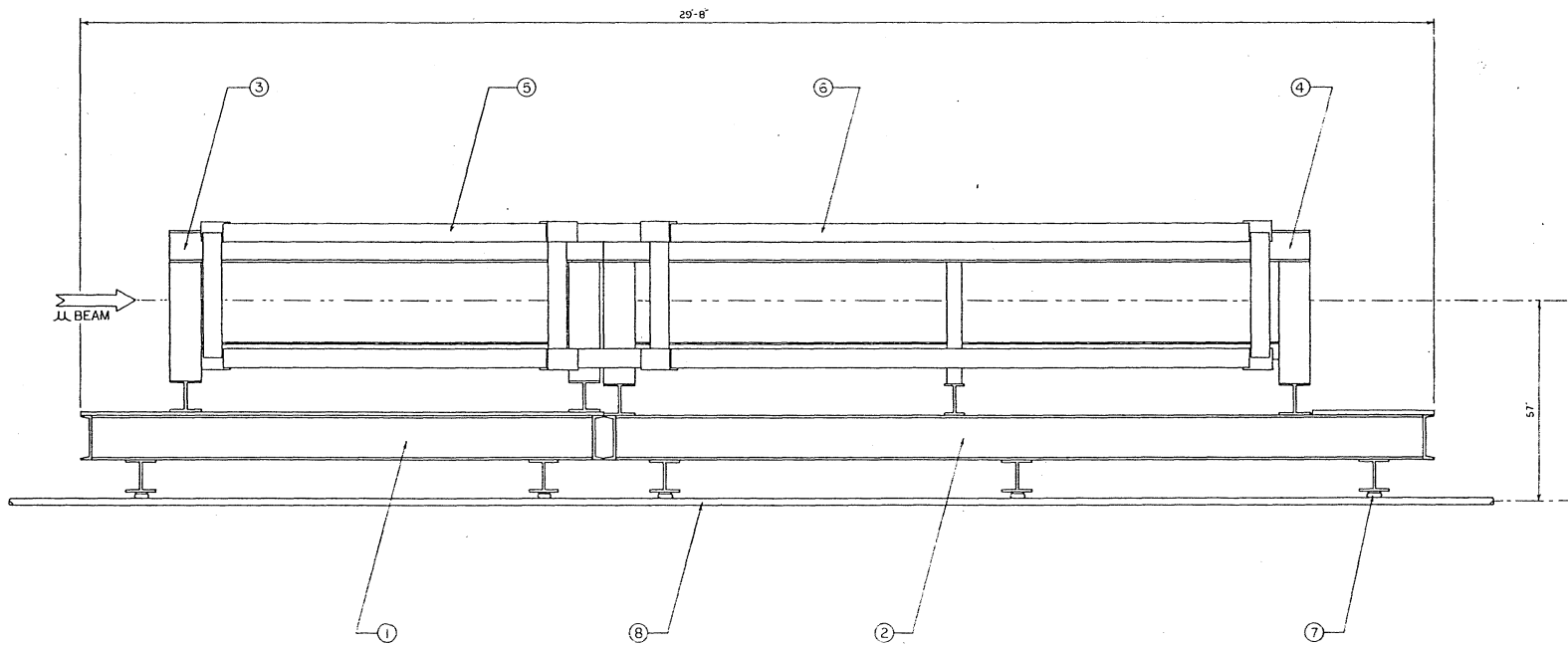
$$E = 13,000 \text{ lbs.}$$

13,000 lbs. is a safe load for the required life time of rolling use.

$\mu$ -beam

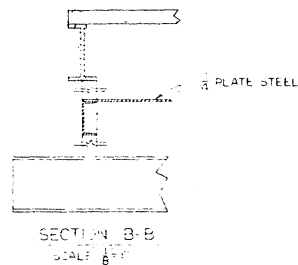
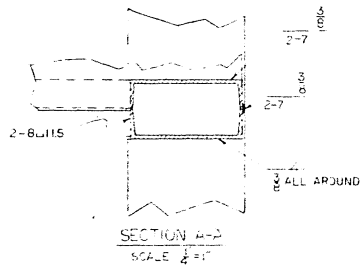
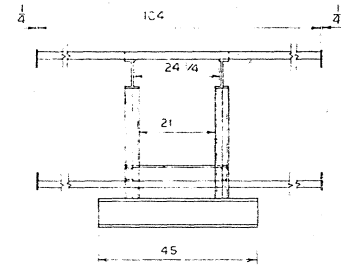
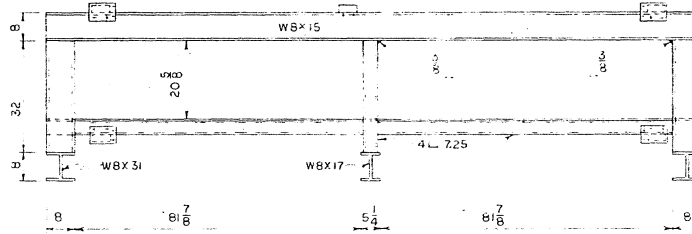
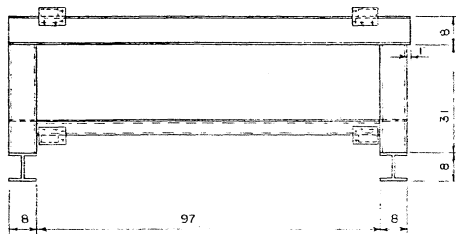
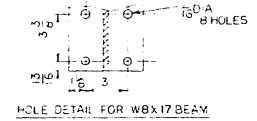
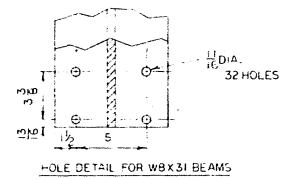
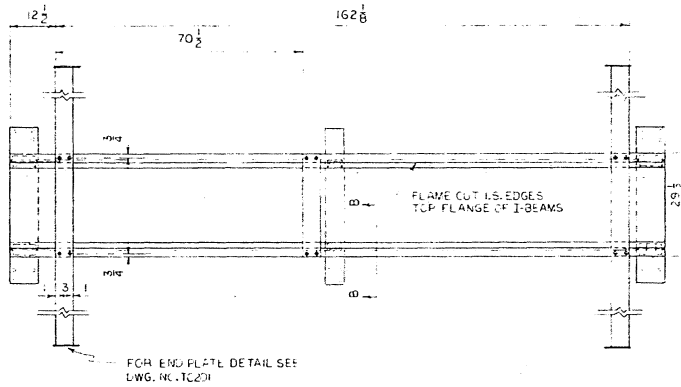
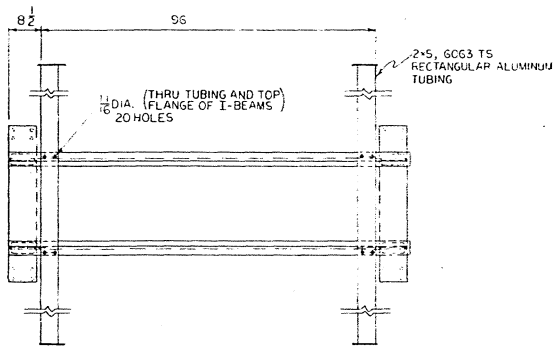


E - 319  
TARGET CALORIMETER



NO.	DESCRIPTION	
1	FRAME #1	
2	FRAME #2	
3	IRON SUPPORT #1	
4	IRON SUPPORT #2	
5	OUTER COUNTER SUPPORT #1	
6	OUTER COUNTER SUPPORT #2	
7	THOMPSON BEARING	
8	THOMPSON RAIL SYSTEM	
MSU TARGET CALORIMETER ASSEMBLY		
MICHIGAN STATE UNIVERSITY COUNTER SPARK CHAMBER LAB EXPERIMENT 3/9		
SCALE	DRAWN BY	DWG NO.
1" = 1'	F. EARLEY	TC 203
DATE	CHECKED BY	
5-17-75		

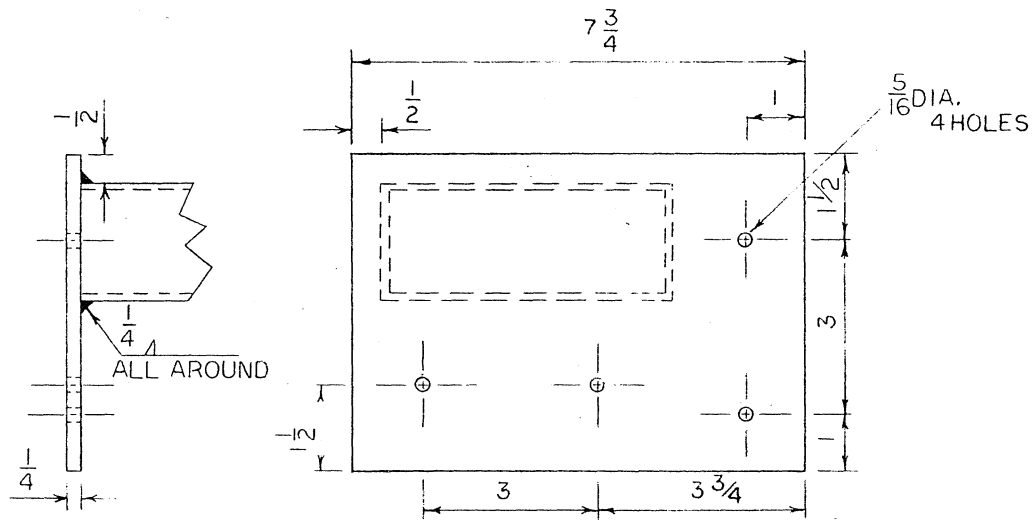




MSU TARGET  
IRON SUPPORT

MICHIGAN STATE UNIVERSITY  
COUNTER SPARK CHAMBER LAB  
EXPERIMENT 319

TOLERANCE: ± 1/16	DRAWN BY: F. EARLEY	DATE:
SCALE: 3/4" = 1"	CHECKED BY:	DWG. NO. TC.202



SECTION A-A END PLATE 16REQ'D

SCALE  $\frac{1}{2} = 1"$

MSU TARGET	
COUNTER SPARK CHAMBER LAB	
DWG. NO. TC 201	DATE 5-13-75



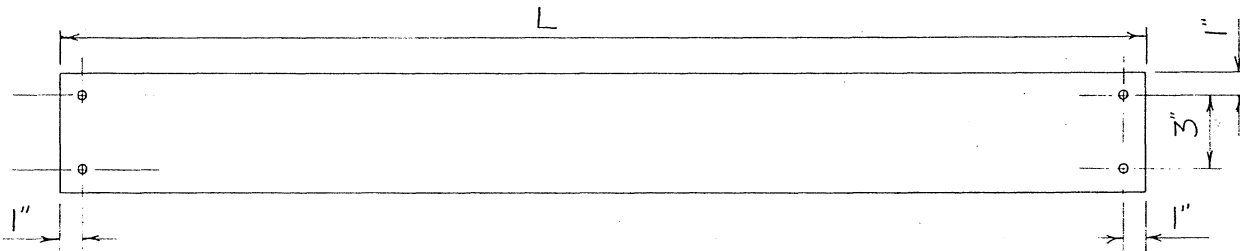
SUBJECT

OUTER OUTER SUPPORT

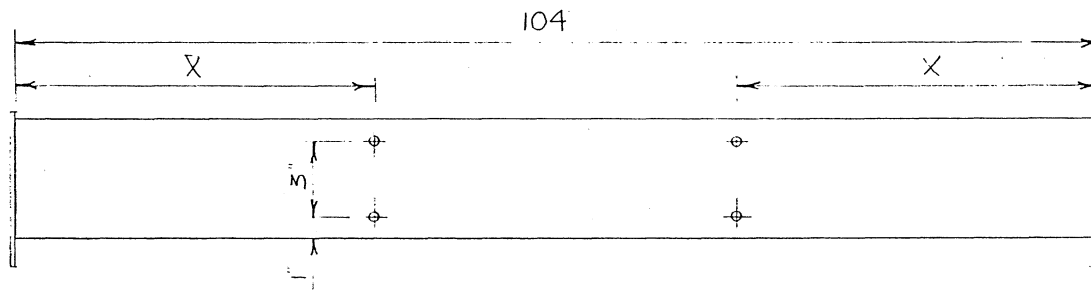
NAME  
FEARLEY

DATE REVISION DATE

MAT'L: 2x5, 6063 TS RECTANGULAR ALUM TUBING  
5/16 DIA  
16 HOLES



L	NUMBER REQ'D
85 1/2	4
151 5/8	4
21 1/2	4
32 7/8	8



4 REQ'D WITH  $X = 33$

4 REQ'D WITH  $X = 103/4$

ALSO REQ'D: 8 ea. END PLATES  $1/4 \times 7 3/4 \times 5 1/2$   
SEE DWG NO TC201 SECTION A-A FOR HOLES



INTRODUCTION TO ASSEMBLY

The assembly assumes that the people involved have available the following, not included, supplies:

- 1) Minimum 15 ton overhead crane
- 2) 2-4 people for some parts of assembly
- 3) 2-14" adjustable wrenches
- 4) 2-four inch paint brushes, thinner and cans for oil-based paint
- 5) Hand electric drill and twist drills for aluminum and steel, drill with 5/8" chuck.
- 6) Sheet Metal Shears
- 7) Hack Saw
- 8) Wood planks 2" x 6" x 4" approximately.

Supplies to be included in assembly are:

- 1) Existing E-26 Target Frame
- 2) New Frame #2
- 3) #1 Iron Support
- 4) #2 Iron Support
- 5) Outer Counter Support Pieces
- 6) 6-Thomson Bearings
- 7) Rubber for Fe to Al Interface
- 8) Cable and winch
- 9) Bolts and nuts
- 10) Paint
- 11) Wire Trough
- 12) Up to 104 scintillation counters
- 13) Up to 103 2" thick iron target plates
- 14) 208 counter clamps.
- 15) 4" x 4" x 36" Frame connect block.

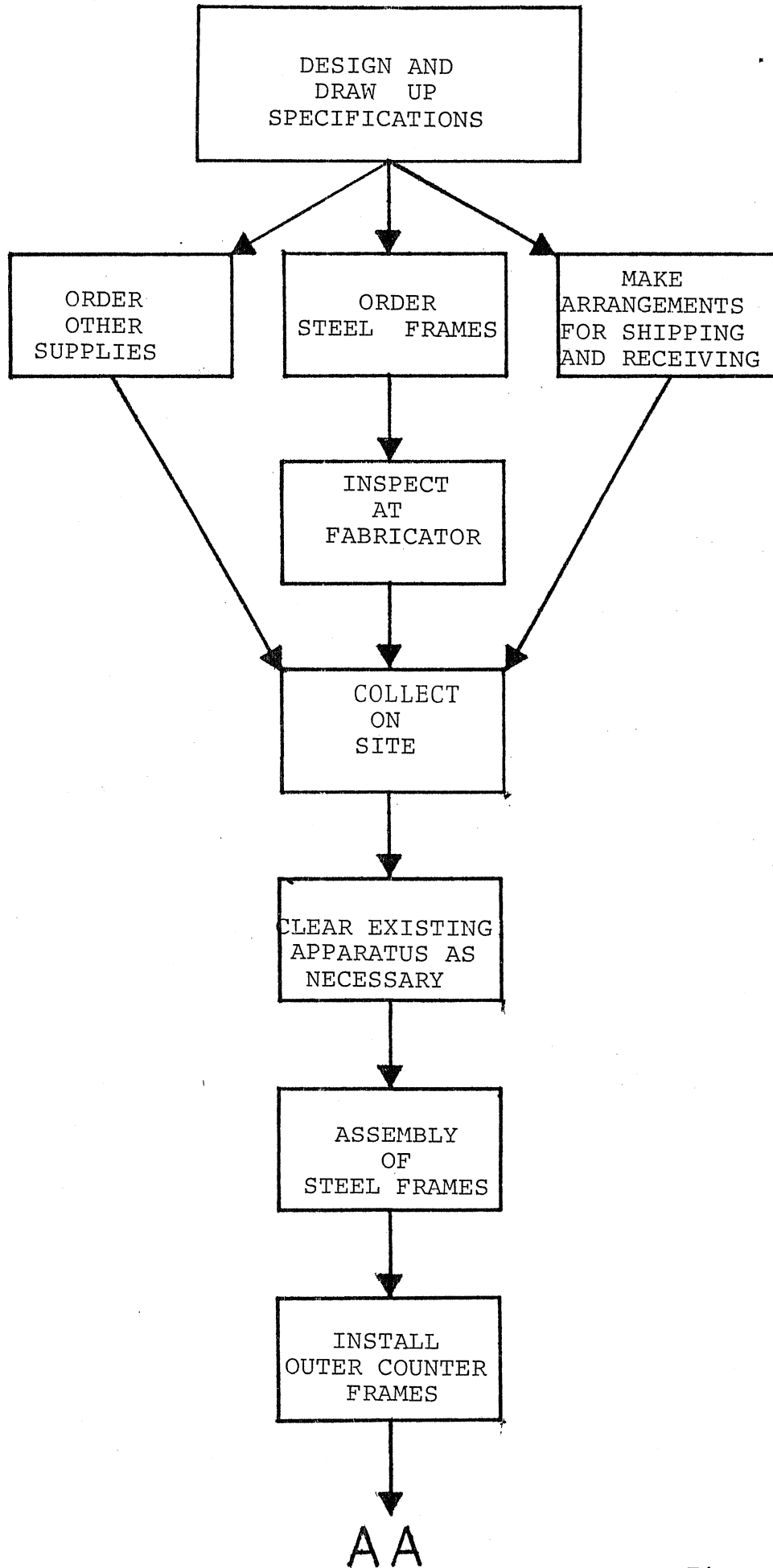


Figure 2

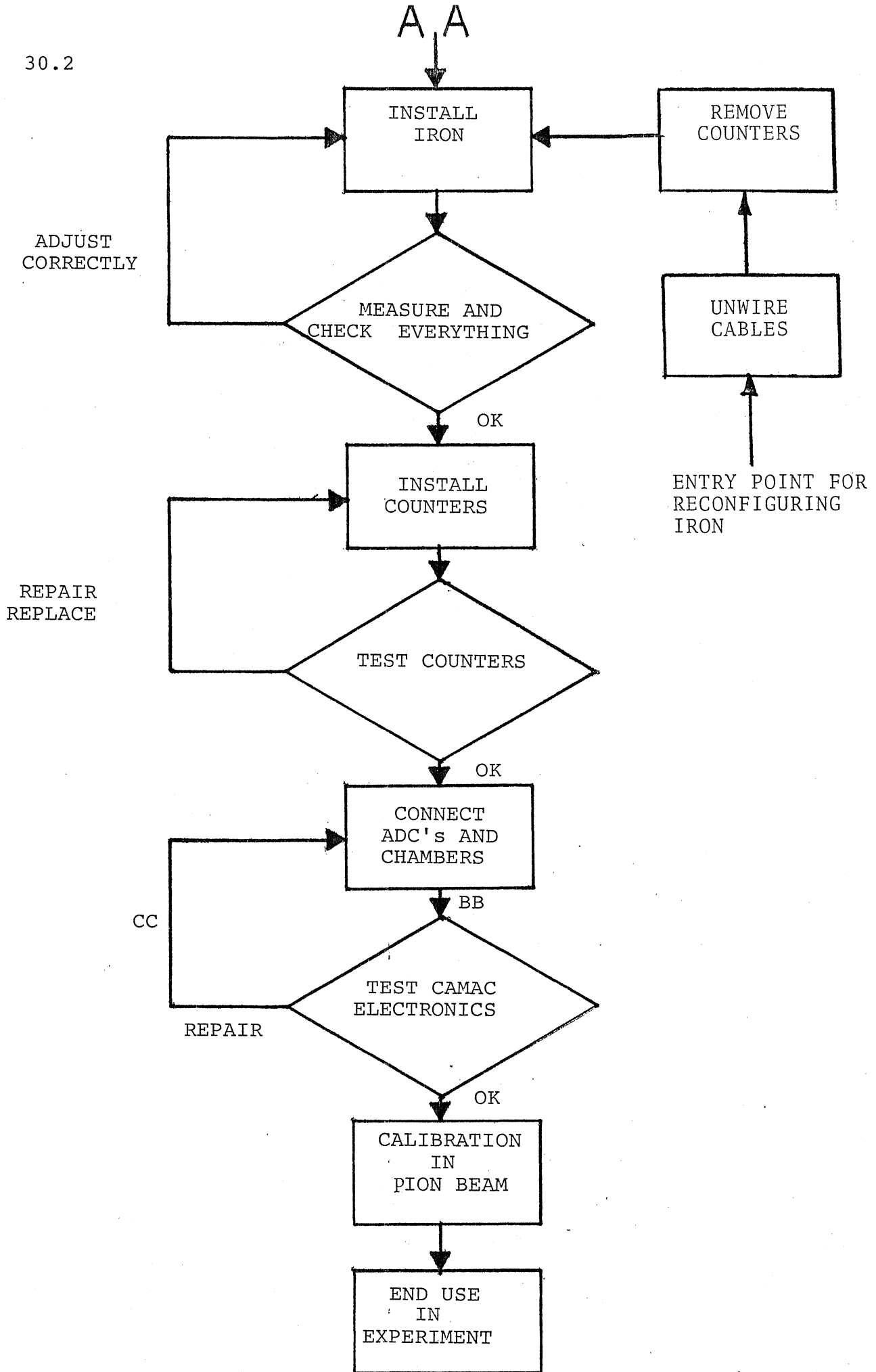


Figure 2

30.31

TARGET FRAME #2 ASSEMBLY

Clear a work area allowing 18 feet of Thomson rail and a workspace of 9 feet by 18 feet on the muon lab floor.

Clear all unnecessary equipment from immediate area and make a path from garage door to rail system 7 feet wide to move frames through.

Collect together into your workspace all necessary tools and materials.

30.32

TARGET IRON PAINTING

Outside of muon lab paint, all of the sections of Target Iron. (Important: the paint fumes may contaminate materials in lab)

Use one coat of rust proofing paint with brush and allow 36-48 hours to dry before moving iron into lab.

30.33 ASSEMBLY PROCEDURE

Frame Painting

While still outside (important, the paint may contaminate scintillator materials in lab) paint the 3 (three) steel frames.

Frame #2  
Iron Support#1  
Iron Support #2

Use two coats of rust proofing paint with brush and allow 36-48 hours to dry before moving frames into lab. DO NOT paint aluminum outer counter support bars or Thomson Bearing.

### 30.34 INSTALLING THE THOMSON BEARINGS

Attach crane to side of frame #2 and lift until the frame stands on its edge. Place the 3 (three) Thomson Bearings in position and bolt them to the 8 (eight) inch I Beam. Using crane, lower frame back down, then connect crane to other side and repeat installing the other 3 (three) bearings.

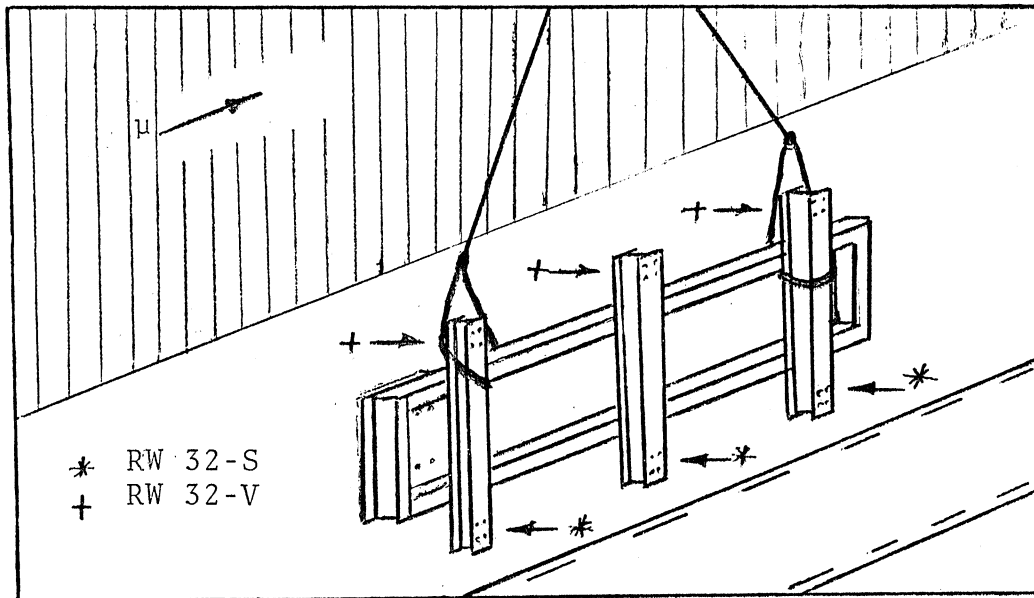


Figure 3

### INSTALLING THE THOMSON BEARINGS

(note: see figure 7)

24 bolts 3/8-24 x 2" and 24 nuts 3/8-24 and 24, 3/8" lock-washers are used to accomplish the assembly. They should be tightened to 50-75 foot-pounds. Then the frame should be returned to its normal position by lowering the crane.

Now the frame should be placed onto the track. First lifting the  $\mu$  beam end about 1 foot off the floor with the overhead crane. Then rotate the entire frame pivoting it on the two downstream Thomson Bearings.

After pivoting, set the end down, then pick up the other end and repeat the scheme until the position of the frame is over the track as shown in Figure 7.

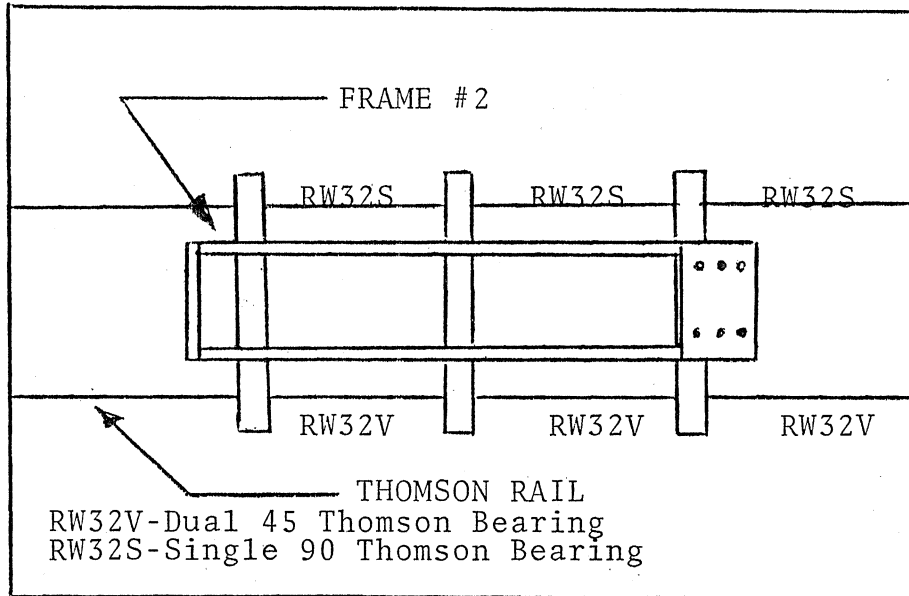


Figure 7

POSITION OF FRAME PRIOR TO MOUNTING ON RAIL

Note:

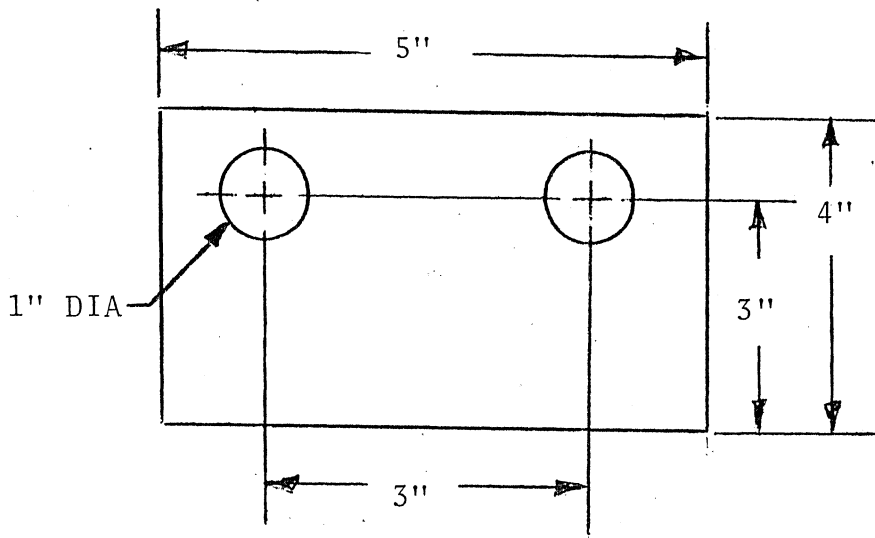
Remember to place wood blocks under bearings when moving frame so as not to damage bearings on cement floor. Now connect crane to both diagonal supports for lifting entire frame about 1 (one) foot. Then carefully align frame with rails and set it down on the Thomson Rail. Now check carefully that the bearings are set onto rail. If not, adjust them. Oil the bearings with light machine oil and move the frame back and forth a few feet.

Note:

Set the Vee Bearings onto the Thomson rail first as they are self aligning.

30.35 INSTALLING THE IRON FRAME

Cut from gasget material supplied 16 steel-to-aluminum interface gasgets as shown.



Note: 1/8" Gasget made of rubber.

Figure 4

Use sheet metal shears. Now unbolt aluminum support bars one at a time and place gasgets between aluminum and steel parts. Then rebolt and tighten to 20-30 ft-lb. Do this to all 8 bars with 16 gasgets.

Fasten crane to diagonals of iron support frame as shown.

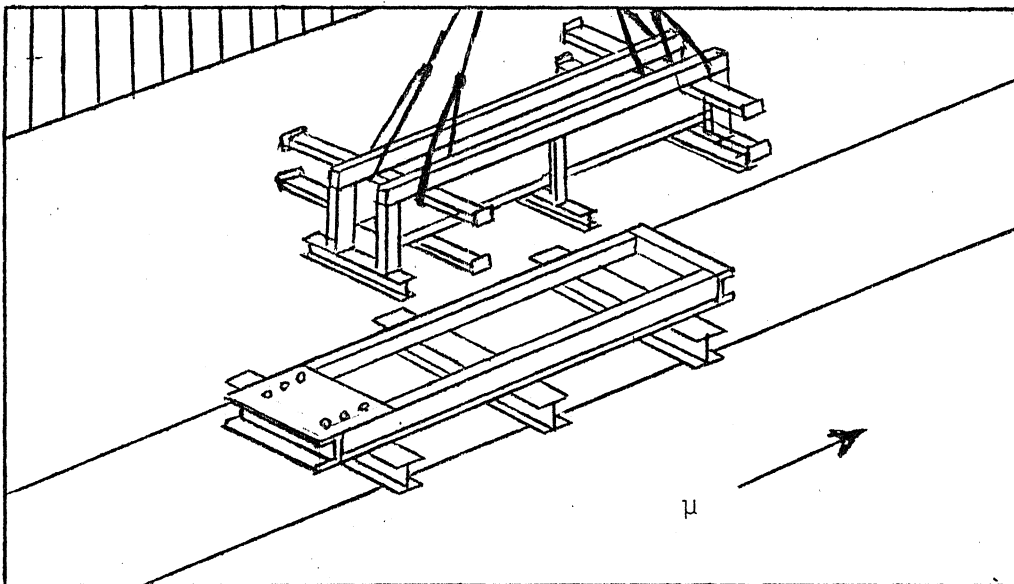


Figure 5

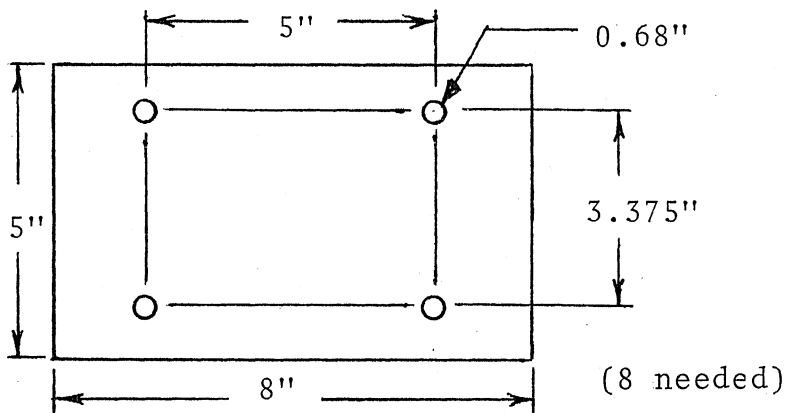
INSTALLING IRON FRAME

## LIFTING IRON SUPPORT ON TO FRAME

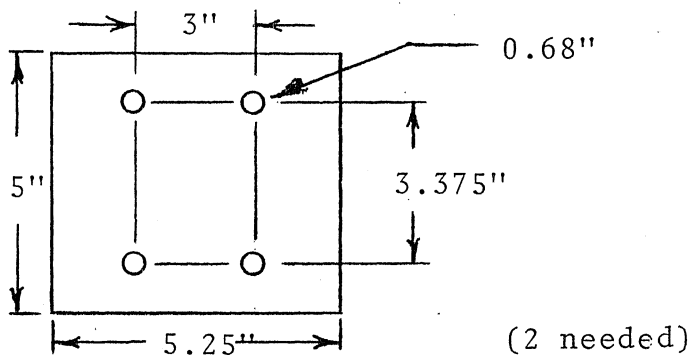
Carefully move into position to align with pre-drilled bolt holes on frame. Then bolt into place using 1/2-12 x 1 1/2" bolts and nuts with washers.

### \*\*Important\*\*

Check beam center for 60" to floor. Beam center is located exactly 10" below support beams that 20" iron hangs on. If, due to variations in structural steel thickness, beam center is more than + 1/2" shims must be placed between frame and Iron Support.



Note: Material is steel. Thickness is whatever is necessary to shim to specifications.



Note: Use these only if necessary.

Figure 6

### HEIGHT SHIM FOR FRAME #2

Inspect Target Frame #2 for loose bolts, bad alignment, or anything that needs correcting.

### 30.36 TARGET FRAME #1 ASSEMBLY

Disconnect all cables to counters and the 2 multiwire proportional chambers. Then remove the two wire troughs connected to the top of the E-26 Target. Clear a useable workspace around the cart with a 15 foot by 8 foot area on one side to place the # 1 Iron Support Frame into.

30.37 PREPARING EXISTING E-26 FRAME #1

The following assemblies will be saved; take care not to disturb them.

Frame #1  
The E-26 Halo Veto Counters  
Front end Cornell Proportional Chamber

Begin by removing the scintillation counters carefully placing each one in a protected place. Then, remove the Target Iron. Unbolt and remove the down stream multiwire proportional chamber. It is important to move it gently so as not to break any of its wires. Remember, these chambers belong to the Cornell Group.

\*\*IMPORTANT\*\*

The existing target angle iron must be cut, so as to remove most of it but leave the Halo Veto Counters and the upstream multiwire proportional chamber and the Halo Veto Counters well supported.

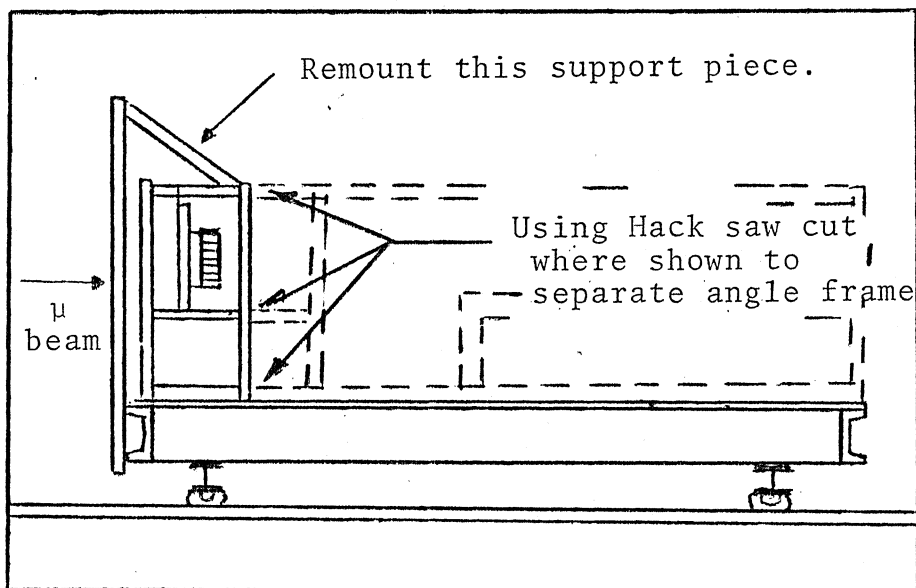


Figure 8

CUTTING EXISTING ANGLE IRON  
(Frame #1)

Cutting existing angles, remount the top Halo Veto Counter support as shown, then cut off excess. Also, make a cut through each base angle as shown, one on each side of Frame (2 cuts). Now unbolt and remove remainder of downstream angle frame disassembling the frame pieces as you proceed.

Clean up loose pieces and check to see that Halo Veto Counter and multiwire proportional chamber are still well supported, brace as necessary.

### 30.38 INSTALLING IRON SUPPORT #1

Lifting the #1 Iron Support Frame with the crane, place it on the #1 Frame (as shown in assembly drawings). **\*\*Important\*\*** Do not jar or impact angle support for multiwire proportional chamber and Halo Veto Counter with Iron Support Frame when moving it. After positioning it with care, mark the necessary hole locations through the 8 inch I Beam on to the 1 inch Steel plate on top of Frame #1 using colored grease pencil. Carefully remove Iron Support Frame off from Frame #1 and set it aside using crane. Drill the holes you have marked first 1/4 inch then after you have made the pilot hole drill them to 5/8 inch (16 holes are necessary). Now lifting the iron support back onto the Frame#1, align it carefully and bolt it into place using 1/2 - 12 x 1.75 bolts nuts and washers (16 required) tightened to about 50-75 foot pounds.

Inspect for careful alignment and that everything is intact and undamaged.

See Figure 5, it shows how to fasten crane to lift the Iron Support Frame.

### 30.385 DRILLING THE FRAME CONNECT HOLES

Drill 12 inches in from outside edge 2 holes 5/8" centered on the c/2 x 20.7 ~ "E" Channel for both frames.

See drawing TC 200, same dimensions are used for both frames

### 30.39 INSTALLING THE ALUMINUM OUTER COUNTER SUPPORT FRAME

Gather together the pieces shown in drawing TC 205 (20 parts) and 120 bolt, nut, and washer sets for 3/8 - 24 x 2"; and 4 (four) connect plates, drawing TC 201.

Gently roll target Frame #1 and Frame #2 together until the iron supports butt into each other. Now, bolt all of the aluminum outer counter support pieces on the aluminum supports using the connect plates between the two frames. (See assembly drawings) Also using 1/2-12 x 10 bolts, connect the 2 target frames together using the frame connect holes with a 4" x 4" x 36" wood block between the two truck frames.

Check the whole assembly for proper alignment.

Move the entire assembly into its final position, note the next step is installing the iron, using the steel cable and winch. The assembly is now too heavy to move by hand.

Align overhead crane over the top of the target.

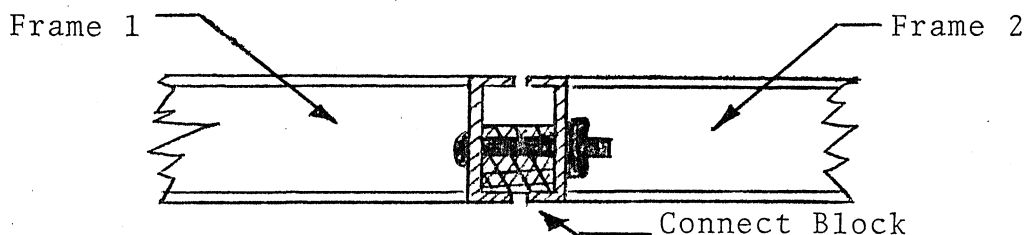


Figure 9

### 30.3A INSTALLING THE TARGET IRON

Lift each slab of iron with the crane with its lifting hook and position it over the top of the target, slowly lower the iron slab into its place in the target. Repeat for as many iron slabs as necessary spacing them according to the spacing requirements of the energy configuration required.

Go over all spacing measurements and adjust as necessary.

Place C clamps on Iron Support Beam just outside of Target Iron for safety so that the last section can not fall off from the target.

### 30.3B INSTALLING THE 20 by 20 COUNTERS

\*\*Important\*\* Be careful with the counters , they are fragile.

Install the counters one at a time by inserting a counter from the side of the target in between the target iron, then clamping the counter into place with two counter clamps.

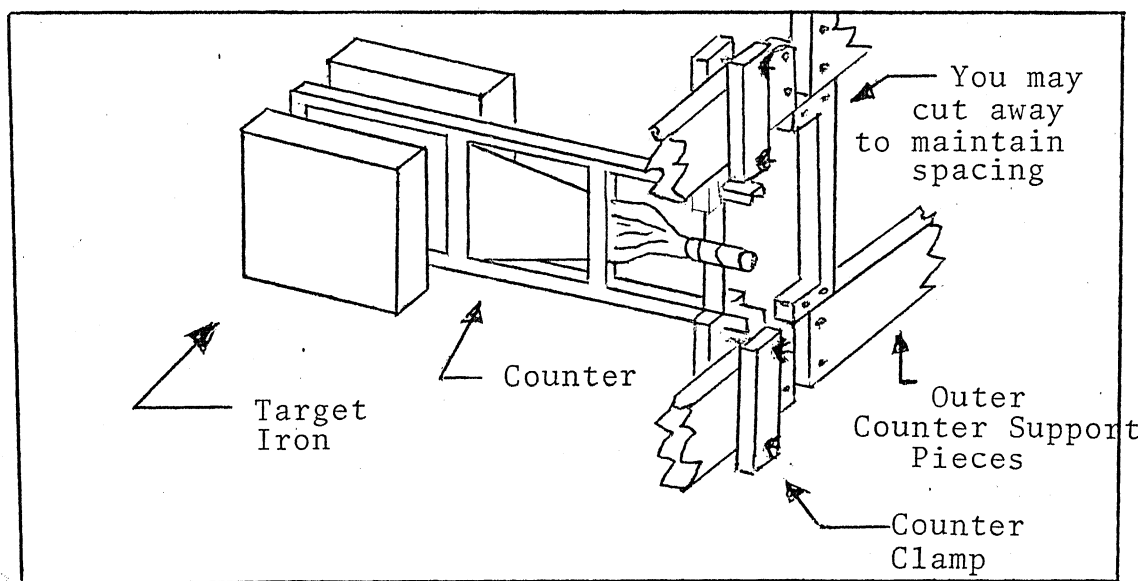


Figure 10

### CLAMPING A COUNTER INTO PLACE

Repeat this process until all of the counters are in place. Then inspect them all for correct installation.

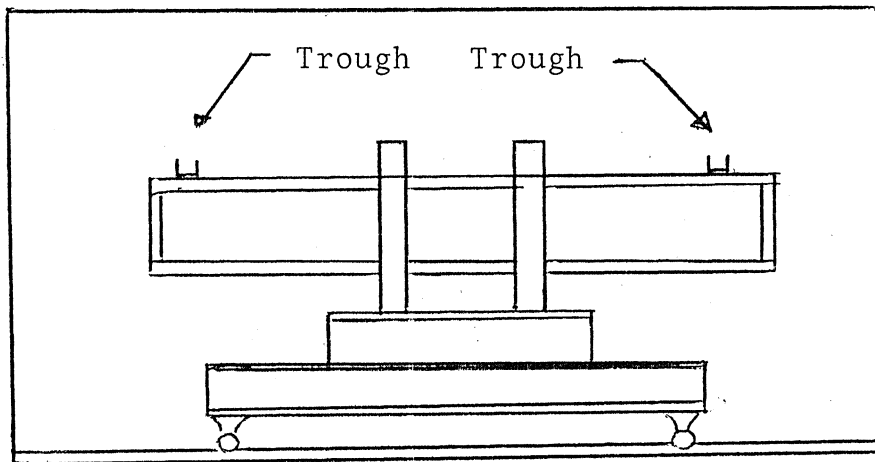
30.3C WIRING THE TARGET

First install two 21 foot lengths of 8" wire trough one on each side of the aluminum support beams running the length of the target.

Fasten them in place with 10 # 8 x 1" screws, 2 per support beam, drill through the plastic into the aluminum and screw into place.

Now connect cables to each counter, one at a time, and mark them with the counter's number on each end. Route the cables into the wire trough, then at one end, flair them into the ceiling towards the (portacamp) CAMAC readout system.

Using light cord, tie the cables into bundles.



END VIEW

Figure 11

#### 30.4 CONCLUSION

The construction of the Michigan State University Instrumented Target involves about 300 man hours over a three month period. One person can do most parts of the construction but 2-4 people are required during some parts of the assembly. Great care must be taken to maintain the best workmanship possible.

Any attempt to make radical changes in the design of this project should result in a careful reconsideration of the inter-relating parts of the entire assembly. The designer is not responsible for any damage resulting from unspecified changes to any of the above assemblies.

Robert Mills

40.10 BOLTS, NUTS AND WASHERS REQUIRED

Thomson Bearings

Frame #2	24 Bolts	3/8-24 x 3"
	24 Nuts	3/8-24
	24 Washers	For 3/8

---

Iron Supports	40 Bolts	1/2-12 x 2
	40 Nuts	1/2-12
	40 Washers	For 1/2

---

Outer Counter Frames	100 Bolts	3/8-24 x 3"
	100 Nuts	3/8-24
	100 Washers	For 3/8

---

Counter Clamps	580 Machine Screws	10-24 x 4"
	580 Wing Nuts	10-24
	1160 Washers	For #8

---

Wire Trough	20 Sheet Metal Screws	#8
-------------	-----------------------	----

---

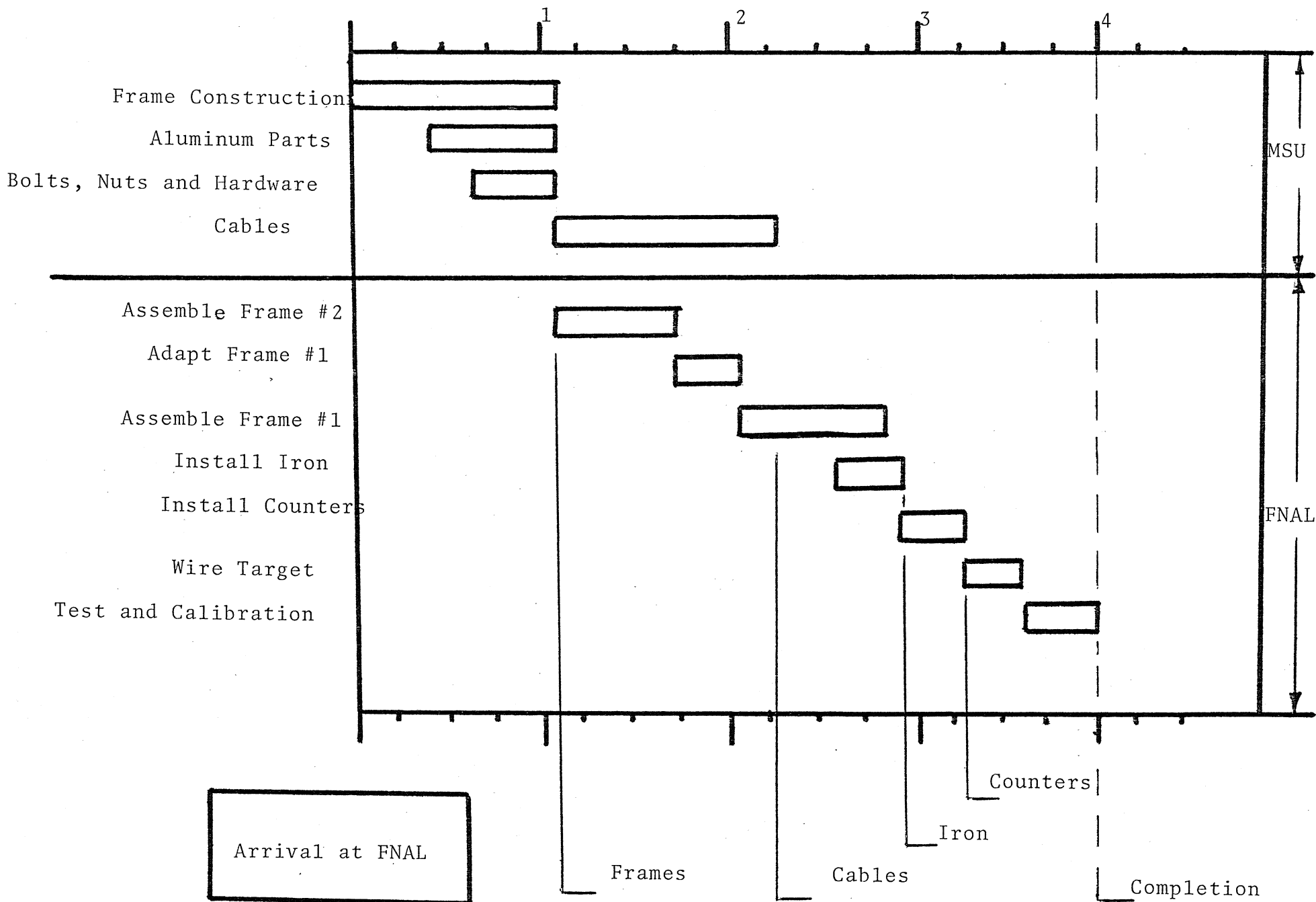
Support Bars	32 Bolts	3/8-24 x 3"
	32 Nuts	3/8-24
	32 Washers	For 3/8

---

Truck Frame Connect	2 Bolts	1/2-12 x 10"
	2 Nuts	1/2-12
	4 Washers	For 1/2

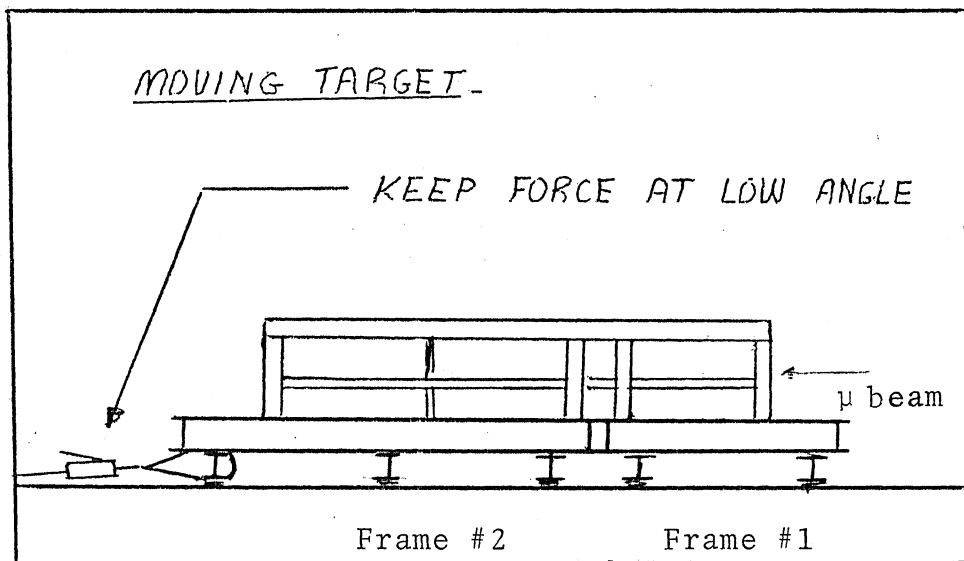
---

TIME LINES FOR TARGET CONSTRUCTION (Time in Months)



#### 40.12 MOVING THE COMPLETED TARGET

Using the block and tackle winch supplied, connect one end to the same side of the target that is the direction you wish to move the target toward. Connect the other end to one of the Thomson Rail ties 10-15 feet farther in that direction take the slack out of the cable and winch the target in the desired direction as much as necessary. If more than 10 feet or so disconnect the tie and move it farther down the line, repeat as often as necessary.



MOVING TARGET ASSEMBLY